# Laser Speckle Imaging For non-Destructive Analysis

by

## Kalomoiris Filippos

## Diploma Thesis

A thesis submitted in partial fulfillment of the requirements for the diploma of
Electrical and Computer Engineering

## Thesis Commitee

Balas Costas, Professor, Supervisor

Kalaitzakis Konstantinos, Professor

Kortsalioudakis Nathanail, Ph.D.

Chania, February 2018

# *Abstract*

When coherent light illuminates a diffuse object, it produces a random interference effect known as speckle pattern. If there is movement in the object either by auto stimulation (e.g. blood flow) or by an external stimulation (e.g. acoustic, thermal, impact) then the speckles fluctuate in intensity. These fluctuations can provide information about the movement. Laser Speckle Imaging is a non-destructive, non-contact, full-field technology that can access these information and build a movement map of the object. This technique has recently become a powerful tool for scientific and industrial analysis in many different fields. Its applications range from non-contact surface analysis and archeology to biomedical science. The work presented in this thesis deals with the design of a Laser Speckle Imaging device that performs, non-contact analysis in impact and acoustic stimulated surfaces, generating spatial and temporal movement mapping with pseudocolors. The implementation employs a sensitive camera, a coherent light source, a light expander, a stimulator and the surface we want to analyze. The light source illuminates the surface and speckle pattern is produced. This pattern is changed by the stimulator and measurements have been recorded with the camera before and during the stimulation. The aforementioned implemented device accomplishes two analyses in order to achieve both spatial and temporal resolution. It also quantifies the stimulation's intensity with no information about the stimulator. These features make our approach ideal for demanding laser speckle imaging applications, such as non-destructive analysis and noninvasive diagnosis.

# Acknowledgements

It is a great opportunity to bestow my heartful regards to all people who have been either directly or indirectly involved in the fulllment of this diploma dissertation.

First and foremost, I would like to express my sincerest gratitude to my professor and supervisor, Professor Constantinos Balas, for giving me the opportunity to deal with such an interesting topic. Not only did he help me completing my studies, but also motivated me to work more eciently and professionally by conducting a lot of extra research, being familiar with experimental devices and gaining valuable knowledge.

Besides my supervisor, I would like to thank the rest of my thesis commitee: Prof. Konstantinos Kalaitzakis and Dr. Nathanail Kortsalioudakis, for their insightful comments and encouragement, but also for the hard question which incented me to widen my research from various perspectives.

My sincere thanks also goes to the whole team of the *Optoelectronics and Imaging Diagnostics Lab*, whose contribution and support have been instrumental. I am really grateful to Rossos Christos (PhD Candidate) for his invaluable help and cooperation, his time, advice and support through the research and implementation of this diploma thesis. I would also like to thank Tsapras Athanasios (PhD Candidate), Kastrinakis Marios (M.sc), Papathanasiou Athanasios (M.sc Candidate), Gkouzionis Ioannis (M.sc Candidate) and Vardoulakis Emmanouil (M.sc Candidate) for their numerous brainstorming discussions, and seless advice.

Furthermore I would like to thank my best friends Adonis , Panagiotis , Trifonas , Themos , Panos , Giorgos and Alexandros for the countless support in whatever decision I made and of course because they were by my side whenever I needed it.

Finally, I must express my very profound gratitude to my beloved parents, Mihalis and Ivelina, and my brother, Dimitris, for providing me with unfailing support and continuous encouragement throughout my years of study and through the process of researching and writing this thesis. This accomplishment would not have been possible without them.

# Contents

# List of Figures

# Chapter 1

# Introduction

## 1.1   Introduction

**Laser Speckle Imaging (LSI)** is an imaging technique which relies on a particular property of the laser. When a coherent light source such as a laser illuminates a rough surface, a pattern is created. This pattern is called speckle. The speckle phenomenon is present with any interfering wave front in fact, such as ultrasounds, and distorts the signal. In LSI however is revealed a *desirable* property from this so-called *undesirable noise*: It carries information about the movement of the scatterers. If there is movement on the surface under investigation either by itself (blood flow) or by a stimulation (acoustic, thermal, impact) then the speckle pattern will change. Changes can be detected and through them the *"movement "* can be quantified. The objective of this thesis was to study and compare the spatial contrast method and the temporal contrast method of *Laser Speckle Imaging* in impact and acoustic stimulated surfaces. We will look to either improve existing processing methods, or to develop new ones.

## 1.2   Thesis Outline

Chapter 2 provides a theoretical backround about nature of light and laser physics.

Chapter 3 presents the technique of interferometry which is a widespread technique with laser. Laser Interferometry can find the displacements of induced objects and surfaces.

Chapter 4 explains the Laser Speckle Imaging and its main principles. It shows how this method work and presents some applications of this method.

Chapter 5 presents the main Set-Up that we used in order to do our implementation.

Chapter 6 presents the Temporal Laser Speckle Imaging device. It describes the Temporal Speckle Contrast algorithm , the additional set-up and all the measurements we have taken.

Chapter 7 presents the Spatial Laser Speckle Imaging device. It describes Spatial Speckle Contrast algorithm , the additional set-up and all the measurements we have taken.

Chapter 8 is the Conclution and the possible future work of our implementation.

# Chapter 2

# Theoretical Background

## 2.1  Nature of Light

About the **Nature of Light** there are two theories have been recognized

### 2.1.1  Particle Theory

First theory is the **Particle Theory (Isaac Newton)**, which is presented to explain the phenomena that were observed concerning light.

According to particle theory, light is a particle with mass, treveling at very high speeds. Light particle can bounce off shiny materials producing reflected beams. For light sources it was believed that they actually generated large quantities of these light particles.

But, many phenomena of light could not be explained by this particle theory such as refraction of light when it passes through optically transparent materials.

### 2.1.2  Wave Theory

The **Wave Theory (C. Huygens)** relates that light is a wave traveling with characteristics similar to those of water waves. But not all phenomena of light can be explained using this theory as well.

### 2.1.3 Dual Nature of Light

Nowadays it is believed that light has two natures. Light travels in small packets of momentu, like particle of mass. The energy contained in each particle $E_p$ is related to the frequency $f$ of light equation. The factor h is known as the Planck constant

$E_p = hf$

Thus light is wave energy traveling with some of the characteristics of a moving particle. The total energy transmitted as light is the sum of th energies of all individual photons emitted. When light travels away from a source then its acts similar to the waves that move across a quiet pond after a small stone is dropped into the water. The waves from a pattern of concentric circles that gets progressively larger as they travel away from the source.

The concept of light wave traveling away from a point source (candle) can be explained by figure 2.1.
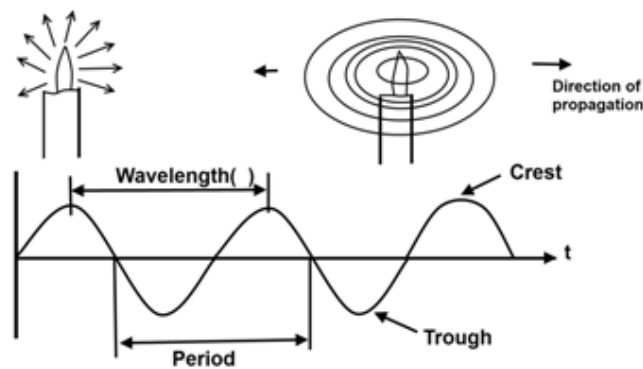


**Figure 2.1:** *Point Source*

### 2.1.4 Characteristics of Light Waves

This light wave defines some very important characerics that are:

- **Ampitude:** The light from the center line to the peak in either the positive or negative direction is called **Amplitude** of the wave. In other words amplitude is the strength of light or the amplitude is related to the strength or intensity of light. The greater the amplitude the greater will be the intensity of the wave. The amplitude of wave is usually measured in units of volts per meter.

- **Frequency:** The number of oscillations or cycles per second is referred to as **Frequency** of the light denoted by $f$. The unit of frequency is Hertz(Hz). The portion of the electro-magnetic spectrum (which light belongs) depends on the frequency or rate at which the light oscillates.

- **Period:** The amount of time required for the one complete oscillation or cycle of the specific light wave is called period of the wave, denoted by $T$. The unit used for period of the wave is second.

  Relationship between Period and Frequency is that: $T = \dfrac{1}{f}$

- **Wave length:** The distance that light travels during the one period of the light wave is called its wave length, denoted by $\lambda$.

### 2.1.5   Diffraction

When light passes throught a narrow opening then it tends to spread out and bends in different directions. The 'spread light as it passes through a narrow opening or along the edge of the barrier is called **Diffraction**.

By figure 2.2 the diffraction can be shown as:
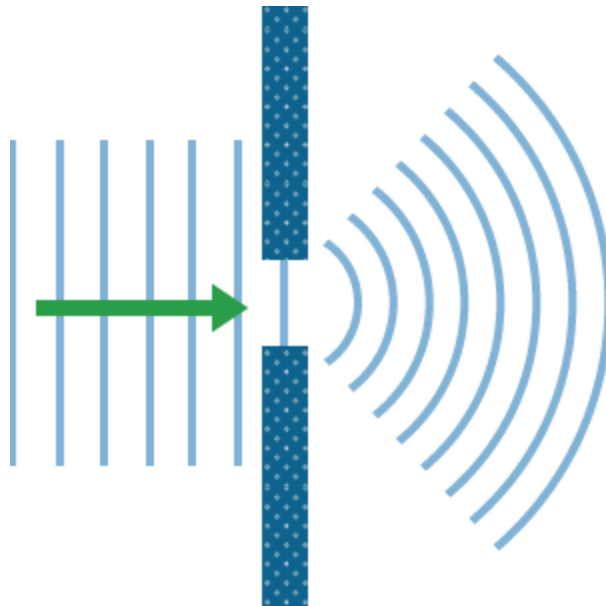


**Figure 2.2:** *Diffraction*

### 2.1.6 Interference

When two or more waves meet at the same place and time and their amplitudes add/subtract to each other, it is called **Interference**. Interference can be either constuctive or destructive.When two waves come close to one another, their effects add together. If the crests, or highest parts of the waves, line up perfectly, the the crest of the combined wave will be the sum of the heights of the two original crests. Likewise, if the lowest parts of the waves (the troughs) line up just right, then the combined trough will be the depth of the two original troughs combined. This is known as **Constructive Interference** as shown in figure 2.3, in which two waves (of the same wavelength) interact in such a way that they are aligned, leading to a new wave that is bigger than the original wave.
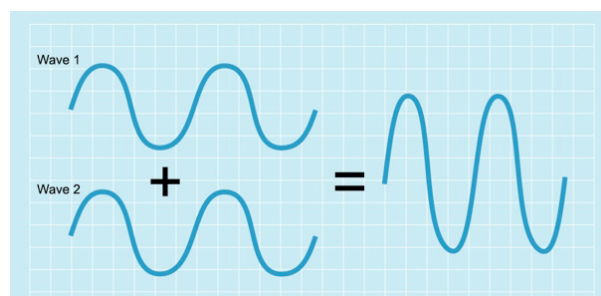


**Figure 2.3:** *Constructive Interference*

However, if two waves are not perfectly aligned, then when the crest of one wave comes along, it will be dragged down by the trough of the other wave. The resulting, combined wave will have crests that are shorter than the crests of either original wave, and troughs that are shallower than either of the incoming waves. This is known as **Destructive Interference** as shown in figure 2.4
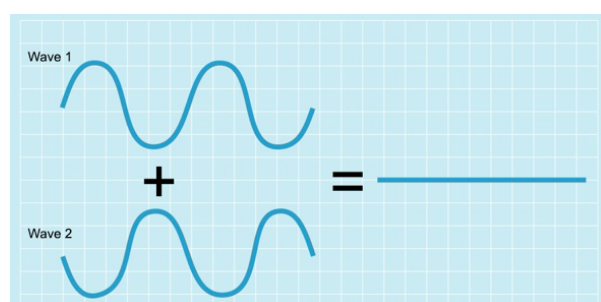


**Figure 2.4:** *Destructive Interference*

### 2.1.7 Young's Double Slit Experiment

The T. Young's double slit experiment is a classical experiment that demonstrate the interference of light waves.

In his experiment Young used a single light source with a small aperture to allow the light to exit and highly filtered light to minimize the number of wavelengths emitted.

The filtered light was then used to illuminate two narrow slights which were placed together. The waves of light heaving the slits spread out and over lapped, causing constructive and destructive interference. Young observed the bright and dark regions on sensitive phorographic film.

Experimental setup can be shown in figure2.5
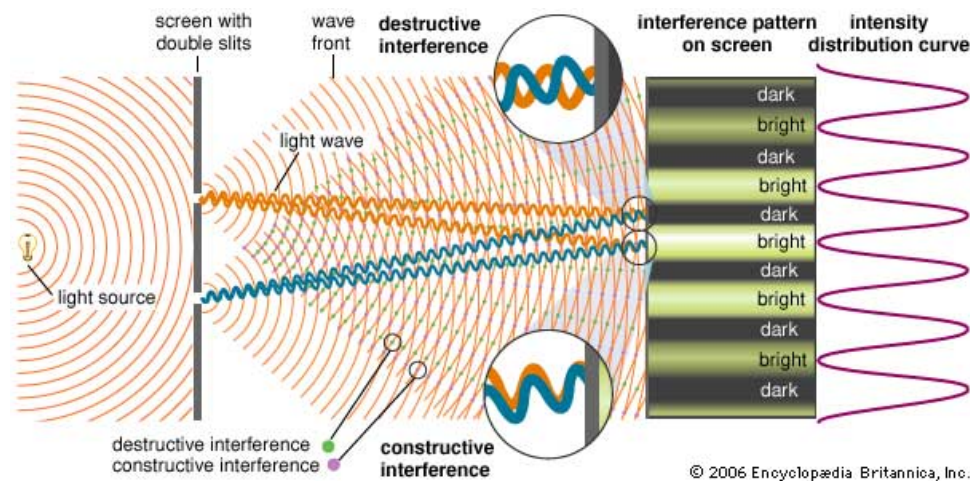


**Figure 2.5:** *Young's Double Slit Experiment*

### 2.1.8 Electromagnetic Spectrum

The **electromagnetic spectrum** is the range of frequencies of electromagnetic radiation and their respective wavelengths. From the **Spectrum** (figure 2.6) it is clear that color is actually depends on wave length and human eyes respond to a narrow range of wave lengths.

The entire electromagnetic spectrum includes waves lengths from 1pm to more than 100km. Waves that are longer than visible light include radio waves, television waves, micro waves and infrared waves. On the other hand waves shorter than visible light are ultraviolet light, x rays, gamma rays.
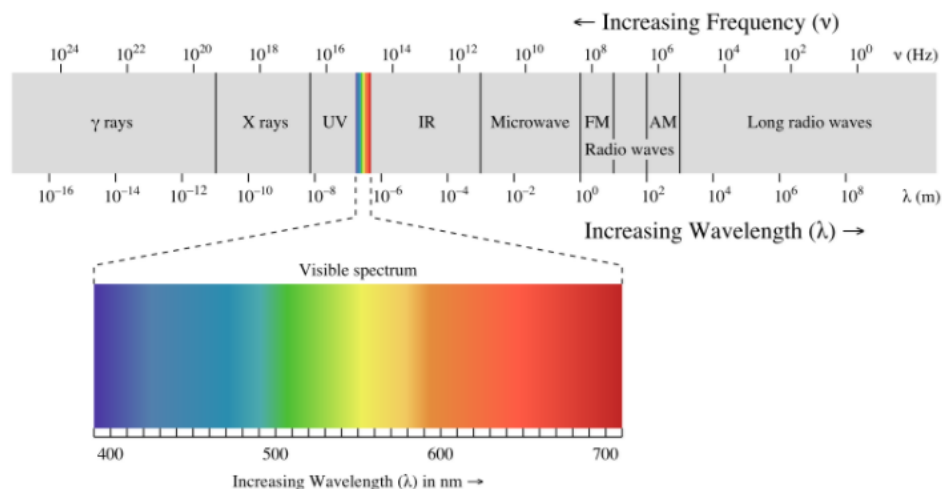
**Figure 2.6:** *Electromagnetic Spectrum*

## 2.2 Laser as a Light Source

A **Laser**(figure 2.7) is a device that emits light through a process of optical amplification based on the stimulated emission of electromagnetic radiation. The term **Laser** originated as an acronym for **Light Amplification by Stimulated Emission of Radiation**. Lasers differ from other sources of light because they emit light coherently. Its spatial coherence allows a laser to be focused to a tight spot, and this enables applications like laser cutting and laser lithography. Its spatial coherence also keeps a laser beam collimated over long distances, and this enables laser pointers to work. Lasers also have high temporal coherence which allows them to have a very narrow spectrum, i.e., they only emit a single color of light. Their temporal coherence also allows them to emit pulses of light that only last a femtosecond. The gain medium of the laser could be solid, liquid, gas, plasma and the spectrum extends, depending on the gain medium, from the infrared to the ultraviolet range.



**Figure 2.7:** *Laser pointers*

### 2.2.1 Principles of laser operation

Laser is photon amplifier combined with a positive optical-feedback mechanism. Positive optical-feedback, which is necessary for lasing, is achieved by two mechanisms:

- One mechanism is consisting of a pair of mirrors between which there is the gain medium that produces the laser. Thus, the radiation leaving the gain medium returns many times to it. So we have a laser **oscillator**.

- The other mechanism is the principle of **stimulated emission**, which says that the probability of photon emission depends on the number of existing photons.

#### 2.2.1.1 Absorption and Emission

Consider an atomic system that consists of two electronic energy states, a lower level state (possibly the ground state)(1) and an excited state (2), with energies $E_1$ and $E_2$ respectively. Assume the atom is in lower level state with energy $E_1$. The electrons of this atom could be excited to state (2), with energy $E_2$ which is much higher than $E_1$, if the atom interacts with radiation with energy density $J$ and frequency $v$, such that the product $hv$ equals the energy difference between the two levels, ie $hv = E_2 - E_1$. This mechanism called **absorption**. The transition from the excited state (2) to the lower level state (1), with the simultaneous emission of a photon with frequency $v$, where $hv = E_2 - E_1$, called **emission**. In a state of thermodynamic equilibrium the rate of excitation is equal to the rate of decay. The decay can be done either automatically after a residence time 10 in the excited state or under the influence of another photon. The first case is called **spontaneous decay**, while the second case is called **stimulated decay** (figure 2.8).
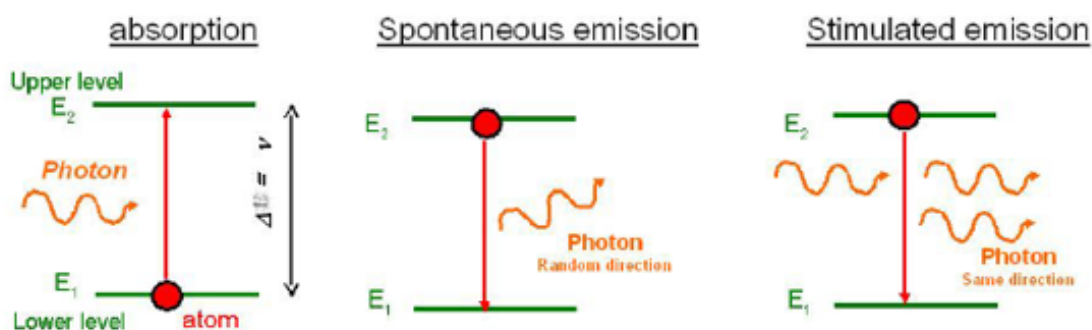


**Figure 2.8:** *Spontaneous vs Stimulated Emission*

### 2.2.1.2    Population Inversion

A **population inversion** occurs when a system (such as a group of atoms or molecules) exists in a state with more population in an excited state than in lower energy states. We know that the rate of stimulated excitation (optical pumping) is equal to the rate of stimulated decay. We also know that there is an additional mechanism of excitation (and even more likely than the above): the spontaneous decay. This means that in a two level system the decay probability is always greater than the probability of excitation and therefore is not possible to produce laser with the use of such material.
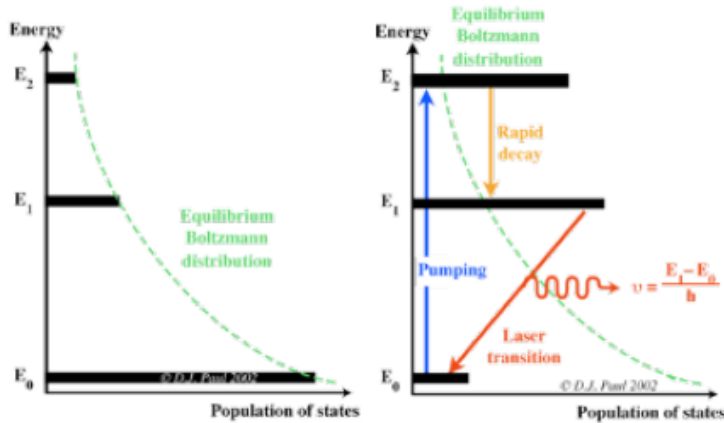


*Figure 2.9:* *Population of States*

A transition from one energy level $En$ to another $Em$ is permissible when not violating the principles of **Energy Conservation, Momentum, Angular Momentum, Spin and Parity**. When a switch is closed for violating one of the above quantities, the transition probability tends to zero, so the characteristic time of transition theory tends to infinity. The average time an atom remains in this state before decay is quite large. The levels in this capacity are called metastable. For comparison for transitions where not violated the above principles those atoms decay very quickly-within $10^{-15}s$, while in the metastable levels atoms remain for a time longer than $10^{-7}s$. The presence of metastable state systems in three levels or more are necessary to produce laser because the decay is very slow and thus population inversion is achieved.

### 2.2.1.3    Gain Medium and Cavity

To preserve the Laser emission should provide positive optical-feedback so that operates as an optical oscillator. The most common type of laser uses feedback from an optical cavity—a pair of mirrors on either end of the gain medium. Light bounces back and forth between the mirrors, passing through the gain medium and being amplified each time. Typically one of the two mirrors, the output coupler, is partially transparent. Some of the light escapes through this

mirror. Depending on the design of the cavity (whether the mirrors are flat or curved), the light coming out of the laser may spread out or form a narrow beam. This type of device is sometimes called a **laser oscillator**(figure 2.10) in analogy to electronic oscillators, in which an electronic amplifier receives electrical feedback that causes it to produce a signal.
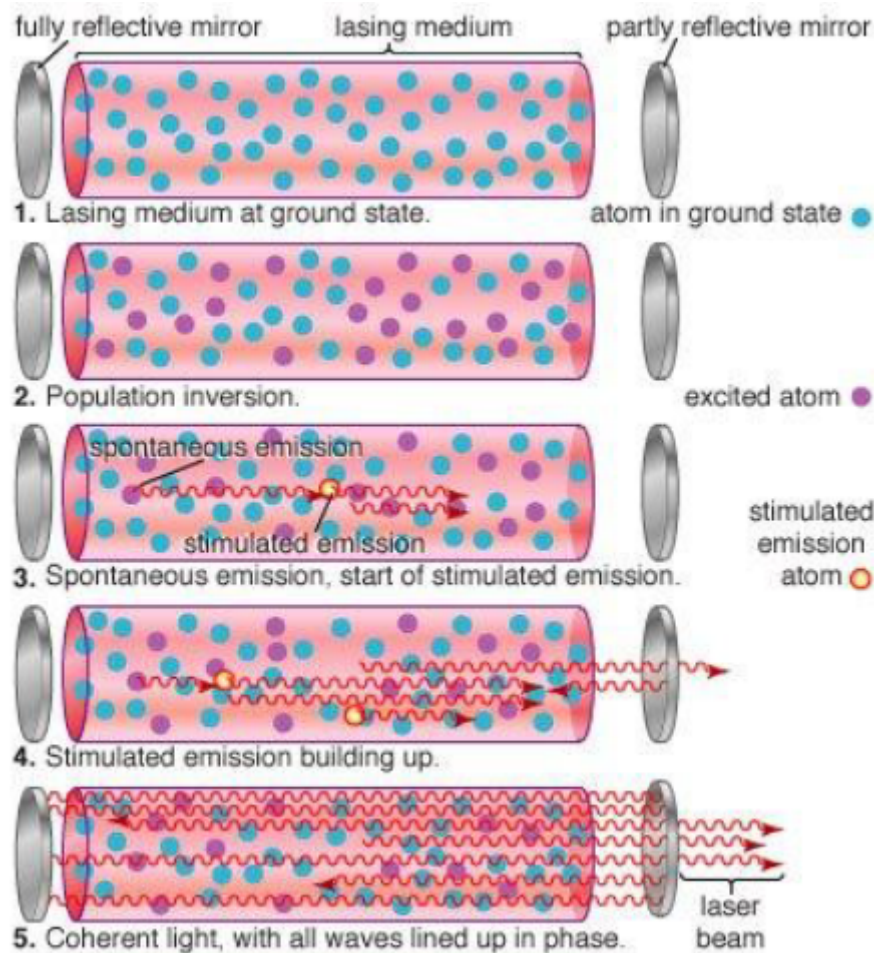


**Figure 2.10:** *Laser Oscillator*

The two parallel mirrors of the cavity forming a resonance cavity around the area of the gain. Only a limited number of wavelengths can exist in such a cavity. This is because the total path ($2L$) traveled by the photon must be an integer multiple of the wavelength of ($p\lambda$) to be supportive contribution. All other wavelengths are disappearing due to destructive contribution. The frequency difference between the permitted modes of oscillation is determined by the length of the cavity. As the length of cavity shortens the greater the difference in frequency and wavelength. Permitted modes refer to these wavelengths are maintained and enhanced in the cavity.

### 2.2.2 Laser Characteristics

Laser light has four unique characteristics that differentiate it from ordinary light:

- **Coherence**

  It is known that visible light is emitted when excited electrons (electrons in higher energy level) jumped into the lower energy level (ground state). The process of electrons moving from higher energy level to lower energy level or lower energy level to higher energy level is called electron transition.

  In ordinary light sources (lamp, sodium lamp and torch light), the electron transition occurs naturally. In other words, electron transition in ordinary light sources is random in time. The photons emitted from ordinary light sources have different energies, frequencies, wavelengths, or colors. Hence, the light waves of ordinary light sources have many wavelengths. Therefore, photons emitted by an ordinary light source are out of phase.(figure 2.11a )

  In laser, the electron transition occurs artificially. In other words, in laser, electron transition occurs in specific time. All the photons emitted in laser have the same energy, frequency, or wavelength. Hence, the light waves of laser light have single wavelength or color. Therefore, the wavelengths of the laser light are in phase in space and time. In laser, a technique called **stimulated emission**2.2.1.1 is used to produce light.(figure2.11b)



*(a)* Incoherent Light            *(b)* Coherent Light
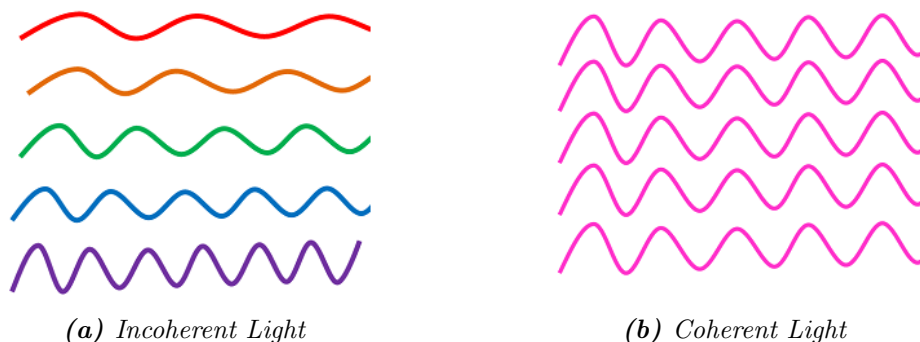
**Figure 2.11:** *Incoherent vs Coherent Light Waves*
(figure)

  Thus, light generated by laser is highly coherent. Because of this coherence, a large amount of power can be concentrated in a narrow space.

- **Directionality**

  In conventional light sources (lamp, sodium lamp and torchlight), photons will travel in random direction. Therefore, these light sources emit light in all directions.

  On the other hand, in laser, all photons will travel in same direction. Therefore, laser emits light only in one direction. This is called **directionality of laser light**. The width

of a laser beam is extremely narrow. Hence, a laser beam can travel to long distances without spreading.



**(a)** *Incoherent Light*      **(b)** *Coherent Light*
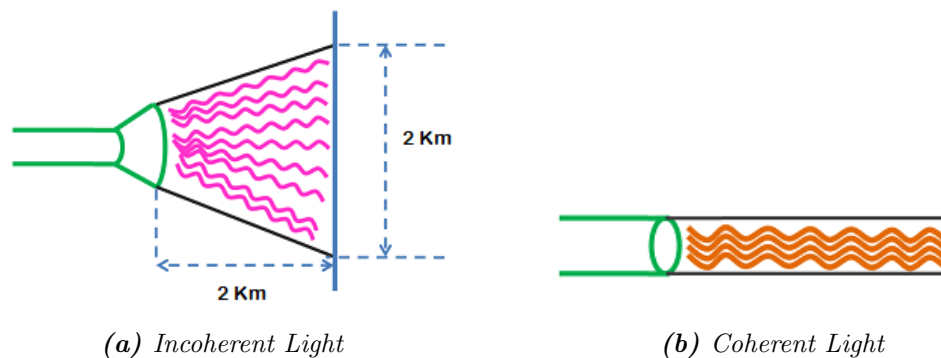
***Figure 2.12:*** *Incoherent vs Coherent Light Waves*
(figure)

If an ordinary light travels a distance of 2 km, it spreads to about 2 km in diameter(figure2.12a). On the other hand, if a laser light travels a distance of 2 km, it spreads to a diameter less than 2 cm (figure2.12b).

- **Monochromatic** light means a light containing a single color or wavelength. The photons emitted from ordinary light sources have different energies, frequencies, wavelengths, or colors. Hence, the light waves of ordinary light sources have many wavelengths or colors. Therefore, ordinary light is a mixture of waves having different frequencies or wavelengths. On the other hand, in laser, all the emitted photons have the same energy, frequency, or wavelength. Hence, the light waves of laser have single wavelength or color. Therefore, laser light covers a very narrow range of frequencies or wavelengths.

- **High Intensity**
  We know that the intensity of a wave is the energy per unit time flowing through a unit normal area. In an ordinary light source, the light spreads out uniformly in all directions.

  If we look at a 100 Watt lamp filament from a distance of $30cm$, the power entering your eye is less than $\dfrac{1}{1000}$ of a watt.

  In laser, the light spreads in small region of space and in a small wavelength range. Hence, laser light has greater intensity when compared to the ordinary light.

  If we look directly along the beam from a laser **(caution: It will cause serious damage)**, then all the power in the laser would enter our eye. Thus, even a 1 Watt laser would appear many thousand times more intense than 100 Watt ordinary lamp.

# Chapter 3

# Laser Interferometry

**Interferometry** is a family of techniques in which waves, usually electromagnetic waves, are superimposed causing the phenomenon of **interference**2.1.6 in order to extract information[8]. Interferometry is an important investigative technique in the fields of astronomy, fiber optics, engineering metrology, optical metrology, oceanography, seismology, spectroscopy (and its applications to chemistry), quantum mechanics, nuclear and particle physics, plasma physics, remote sensing, biomolecular interactions, surface profiling, microfluidics, mechanical stress/strain measurement, velocimetry, and optometry.[9]

## 3.1   Basic Principles

**Interferometry** makes use of the principle of superposition to combine waves in a way that will cause the result of their combination to have some meaningful property that is diagnostic of the original state of the waves. This works because when two waves with the same frequency combine, the resulting intensity pattern is determined by the phase difference between the two waves. Waves that are in phase will undergo constructive interference while waves that are out of phase will undergo destructive interference. Waves which are not completely in phase nor completely out of phase will have an intermediate intensity pattern, which can be used to determine their relative phase difference.

By using two light beams (usually by splitting one beam into two), an interference pattern can be formed when these two beams superpose. Because the wavelength of the visible light is very short, small changes in the differences in the optical paths (distance travelled) between the two beams can be detected (as these differences will produce noticeable changes in the interference pattern). Hence, the optical interferometry has been a valuable measurement technique for more than a hundred years. Its accuracy has been improved with the invention of **Lasers**.

## 3.2 Interferometers

An **Interferometer** is an optical device which utilizes the effect of interference2.1.6. Typically, it starts with some input beam, splits it into two separate beams with some kind of beam splitter (a partially transmissive mirror), possibly exposes some of these beams to some external influences (e.g. some length changes or refractive index changes in a transparent medium), and recombines the beams on another beam splitter. The power or the spatial shape of the resulting beam can then be used e.g. for a measurement.

### 3.2.1 Michelson Interferometer

The **Michelson Interferometer** is a common configuration for optical interferometry and was invented by *Albert Abraham Michelson*. Using a beamsplitter (figure 3.1), a light source is split into two arms. Each of those light beams is reflected back toward the beamsplitter which then combines their amplitudes using the superposition principle. The resulting interference pattern that is not directed back toward the source is typically directed to some type of photoelectric detector or camera. For different applications of the interferometer, the two light paths can be with different lengths or incorporate optical elements or even materials under test.
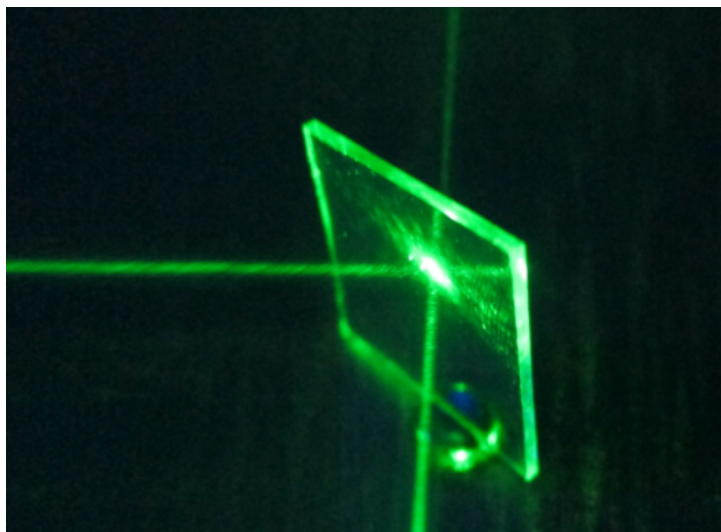


**Figure 3.1:** *Beam Splitter*

The **Michelson interferometer** (among other interferometer configurations) is employed in many scientific experiments and became well known for its use by *Albert Michelson* and *Edward Morley* in the famous *Michelson-Morley experiment* (1887)[10] in a configuration which would have detected the earth's motion through the supposed luminiferous aether that most physicists at the time believed was the medium in which light waves propagated. The null result of that

experiment essentially disproved the existence of such an aether, leading eventually to the *special theory of relativity*[28] and the revolution in physics at the beginning of the twentieth century. In 2016, another application of the Michelson interferometer, *LIGO* [29], made the first direct detection of gravitational waves[11]. That observation confirmed an important prediction of general relativity, validating the theory's prediction of space-time distortion in the context of large scale cosmic events (known as strong field tests).
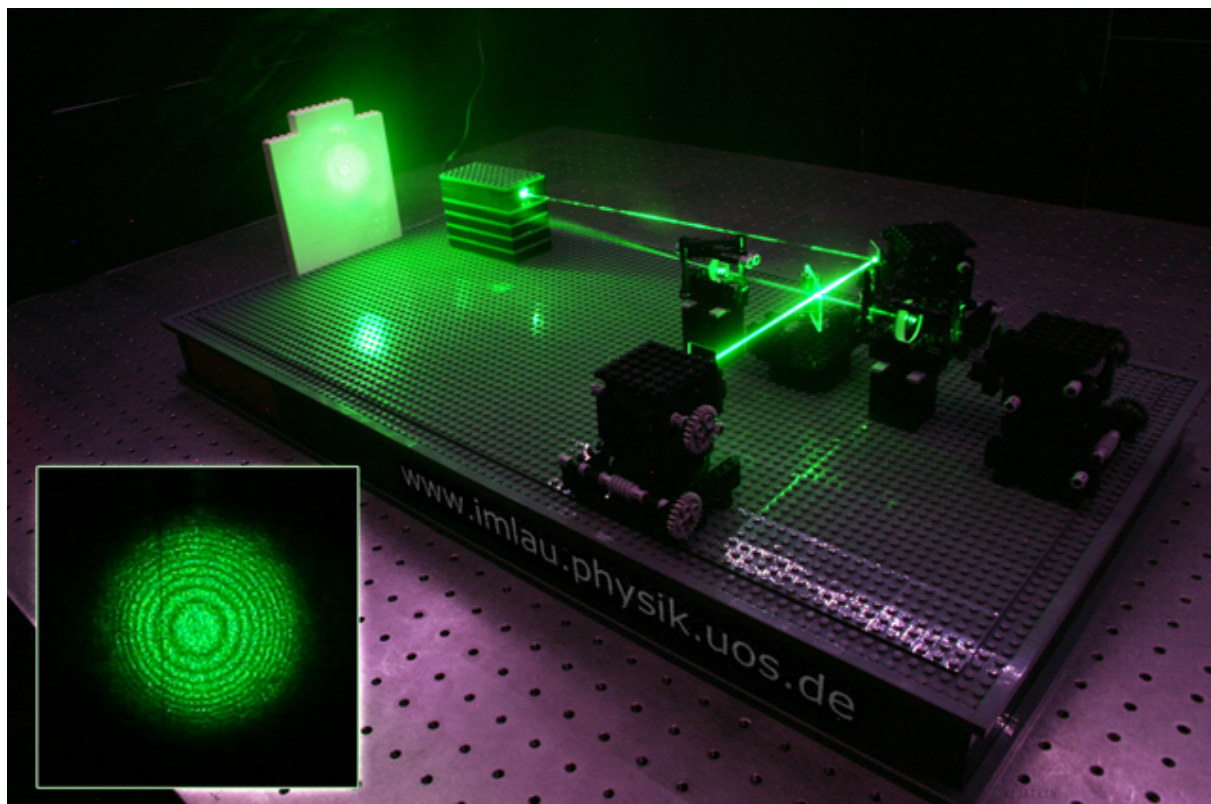


**Figure 3.2:** *Michelson Interferometer*

### 3.2.1.1 Configuration

A **Michelson Interferometer** consists minimally of mirrors M1 and M2 and a beam splitter M. In figure 3.3, a source S emits light that hits the beam splitter (in this case, a plate beamsplitter) surface M at point C. M is partially reflective, so part of the light is transmitted through to point B while some is reflected in the direction of A. Both beams recombine at point C' to produce an interference pattern incident on the detector at point E (or on the retina of a person's eye)(figure 3.4).
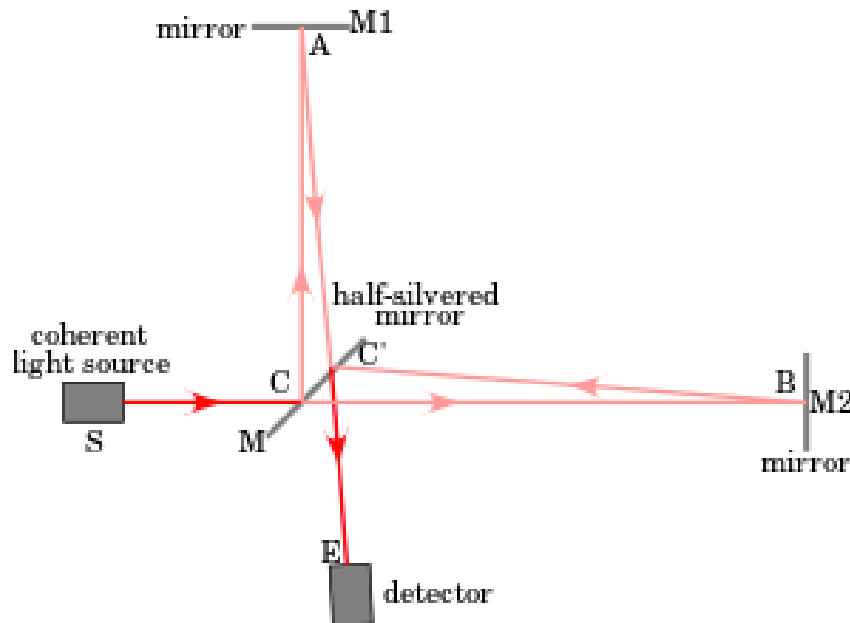


*Figure 3.3: Michelson Interferometer (graphic)*
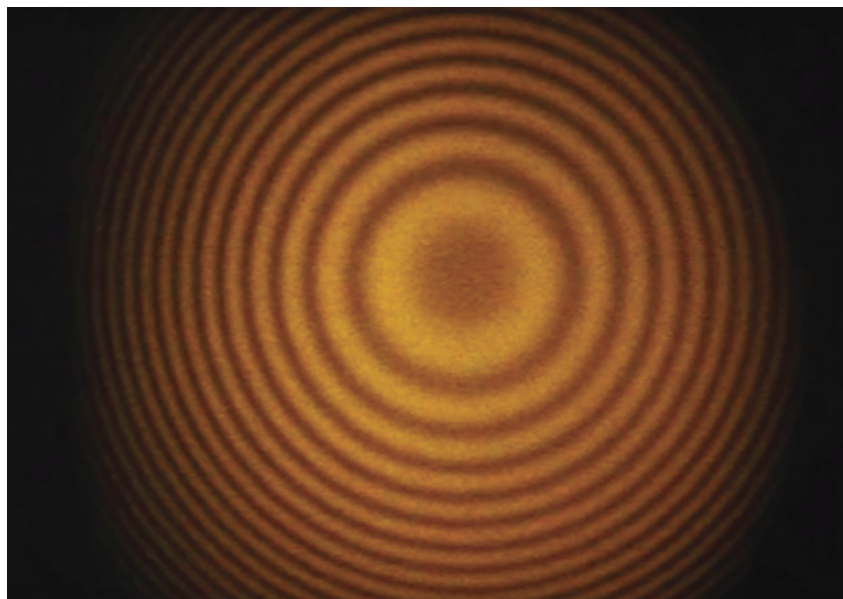


*Figure 3.4: Fringe pattern formed by the Michelson interferometer*

### 3.2.2 Mach-Zehnder Interferometer

The **MachZehnder Interferometer** was developed by the physicists *Ludwig Mach* and *Ludwig Zehnder*. As shown in Figure 3.5, it uses two separate beam splitters(BS) 3.1 to split and recombine the beams, and has two outputs, which can be sent to photodetectors. The optical path lengths in the two arms may be nearly identical (as in the figure), or may be different. The distribution of *optical powers* [30] at the two outputs depends on the precise difference in optical arm lengths and on the wavelength (or optical frequency).

If the interferometer is well aligned, the path length difference can be adjusted (e.g. by slightly moving one of the mirrors) so that for a particular optical frequency the total power goes into one of the outputs. For misaligned beams (e.g. with one mirror being slightly tilted), there will be some fringe patterns in both outputs, and variations of the path length difference affect mainly the shapes of these interference patterns, whereas the distribution of total powers on the outputs may not change very much.
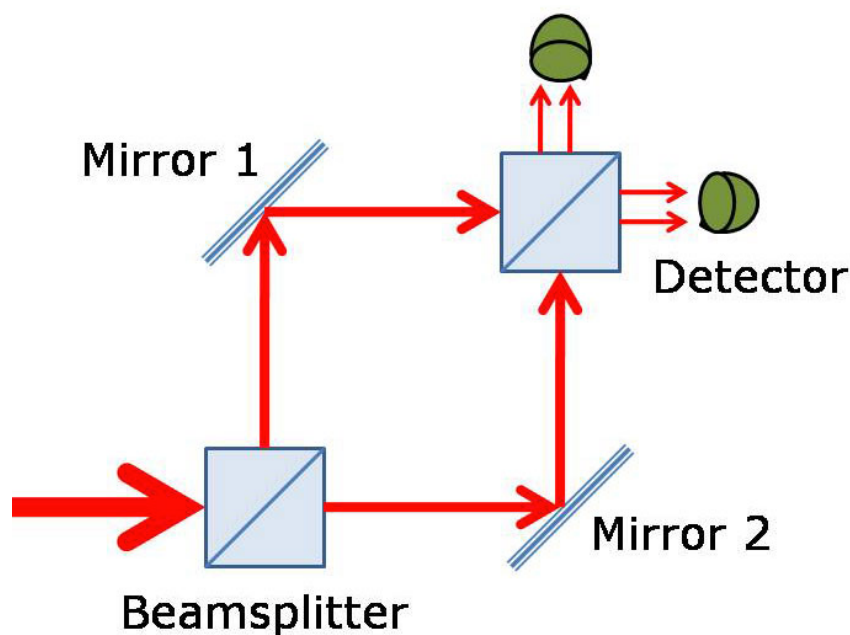


**Figure 3.5:** *Mach-Zehnder Interferometer*

### 3.2.3 Fabry-Perot Interferometer

A **FabryPerot Interferometer** (Figure 3.6) consists of two parallel mirrors, allowing for multiple round trips of light. (A monolithic version of this can be a glass plate with reflective coatings on both sides.) For high mirror reflectivities, such a device can have very sharp resonances (a high finesse), i.e. exhibit a high transmission only for optical frequencies which closely match certain values. Based on these sharp features, distances (or changes of distances) can be measured with a resolution far better than the wavelength. Similarly, resonance frequencies can be defined very precisely.
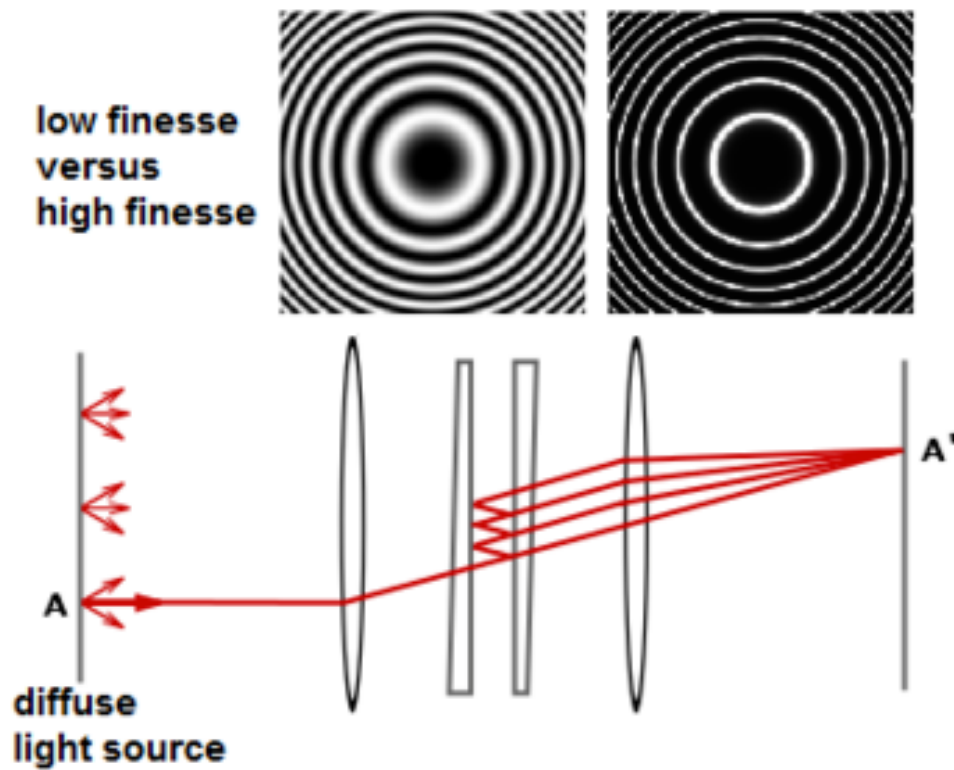


**Figure 3.6:** *Fabry-Perot Interferometer*

### 3.2.4 Sagnac Interferometer

A **Sagnac Interferometer** (named after the French physicist *Georges Sagnac*) uses counterpropagating beams in a ring path, realized e.g. with multiple mirrors (as in Figure 3.7) or with an optical fiber. If the whole interferometer is rotated e.g. around an axis which is perpendicular to the drawing plane, this introduces a relative phase shift of the counterpropagating beams (Sagnac effect). The sensitivity for rotations depends on the area covered by the ring, multiplied by the number of round trips (which can be large e.g. when using many turns in an optical fiber). It is possible e.g. to obtain a sensitivity which is sufficient for measuring the rotation of the Earth around its axis.
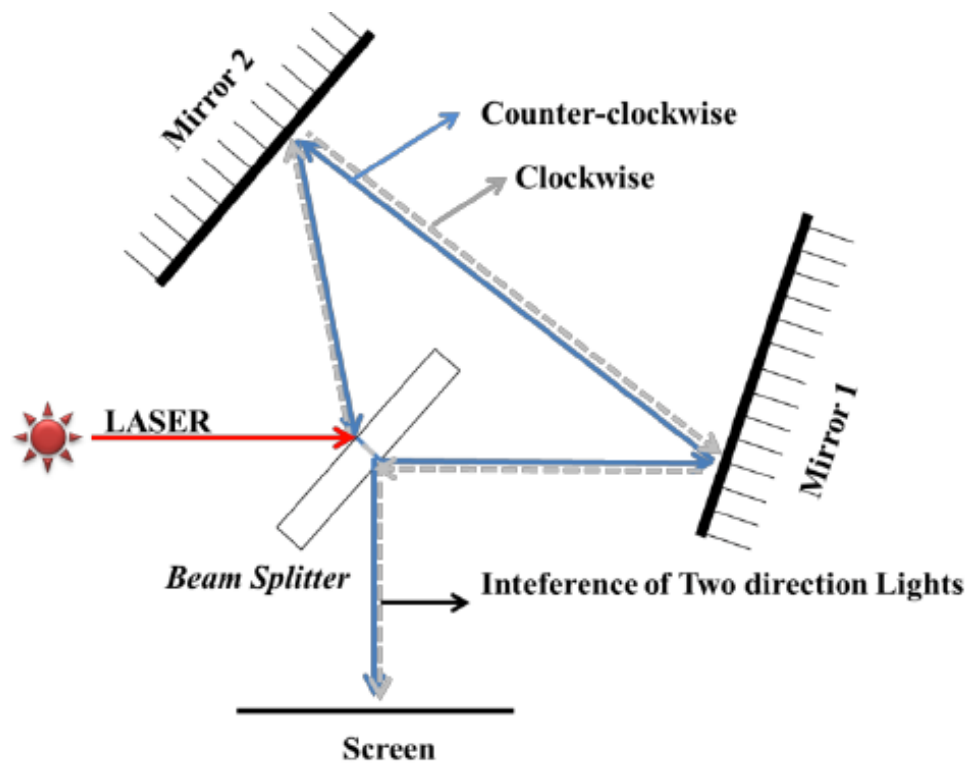


**Figure 3.7:** *Sagnac Interferometer*

Sagnac interferometers are used e.g. in inertial guidance systems.

### 3.2.5 Common-Path Interferometers

Some interferometers use a common beam path but different polarizations for the two beams. This has the advantage that fluctuations of the geometric path length do not affect the interferometer output, whereas the interferometer can be a sensitive detector for birefringence.

## 3.3 Digital Speckle Pattern Interferometry

### 3.3.1 Speckle Pattern

A **Speckle Pattern** (figure 3.8) is an intensity pattern produced by the mutual interference of a set of wavefronts[12]. This phenomenon has been investigated by scientists since the time of Newton, but speckles have come into prominence since the invention of the laser and have now found a variety of applications. The term speckle pattern is also commonly used in the experimental mechanics community to describe the pattern of physical speckles on a surface[13],[14] which is useful for measuring displacement fields via digital image correlation. Speckle patterns typically occur in diffuse reflections of monochromatic light such as laser light. Such reflections may occur on materials such as paper, white paint, rough surfaces, or in media with a large number of scattering particles in space, such as airborne dust or in cloudy liquids.
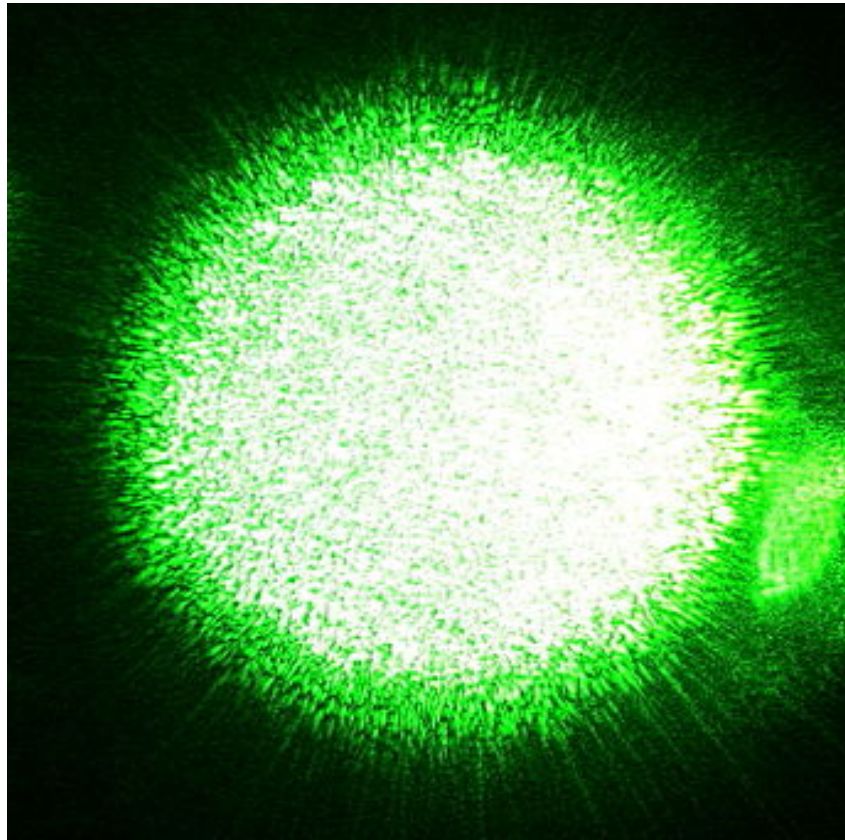


***Figure 3.8:*** *Speckle Pattern*

### 3.3.2 Digital Image Correlation

**Digital Image Correlation (DIC)** is the simplest interferometric method which can be adopted to the analysis of surface damage [15]-[16]-[19] .

The diagram of the optical setup is shown in figure 3.9.The surface investigated is illuminated by a laser beam and the scattered light is recorded by digital camera. A narrow band interferometric filter is placed in front of the camera. This filter blocks all wavelengths different from the waveleght which is the output of our laser light, allowing the instrument to be used in the ambient light. During the measurement, the camera is recording a speckle image —a granular pattern of bright and dark spots —which results from mutual *interference* of the reflected laser light. When a deformation of the same order as the wavelength of the laser appears on the surface investigated, a change in the speckle pattern occurs. The change can be visualized by digital subtraction of the acquired and stored images.

For example: If The surface is heated with a flow of warm air for a few seconds an increase of the surface temperature by approximately $2 - 3^oC$ is sufficient for producing high contrast images. Immediately after heating, a speckle pattern on the surface investigated is recorded as a reference image, then the consecutive images are subtracted arithmetically using the computer and the difference is displayed on the monitor. Local inhomogeneities or structural faults of the surface undergo cooling at different rates, which leads to local out-of-plane displacements visible as bright areas. In this way, features of the painted surface such as delaminated areas of a paint layer or cracks can be detected.
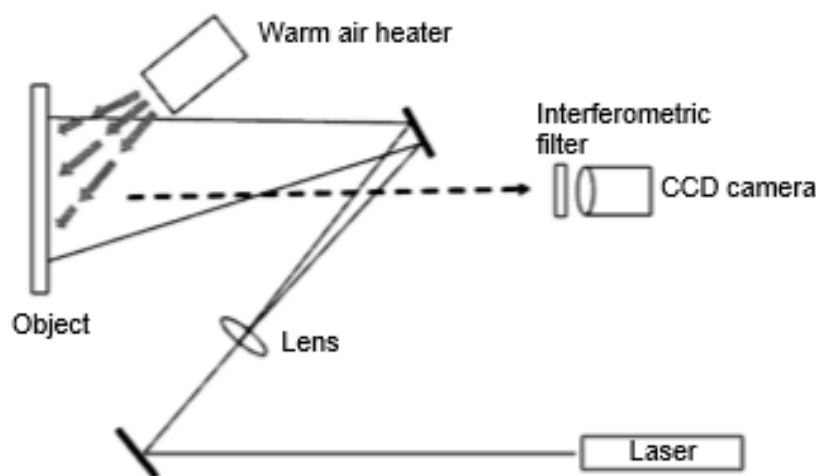


**Figure 3.9:** *Digital Image Correlation setup with warm air heater*

In fact, **Digital Image Correlation** provides quantitative information on the number of cracks in the surface layer and their length. Consequently, a precise comparison between preservation

states of the object before and after any potentially dangerous event, or just at different points in time, is possible. It should be stressed that damage of the design layer is detected at an early stage long before the object needs any conservation treatment. Therefore, this very simple diagnosing technique can be used in preventive conservation as an early-warning system.

DIC is an attractive technique as it is easy to apply, the interpretation of the results is simple, and a useful visualization of damage is obtained. However, as will be shown below, DIC is less sensitive than the full **DSPI**3.3.3 in providing more quantitative characteristics of the damage.

### 3.3.3 Digital Speckle Pattern Interferometry for thermally-induced surface deformation

The diagram of the optical setup is shown in figure 3.10.The instrument was developed from the DIC system by dividing the laser beam into two beams, called object and reference beams, using a *beam splitter*(figure 3.1). The object beam illuminates (as before) the surface investigated while the reference beam passes through magnifying lenses and a ground glass and is merged with the beam reflected from the object using a beam-splitter cube. The object and reference beams superimpose coherently producing an interferogram recorded by a camera.
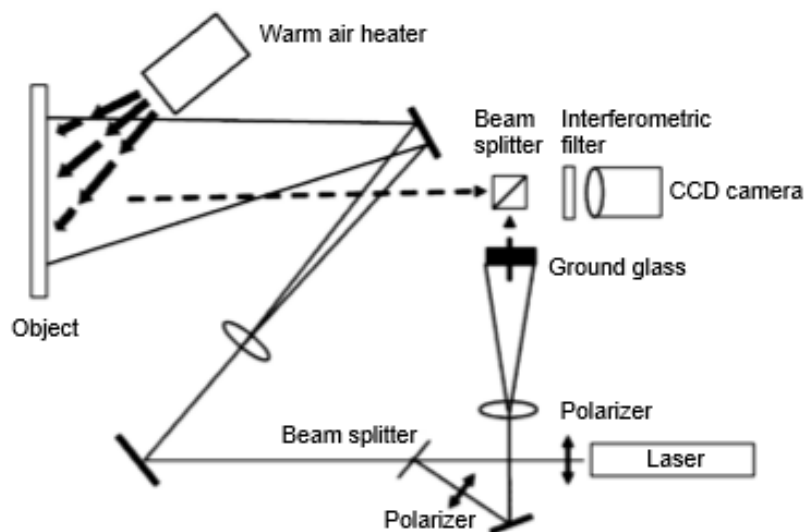


**Figure 3.10:** *Digital Speckle Pattern Interforometry setup with warm air heater*

By using a ground glass in the reference beam path the speckled reference beam is obtained but information about the surface contained in the interferogram is unchanged[18]. Typically, the **DSPI** systems combining the object and reference beams require a specific lens system which ensures that the reference beam appears to the detector as if it originated at the centre of the exit pupil of the imaging optical system. Using ground glass in the reference beam path has two

advantages at the cost of some reduction of image quality. Firstly, it avoids a complicated and expensive lens system for the reference beam. Secondly, the reference beam does not need to be realigned when the distance from the object, or size of the analyzed area, is changed, which is very convenient for an operator. Realigning the instrument, while recording data, is very simple, as it is carried out by focusing imaging optics and choosing the intensity of the reference beam by rotating one of the linear polarizers in the reference beam path. Polarizers are used only for adjusting proper ratio between object and reference beams and can be substituted by a neutral density filter, if required.

As in the case of DIC, the recorded interferograms contain information about the surface shape so one can analyse inhomogeneities of the surface by subtracting consecutive image during the cooling process. The intensity of the light in the plane of interferogram is given by:

$$I_{01}(r) = I_o + I_r + 2\sqrt{I_o I_r} \cos\left[\varepsilon(x, y)\right]$$

where x and y define the position of a pixel in the plane of the interferogram, $I_o$ and $I_r$ are intensities of the object and reference beams, respectively, $\varepsilon$ is a random phase difference between the object and reference beams at point $(x, y)$.

The movement of the surface (caused by the cooling process) creates an additional phase $\Delta\varepsilon(x, y)$ in the recorded interferogram:

$$I_{02}(r) = I_i + I_r + 2\sqrt{I_i I_r} \cos\left[\varepsilon(x, y) + \Delta\varepsilon(x, y)\right]$$

Therefore, subtraction of the interferograms $I_{01} I_{02}$ leads to the image with dark for $\Delta\varepsilon = 2n\pi$ and bright for $\Delta\varepsilon = (2n + 1)\pi$ fringes. Fringes become clustered and distorted around local surface deformations and may be used as a guide to the identification of any heterogeneities in the under examination layer.



*(a) DIC image*          *(b) DSPI image*
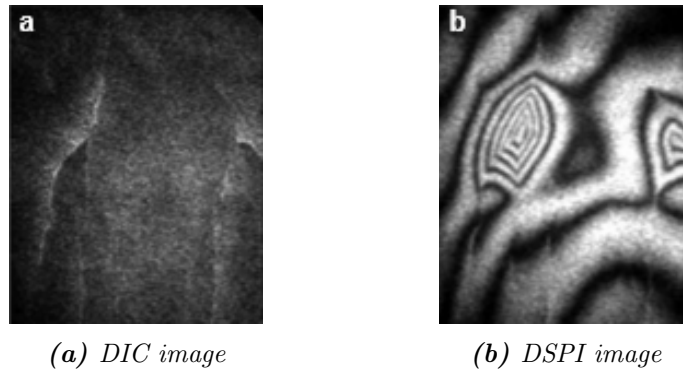
*Figure 3.11:* *(a) Tracing damage on the same surface with DIC and (b) with the thermally-induced DSPI*

### 3.3.4 Digital Speckle Pattern Interferometry for sound-induced surface deformation

The diagram of the optical setup is shown in figure 3.12. There are two differences in comparison to the Digital Speckle Pattern Interferometry for thermal-induced surface deformation system (figure3.10). The heater is replaced by a loudspeaker which emits sound waves inducing vibration of detached fragments of the under examination layer, and a phase shifter is placed in the object beam path.
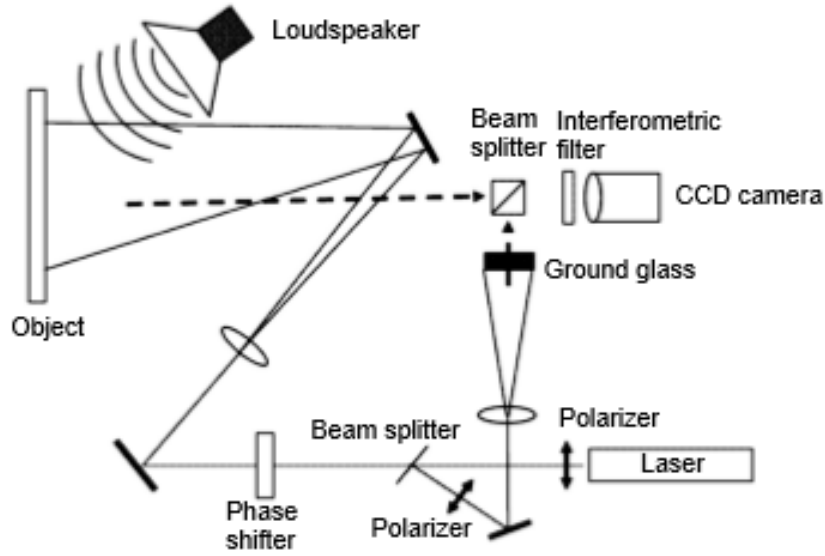


**Figure 3.12:** *Digital Speckle Pattern Interforometry setup with loudspeaker*

The measurement consists in analysing a sound-induced vibration of the surface investigated. A signal with controlled frequency and amplitude is generated and the soundwave can induce vibrations of delaminated parts of a design layer when the generated wave is close enough to the resonant frequency. Generally, for an object vibrating with frequency $\omega$ , the intensity of light in the plane of the interferogram is given by:

$$I(x,y) = I_i + I_r + 2\sqrt{I_i I_r} \cos\left[\varepsilon(x,y) + \Delta\varepsilon(x,y,\omega)\right]$$

The symbols used in this equation have the same meaning as in the previous equations. But in case of the induced vibration of the surface, an additional phase shift $\Delta\varepsilon$ resulting from the vibration of the object appears as an argument of the *cos* function. For the object beam perpendicular to the illuminated surface:

$$\Delta\varepsilon(x,y,\omega) = \frac{4\pi\delta z(x,y)}{\lambda} cos(\omega t)$$

where $\lambda$ is a wavelength of the laser light and $\delta z$ is an out-of-plane displacement of the surface. Note that $\Delta\varepsilon = 0$ for a still object. When the time of measurement is much longer than the vibration period, the intensity of light in the plane of the interferogram can be represented as [20] :

$$I(x,y) = I_o + I_r + 2\sqrt{I_o I_r}\cos\left[\varepsilon(x,y)\right]J_o\left(\frac{4\pi}{\lambda}\delta z(x,y)\right)$$

where $J_0$ represents the zero-order Bessel function of the first kind and $\delta z$ is twice the vibration amplitude. The final image is obtained by the subtraction of interferograms for the still and vibrating object and is given by [18]:

$$I(x,y) = 2\sqrt{I_o I_r}\cos\left[\varepsilon(x,y)\right]\left[1 - J_o\left(\frac{4\pi}{\lambda}\delta z(x,y)\right)\right]$$

This equation provides information on the amplitude of the object vibration, but the information is still relative because the intensity of light as well as the initial random phase $\varepsilon(x,y)$ are unknown. It is assumed that the intensity of light is constant during the time of the measurement and that its value is irrelevant for the final result of the analysis.



*Figure 3.13: Photograph of the Digital Speckle Pattern Interforometry setup with loudspeaker*
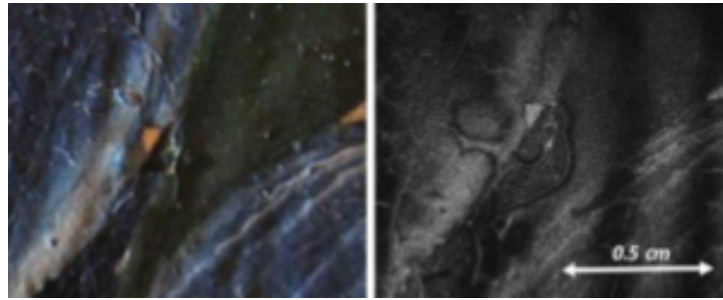
**Figure 3.14:** *Fringe pattern showing an area of thick paint.*
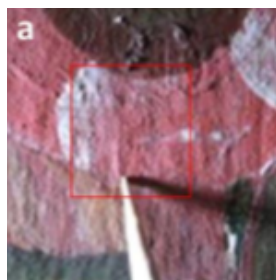


**(a)** *Photograph of the investigated area*
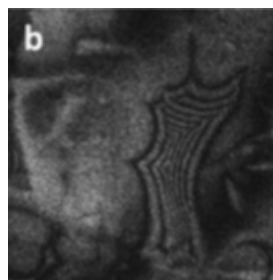
**(b)** *A contour of the detachment revealed by a cluster of distorted fringes*
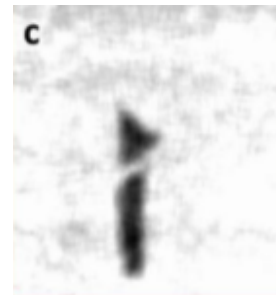
**(c)** *The analysis of sound-induced vibration of the surface*

**Figure 3.15:** *A detachment of the paint layer*
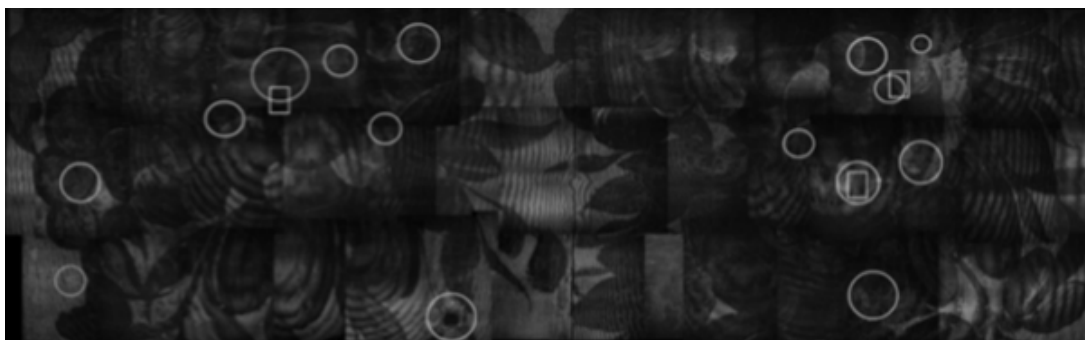


**Figure 3.16:** *Irregular or problematic areas on a painting as detected by DSPI, marked by rectangles and ovals, respectively*

# Chapter 4

# Laser Speckle Imaging

## 4.1 Principles of Speckles

When the Laser was invented in the early 1960s , its first users noticed, when the laser light bit on a matt surface such as paper or unpolished metal or glass, a high-contrast grainy pattern. This effect was initially called *granularity*[6] but soon the name *Speckle* became more popular.

When an image is formed of a rough surface which is illuminated by a coherent light such as a *Laser Beam*, a speckle pattern is observed in the image plane. This is called a *subjective speckle pattern*, or simply *image speckle*. It is called subjective because the detailed structure of the speckle pattern depends on the viewing system parameters. For instance, if the size of the lens aperture changes, the size of the speckles also changes. If the position of the imaging system is altered, the pattern will gradually change and will eventually be unrelated to the original speckle pattern.

When laser light which has been scattered off a rough surface falls on another surface, it forms an *objective speckle pattern*. If a photographic plate or another 2-D optical sensor is located within the scattered light field without a lens, a speckle pattern is obtained whose characteristics depend on the geometry of the system and the wavelength of the laser. Objective speckles are usually obtained in the far-field (also called Fraunhofer region) and called *far field speckles*. Speckles can be observed also close to the scattering object, in the near field (also called Fresnel region). This kind of speckles are called *near field Speckles*.
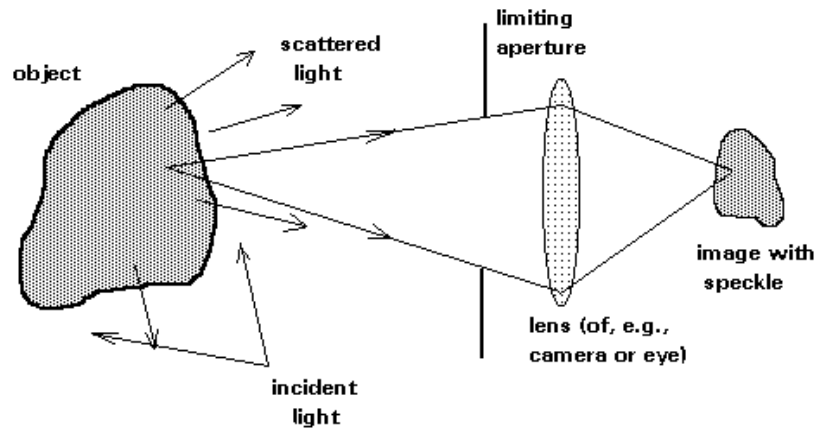
***Figure 4.1:*** *The formation of image speckle*
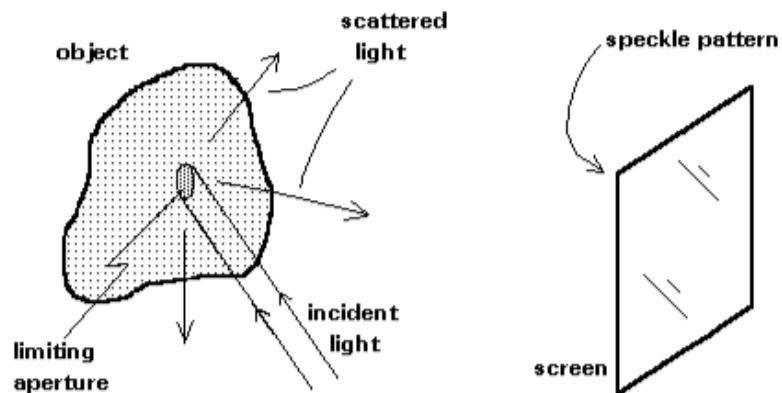


***Figure 4.2:*** *The formation of far-field speckle*

Rigorously, a speckle pattern is a random intensity pattern produced by the mutual interference of a set of wavefronts. In optics, a wavefront is the locus (a line, or, in a wave propagating in 3 dimensions, a surface) of points having the same phase. Thus the phenomenon can be observed with different media such as radio waves, or coherent light as in lasers.

Speckle is often regarded as a nuisance, or noise, and therefore speckle removal techniques or algorithms have been developed for many applications. However,speckle hab been studied and soon began to appear direct applications of the phenomenon.[12]

## 4.2 The speckle Contrast

Assuming ideal conditions for producing a speckle pattern —single-frequency laser light and a perfectly diffusing surface with a Gaussian distribution of surface height fluctuations —it can be shown that the standard deviation of the intensity variations in the speckle pattern is equal to the mean intensity. In practice, speckle patterns often have a standard deviation that is less than the mean intensity, and this is observed as a reduction in the contrast of the speckle pattern. The standard measure of a speckle pattern is known as the contrast K, which is shown below in Equation.

$$K = \frac{\sigma_I}{\langle I \rangle}$$

The contrast is a metric of the variation in the intensity of the speckle pattern and is defined as the ratio of standard deviation, $\sigma_I$, to the mean intensity, $\langle I \rangle$, of the speckle pattern. If the speckle pattern is formed from light scattering off a dynamic medium, the variable of contrast can be utilized to infer information about motion of the dynamic medium .
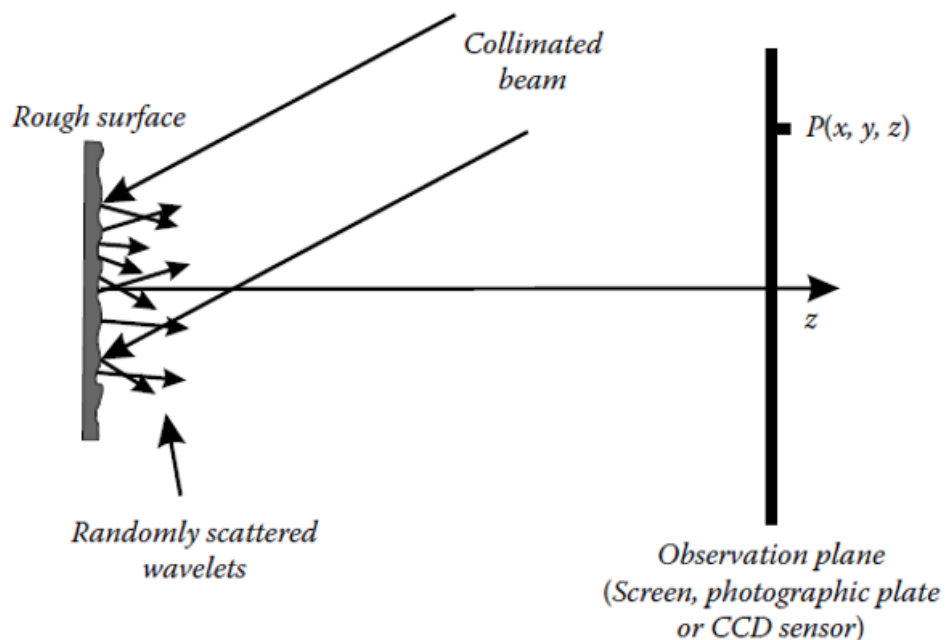


**Figure 4.3:** *The physical origin of speckle pattern: diffuse reflection of coherent light from a rough surface*

## 4.3 Full field technique

Full-field imaging, without scanning, of the area of interest is achieved with **Laser Speckle Imaging (LSI)**. The area is illuminated by a laser beam and a photograph is taken, in its simplest early form, then called single-exposure speckle photography [5]. The speckle would be *freezed* using a very short exposure time and a high-contrast speckle pattern will be resulted. Whereas a long exposure time would allow the speckles to average out, leading to a low contrast. Conversely, using an exposure time that is of the same order as the correlation time of the intensity fluctuations, would lead to high contrast in static parts of the image, but low contrast *blurred* in the moving parts of the image. Then the velocity distribution in the field of view can be mapped as variations in speckle contrast.

## 4.4 Time-varying speckles

When in an object lighted by a laser there is motion, then speckle pattern changes. For small movements of a solid object, the speckles move with the object and they remain associated but for larger motions, they decorrelate and the speckle pattern changes completely.

So if the frequency spectrum of the fluctuations is dependent on the velocity of the motion, it is possible to obtain information about the motion of the scatterers from a study of the temporal statistics of the speckle.

## 4.5 Spatial and Temporal Speckle Contrast

Speckle arises from the random interference of coherent light 4.1. Whenever coherent light interacts with a random scattering medium, a photodetector will receive light that has scattered from varying positions within the medium resulting in constructive and destructive interference, producing a randomly varying intensity pattern known as speckle. If scattering particles are moving, this will cause fluctuations in the interference, which will appear as intensity variations. The temporal and spatial statistics of this speckle pattern provide information about the motion of the scattering particles. The motion can be quantified by measuring and analyzing either the temporal variations or the spatial variations.

### 4.5.1 Spatial Contrast Imaging

Accurate estimation of the speckle contrast from spatial statistics [4]

**Spatial Contrast Imaging** [7], the most common approach, implements a sliding, square structuring element $N_{pixels}$ of $8 \times 8$ or $16 \times 16$ pixels to calculate the local speckle contrast $K$ as the standard deviation of pixel intensities $\sigma_I$ divided by the mean intensity $\langle I \rangle$ within the element boundaries.Clearly a larger value of $N_{pixels}$ will give a more accurate estimate of the speckle contrast, but at the expense of spatial resolution. If the window size is too small, then the large variation in the estimate of the speckle contrast will reduce sensitivity . A survey of the literature [26] indicates that the community has empirically settled on a window size of $8 \times 8$ pixels as a reasonable trade-off between spatial resolution and uncertainty in the estimated speckle contrast, but this all depends on camera resolution, speckle size, and desired contrast resolution. The algorithm of *Spatial Contrast Imaging* requires only one raw speckle image to compute a contrast image, and therefore offers high-temporal resolution at the expense of spatial resolution because of the use of the structuring element.
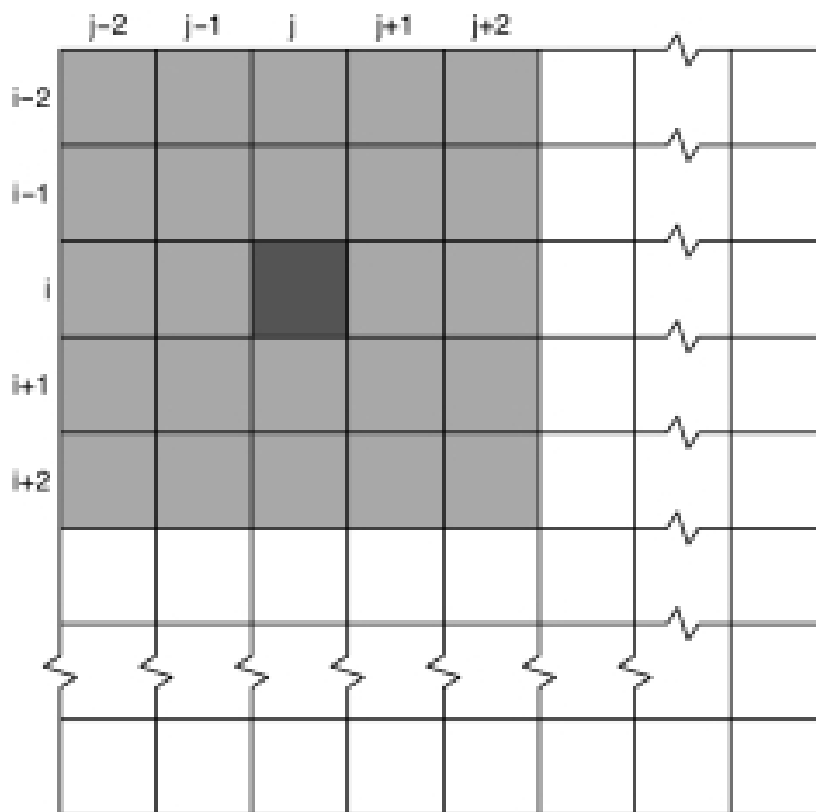


***Figure 4.4:*** *Schematic overview of the way the contrast is calculated in Spatial Contrast Analysis*

### 4.5.2 Temporal Contrast Imaging

In order to circumvent the reduction in spatial resolution[3]a temporal algorithm that calculates a speckle contrast image by computing $K$ for each pixel across a sequence of images developed. This approach requires a minimum of 5 statistically independent images and is associated with better spatial resolution at the expense of temporal resolution and called **Temporal Contrast Imaging**[7]. Recent studies describe results that support the use of the temporal algorithm to analyze raw speckle images and it has been proved that the temporal algorithm is more accurate than the spatial algorithm.
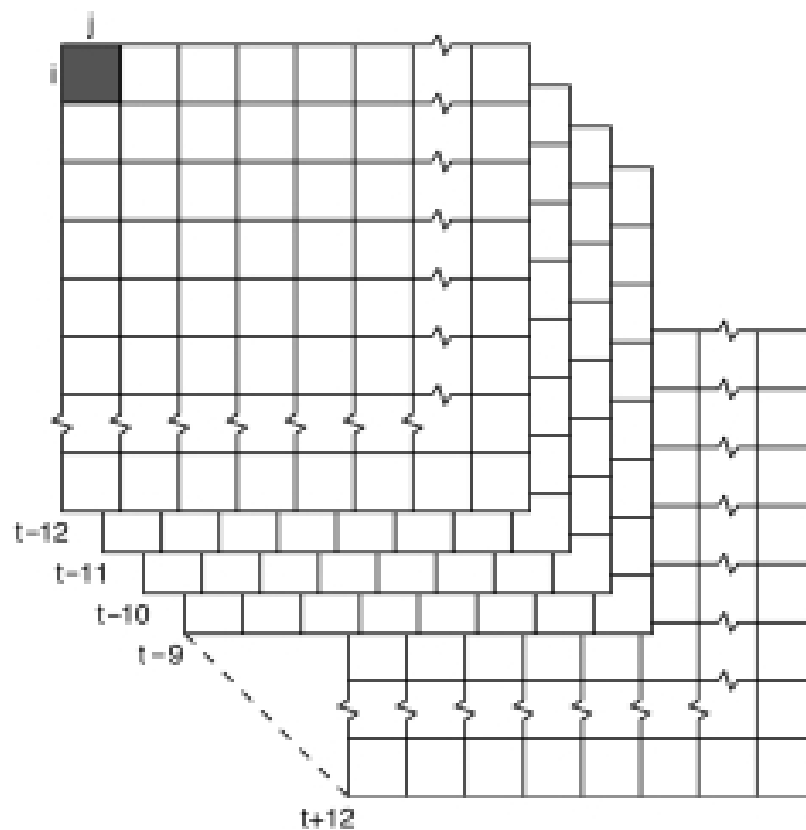


***Figure 4.5:*** *Schematic overview of the way the contrast is calculated in Temporal Contrast Analysis*

### 4.5.3 Spatial vs Temporal Contrast Imaging

**Speckle Contrast** can be estimated from either the spatial statistics or the temporal statistics. The *spatial statistics*[4] offers better temporal resolution but at the expense of spatial resolution because of the requirement to use a sufficiently large window of image pixels in the calculation. If the pixel size is too small relative to the speckle size, then speckle contrast will be underestimated and sensitivity to spatial and temporal variations in speckle contrast will degrade. Ideally, the speckle size is twice as large as a pixel and the contrast is estimated from at least $8 \times 8 = 64$ pixels. The *temporal statistics*[4] on the other hand offer better spatial resolution at the expense of temporal resolution. If temporal samples are statistically independent, i.e., the time between samples is greater than the correlation time, then a minimum of only 5 samples is required to accurately estimate the speckle contrast and have good sensitivity to spatial and temporal variations in speckle contrast. For typical brain applications, the correlation time is approximately 5 ms. Thus, given an image sample every 10 ms, temporal speckle contrast could be estimated every 50 ms with pixel spatial resolution. Compare this with spatial speckle contrast, which can be estimated at the camera frame rate with a resolution of $8 \times 8$ pixels. Note that while this spatial resolution difference is important on the surface of the sample, it is quickly blurred by photon scattering beneath the surface of the tissue.

Spatial and temporal statistics do have important differences when it comes to the treatment of static scattering. Static scattering will produce an additive offset to the spatial speckle contrast. If this is not properly calibrated, then the absolute speckle contrast will overestimated and relative changes in the speckle contrast will underestimated. Static scattering does not produce an additive offset in the temporal speckle contrast, but instead scales the speckle contrast by a factor related to the relative contribution of statically and dynamically scattered photons. While this confounds estimates of the absolute speckle contrast, the scale factor generally cancels when estimating relative changes in speckle contrast.

Computational efficiency has plagued the calculation of speckle contrast, usually requiring much more computational time than data acquisition time, thus preventing real-time visualization. While temporal speckle contrast is generally less computationally expensive than spatial speckle contrast,[2] it has been recently developed some improved algorithms that enable speckle contrast calculation at rates that exceed image acquisition rates so that the acquisition time is now the limiting factor in the temporal resolution[21]. As a result, true real-time calculations of speckle contrast changes are now possible.

## 4.6 Applications

**Laser Speckle Imaging** and related techniques[4] have been used in a large number of blood flow imaging applications in tissues such as the retina, skin, and brain. These tissues are particularly well suited for LSI since the microvasculature of interest is generally superficial. Because of its measurement geometry LSI is unable to sense blood flow in deep tissues. One of the earliest uses of speckle imaging was in the retina, where the vasculature and blood flow of interest is accessible[22]. More recently, LSI has become one of the most widely used methods for *in vivo* imaging of blood flow in the brain, particularly in small animal models of both normal and diseased brain.

Except for blood flow imaging applications, LSI have been used for surface tampering detection [23]. In addition there are some applications in order to detect erosion in all kind of surfaces.

### 4.6.1 Skin Perfusion

Full-field monitoring of skin perfusion was one of the earliest uses of LSI[24]. Initially, skin was a convenient *in vivo* test sample. However, images of skin perfusion are complicated by the fact that the majority of the vasculature is contained beneath a layer of tissue that has few blood vessels. Therefore, it is usually difficult to monitor flow in single vessels in the skin, although LSI is able to quantify overall perfusion in the capillary bed.
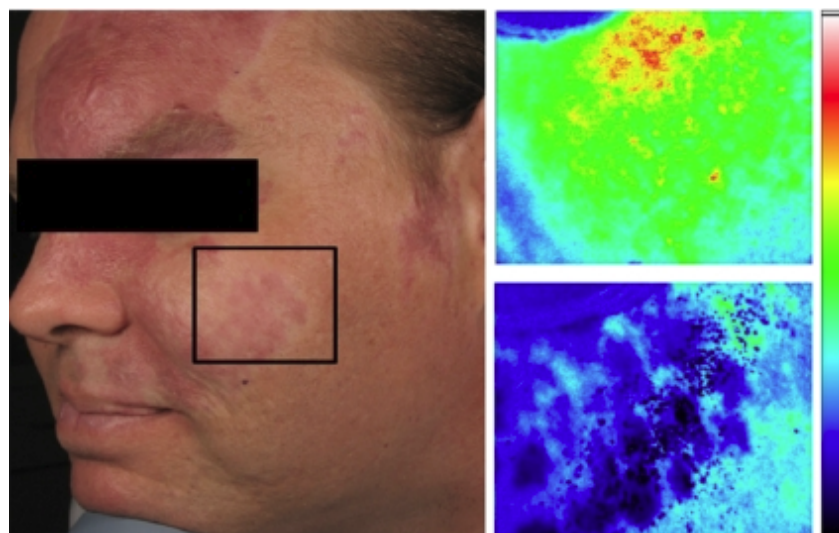


**Figure 4.6:** *Illustration of LSCI for monitoring PWS treatment. Left: Photograph of patient with PWS in the area indicated by the rectangle. LSI images were acquired immediately before (upper) and 15 minutes after (lower) laser therapy.*

### 4.6.2 Retinal Blood Flow

Another application of LSI and related techniques was in visualization and quantification of blood flow in the retina in both animals and humans[4]. Since the retina is accessible and blood flow is an important indicator in a variety of ophthalmology conditions, considerable effort has been invested in developing blood flow imaging methods for the eye. Speckle-based imaging of retinal blood flow has been performed with diode lasers as well as argon ion lasers that are coupled into fundus cameras. Applications in the retina have included analysis of the effects of a wide range of pharmacological agents on blood flow as well as analysis of flow around the optic nerve head. Despite the large number of reports of the use of speckle techniques for measuring retinal blood flow, however, very few images of retinal blood flow in humans have been reported. The majority of studies have reported average flow values that are calculated from images without showing any spatial maps of blood flow.
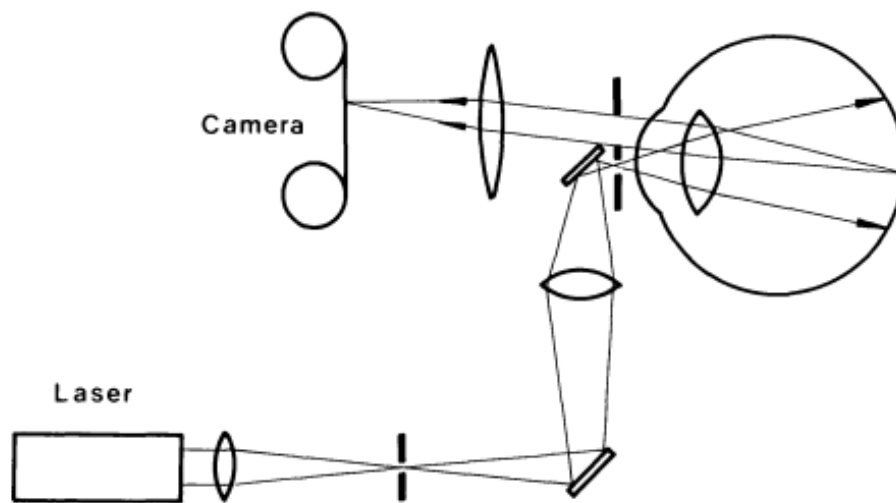


***Figure 4.7:*** *Experimental Laser Speckle Imaging Setup for Retinal Blood Flowmetry*

### 4.6.3 Brain Applications

For most applications in the brain, a portion of the skull is either thinned or removed and saline or mineral oil is placed on the surface to improve image quality by minimizing the effects of static scattering elements. Most applications in the brain involve quantifying the changes in speckle contrast at each pixel as an indication of the relative cerebral blood flow.

An illustration of the ability of LSI to image the spatiotemporal changes in cerebral blood flow (CBF) following functional activation is given in Figure 4.8. A $5 \times 5$-mm area of cortex was imaged in a rat through a thinned skull as the forepaw of the rat was stimulated with electrical pulses. The stimulus was applied for $10s$ with $0.5mA$ and 20 trials were repeated. The speckle contrast images at each time, relative to the stimulus were averaged. Speckle contrast values were converted to speckle correlation decay times ($\tau_c$) at each pixel in all images, and ratios of the inverse of the decay times were used as a measure of the relative changes in CBF.
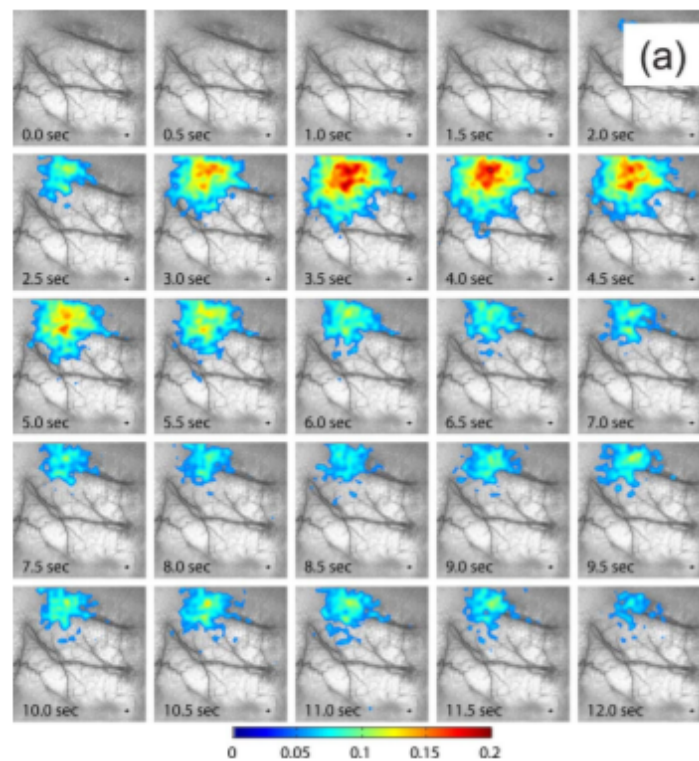


**Figure 4.8:** *Imaging of stimulus induced changes in blood flow in the brain. Sequence of images showing the percent changes in blood flow in response to 10 s of forepaw stimulation*

### 4.6.4 Surface Tampering Detection

Many cases, including law enforcement and security, require detecting whether physical objects have been tampered. Often, the contact is subtle and cannot be detected with the naked eye or by comparing a pair of photographs taken before and after the incident (figure 4.9(d)(e)).A new technique has been proposed[23] to detect surface changes for cases where traditional imaging is insufcient. This technique makes use of the speckle generated by laser illumination and exploits the fact that the precise speckle pattern observed from a given viewpoint depends on the phase of the light wavefront and, therefore, is sensitive to tiny perturbations of the imaged surface (figure 4.9(a-c)). It focuses on the situation where surface tampering is subtle, where only the phase, and not the intensity of the light reaching the camera might be altered. To address this problem, laser speckle imaging is leveraged. A laser speckle image encodes phase information, because speckle4.1 originates from the constructive and destructive interferences of waves reected at different points of the surface. Phase differences come from the variation in travel distance, which is affected by tiny changes in the surface geometry. If the surface prole is altered by an amount as small as the laser wavelength, the speckle pattern is modied .

Figure 4.9 shows: Top left:The prototype setup that combines an SLR with a consumer pico laser projector and an expirement that compare the similarity maps of laser speckle and incoherent illumination photos. Bottom left: The granular pattern, called speckle. (a),(b) Images of a wall illuminated by the laser projector. Between (a) and (b), the wall was touched gently. The speckle similarity map is computed in (c) reveals where the wall was touched. Without the laser projector, the images before and after the incident (d) and (e) reveal no difference, as shown in the similarity map (f).
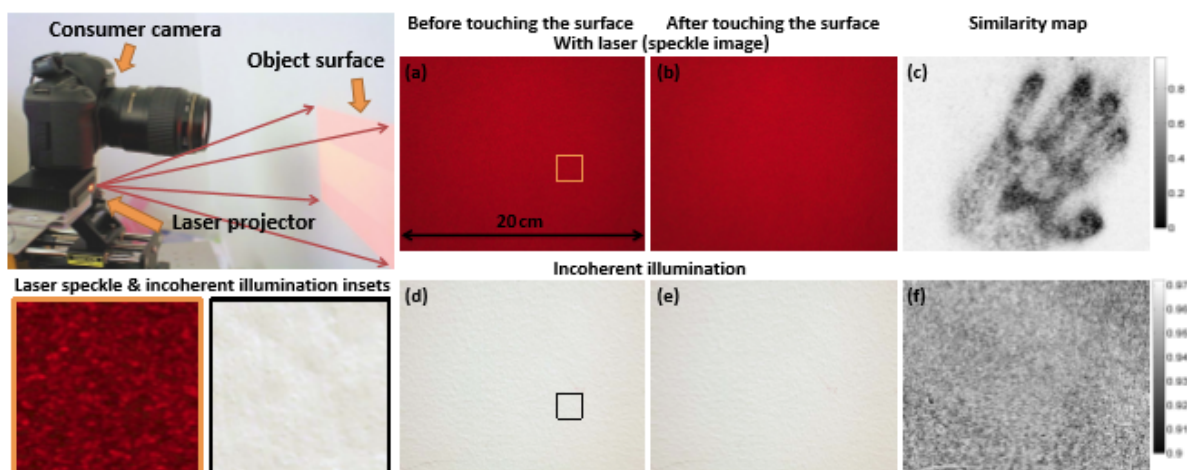


***Figure 4.9:*** *Surface Tampering Detection setup and results*

### 4.6.5 Dental Erosion Detection

Tooth erosion is defined as change in the ultrastructure of the enamel, which is currently assessed only using clinical diagnostics. Erosion is highly prevalent, affecting more than 50% of the population under five years of age and up to 77% of elderly individuals. Tooth wear is a natural process caused by friction during chewing and brushing as well as exposure to acidic foods and beverages. This process becomes pathological when the degree of destruction compromises the function and esthetics of the teeth, with the emergence of sensitivity, which can range from mild discomfort to the impossibility of ingesting certain substances

The ability of **Laser Speckle Imaging** to allow the evaluation of dynamic features in tissues using a non-invasive, non-destructive cost-effective, real-time method has stimulated the academic community to focus their efforts on the study of this method in the time domain (dynamic speckle analysis). However, the analysis of speckle patterns in the spatial domain also contains information on the microstructure and heterogeneities of the surface, which can be explored by applying the proper statistical analysis. So with the LSI it is possible to acquire information on the microstructure of some surfaces and detect minimal changes and furthermore to analyse the structure of enamel[25].

In Figure 4.10 some expirement samples that were placed inside a plastic tube (a). Each sample was imaged under white (b) and laser (c) illumination. (d) presents the speckle contrast imaging in which a false color algorithm was applied to increase the visual contrast. Each raw image was manually trimmed to obtain a $700 \times 700$ pixel image (e) containing the region of interest with a sample of the non-eroded tissue (right) and a sample of eroded tissue (left).
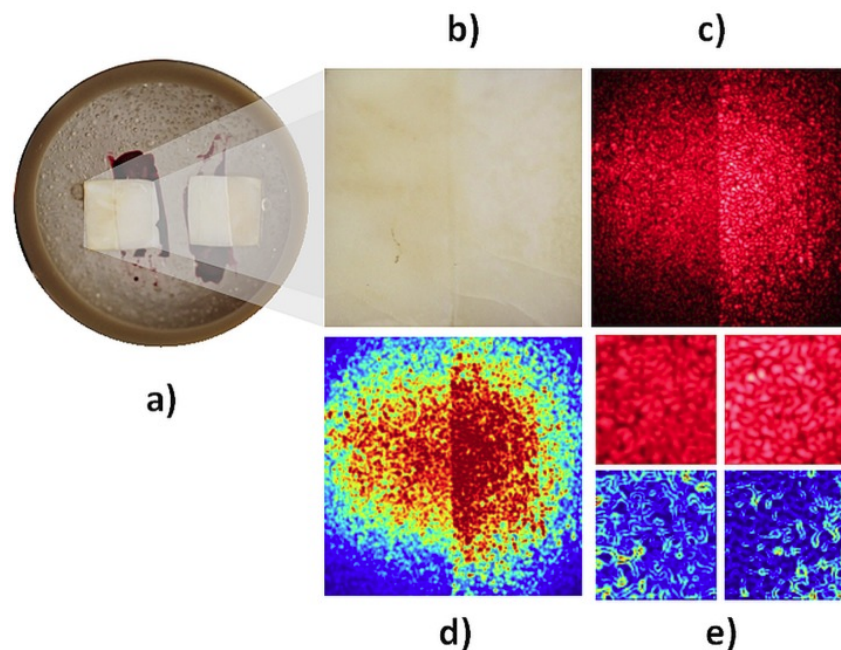


**Figure 4.10:** *Dental Erosion Detection Expirement*

# Chapter 5

# Laser Speckle Imager Setup

In order to built a **Laser Speckle Imager** we needed to design the setup . The LSI experimental procedure consists of a few basic elements which are: a coherent light source, i.e. laser, a light expander, the imaged object and a camera used to capture the images as shown in figure 5.1. Except from these we can use different types of stimulators depending the object we want to study.
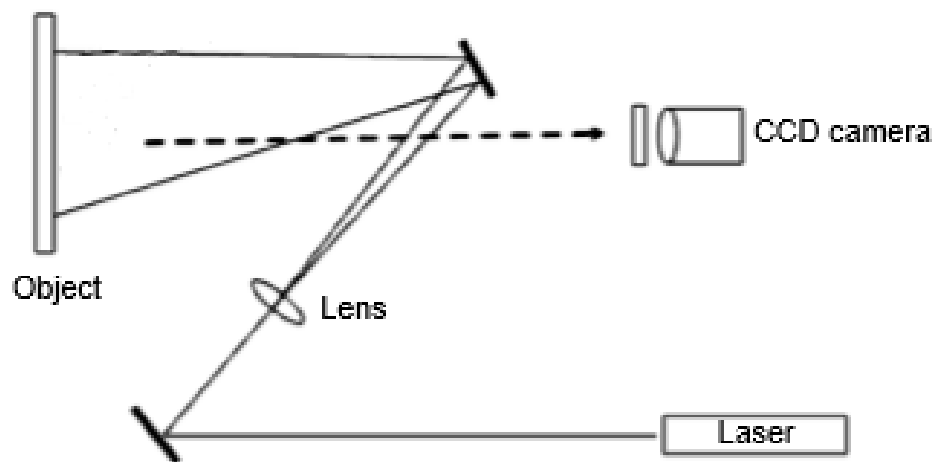


**Figure 5.1:** *Simple LSI Setup*

## 5.1 Camera

The **ZWO ASI178MC** (figure 5.2)is a sensitive and state-of-the-art color astronomy camera with 6.4M resolution and USB 3.0. Built around the Sony IMX178 back-illuminated image sensor, this advanced camera has a resolution of $3096 \times 2080$ with $2.4\mu m$ square pixel size. With 14 bit ADC and extremely low read noise (2.2e - 1.4e), this high-sensitivity camera is ideal for high-resolution astronomical imaging and works well for microscopy imaging as well.

The heart of this color camera is a Type 1/1.8" CMOS sensor with 8.92 mm diagonal. This advanced sensor incorporates Sony's Exmor R technology that enables high-speed processing, low noise, and low power dissipation using column parallel A/D conversion with the back-illuminated sensor. The sensor also incorporates Sony's STARVIS technology features a sensitivity of $2000mV+$ per 1 micron square and allows high image quality in the visible-light. The 14-bit ADC enables high dynamic range and reduced quantization noise and dark random noise. This makes for cleaner image quality in light and dark areas when imaging objects with high contrast. The rolling shutter and fast USB 3.0 interface on the camera allow transfer rates of up to 60 frames per second at full $3096 \times 2080$ resolution. At reduced resolution of $640 \times 480$, download rates up to 253 fps become possible. The camera enables exposure times of $32\mu s$ to $1000s$ (16.7 minutes).

Quantum Efficiency and Read Noise are the most important parameters to measure the performance of a camera. Higher Quantum Efficiency and lower Read Noise are needed to improve the SNR of an image. Read Noise includes pixel diode noise, circuit noise and ADC quantization error noise, and the lower the better. The Read Noise of the ASI178 cameras is extremely lower when compared with traditional CCD cameras. It is even lower when the camera is set at a higher gain. Depending on your target, you can set the Gain lower for higher Dynamic Range (longer exposure) or set the Gain higher for lower noise (such as short exposure or lucky imagig).



**Figure 5.2:** *ZWO ASI178MC*

| Sensor | 1/1.8″ CMOS IMX178 |
|---|---|
| Resolution | 6.4 Mega Pixels 3096×2080 |
| Pixel Size | 7.4mm×5mm |
| Diagonal | 8.92mm |
| Exposure Range | $32\mu s - 1000s$ |
| ROI | Supported |
| ST4 Guider Port | Yes |
| Focus Distance to Sensor | 12.5mm |
| Shutter Type | Rolling Shutter |
| Protect Window | AR window |
| OS Compatibility | Mac, Windows, Linux |
| Interface | USB3.0/USB2.0 |
| Bit Rate | 14bit output (14-bit ADC) |
| Adaptor | 2″/1.25″/M42X0.75 |
| Dimension | $\phi62$mm×36mm |
| Weight | 120g or 4.2 ounces (without lens) |
| Working Temperature | $-5°C - 45°C$ |
| Storage Temperature | $-20°C - 60°C$ |
| Working Relative Humidity | $20\% - 80\%$ |
| Storage Relative Humidity | $20\% - 95\%$ |

**Figure 5.3:** *Camera technical details*
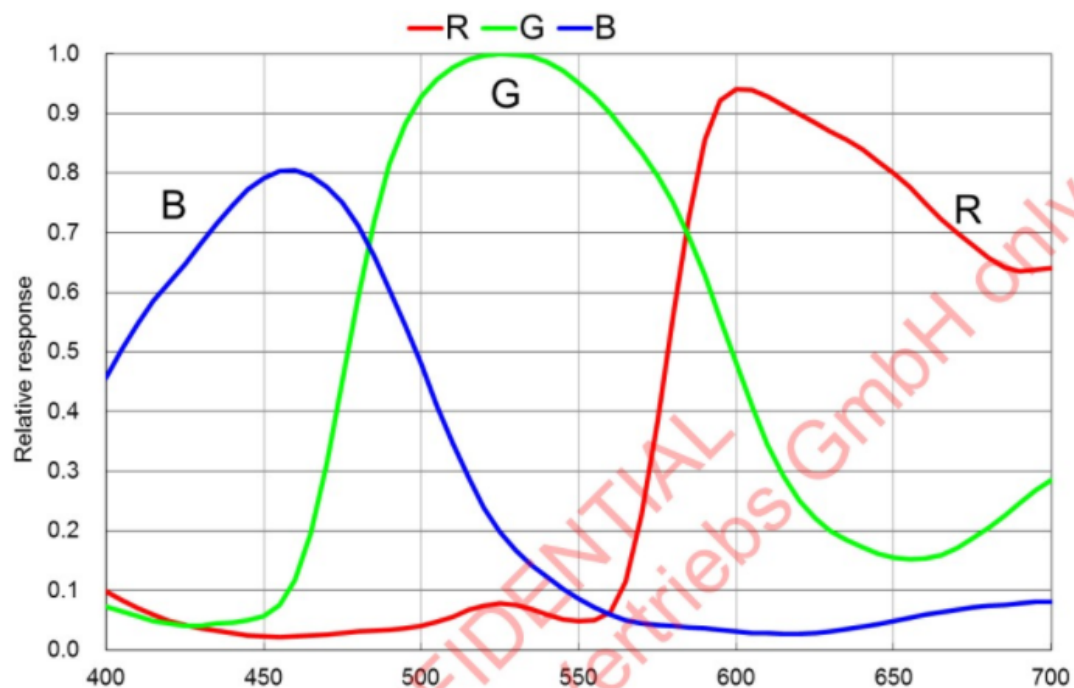


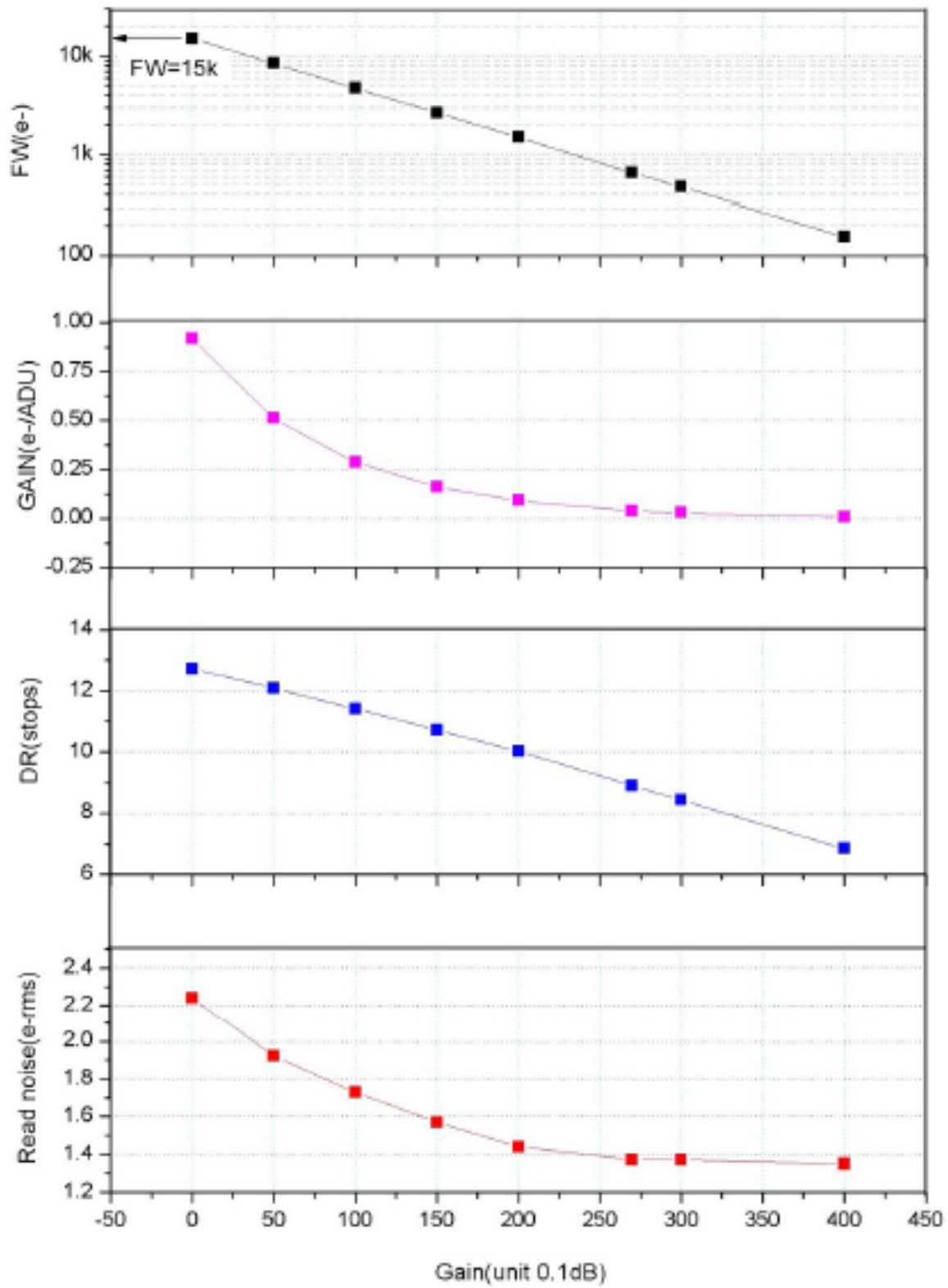**Figure 5.4:** *Relative QE Curve*

**Figure 5.5:** *Read noise, full well, gain and dynamic range for ASI178*

## 5.2 Coherent Light Source

### 5.2.1 LaseRock

**LaseRock** 5.6 is a coherent light source that developed in electronics lab from Christos Rossos during his M.Sc. This source was developed for scientific and medical applications having laser modules with selected emission wavelengths that could be useful for various applications for example exciting as much as possible Alexa Fluor family of fluorescent dyes (Alexa Fluor is a family of fluorescent dyes that used as cell and tissue labels in fluorescence microscopy and cell biology). We, as we have discussed above, need a source of coherent light in order to produce a speckle pattern. So this light source seems perfect for our goal .

The design specifications of our coherent light source are the following:

- Laser module optical power up to 1Watt.

- High efficiency Laser drivers.

- Light multiplexing using a liquid light guide.

- Selected Wavelengths: this design has four available laser wavelengths: 405nm, 450nm, 532nm and 635nm .



**Figure 5.6:** *The Coherent Light Source*

### 5.2.2 Laser Components

There are several types of lasers available like solid-state, gas, dye and diode lasers. The types of lasers that have been used are diode lasers because compared to most laser types, diode lasers are less expensive and more compact making them ideal for small electronic devices. Diode lasers use much less power than most types of lasers. While gas and solid-state lasers require a power supply in kilo-volts, diode lasers typically run on small voltage. Nevertheless, due to continuous development in laser diode technology, laser diodes have been developed that have got high optical power. So, the diode lasers that this source contain are the following:

- **405nm Laser Diode**

  The Sony SLD3237VF continuous wave laser diode is very efficient and has a 200mW optical output power. The diode structural material is the gallium nitride crystal. Also, its guaranteed high-temperature operation up to $85^{o}C$ assures reliability at high temperature operation. Its operating voltage is 5V and operating max current is 260mA. The package of the laser diode is the TO-38 (5.6mm). Its working life is more than 10000 hours.



*Figure 5.7:* *Sony SLD3237VF Laser Diode*

- **450nm Laser Diode**

  The LD-450-1600MG by Roithner is a continuous wave laser diode is very efficient and has a 1600mW optical output power. The diode structural material is the gallium nitride crystal. Also, its guaranteed high-temperature operation up to $70C$ assures reliability at high temperature operation. Its operating voltage is 4.8V and operating max current is 1.5A. The package of the laser diode is the TO-38 (5.6mm). Its working life is more than 10000 hours.

**Figure 5.8:** *Roithner LD-450-1600MG Laser Diode*

- **532nm Laser Diode**

  The HK-E03421 by Laserpointerpro is a continuous wave laser diode and has a 200mW
  optical output power. The diode structural material is YGA. Also, it is guaranteed high-
  temperature operation up to $40^oC$ assures reliability at high temperature operation. Its
  operating voltage is 3V and operating max current is 1A. The package of the laser diode
  is a laser pointer package. The laser pointer disassembled in our lab and only the laser
  diode package left TO-38 (5.6mm). Its working life is more than 10000 hours.



**Figure 5.9:** *Laserpointerpro HK-E03421*

- **635nm Laser Diode**

  The RTL635-150-TO3 by Roithner is a continuous wave laser diode, is very efficient and
  has a 150mW optical output power. The diode structural material is AlGaInP. In contrast
  to the other diode lasers which could operate in high temperatures, RTL635-150-TO3 laser
  diode cannot operate in high temperatures and the diode must have a temperature between
  $10^oC$ and $25^oC$. When operating over the temperature range there is a loss of 20% in
  optical output power. For this reason, we must keep the laser module temperature in the
  operating temperatures that manufacturer suggests. The expected lifetime is the half of
  the laser diode's lifetime and it is expected at 10000 hours but it can be shortened by high
  temperatures. The operating voltage is 2.3V and operating max current is 650mA. The
  package of the laser is TO3.
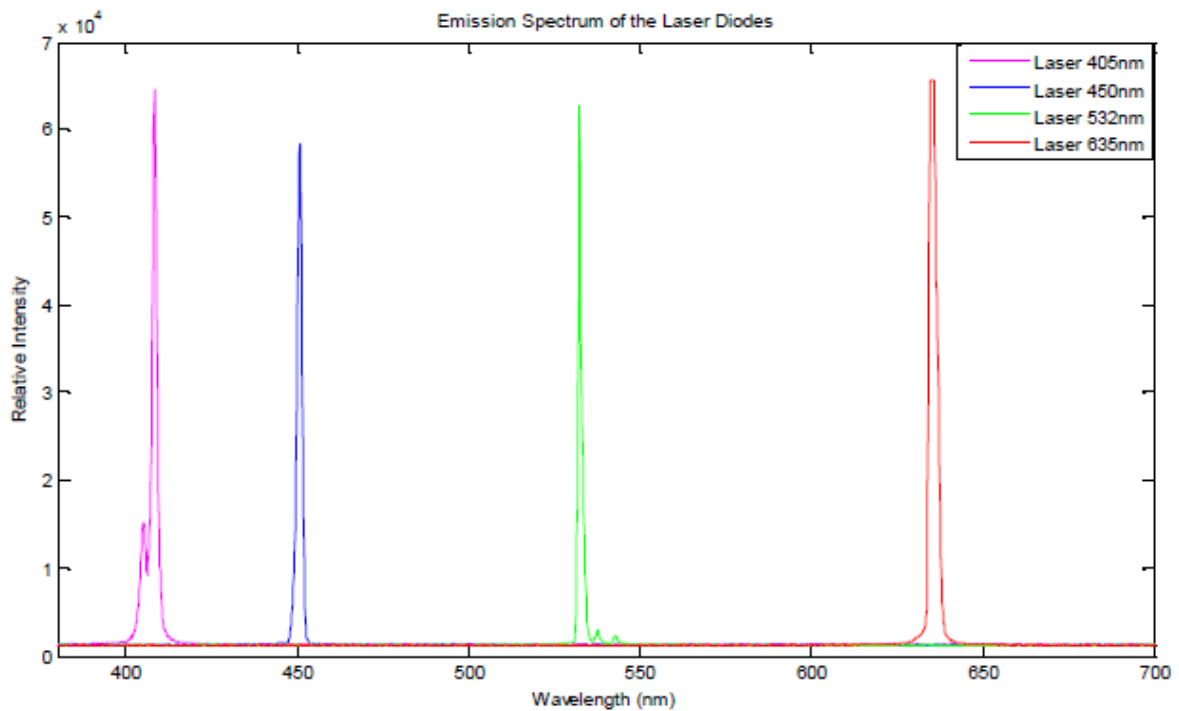
*Figure 5.10:* *Roithner RTL635-150-TO3 Laser Diode*



*Figure 5.11:* *Lasers' Emission Spectra*

## 5.3 Coherent Light Beam Expander

In order to expand our coherent light beam we do not use a typical expander. We use a liquid light guide. The lasers spot will fall on the liquids light guide tip and will be transmitted to the other tip expanded as in figure 5.12.

Liquid light guides are clearly superior to light guides made of silica fiber bundles by the very nature of their design. A liquid light guide is much like a single silica fiber with a very large diameter. It has the cross-section of an open pipe, transmitting light with total reflectance using all the space available. Silica fiber bundles, in contrast, are like many small tubes in a larger pipe with spaces between the individual strands remaining unused. These dead spots do not transmit light. This is why liquid light guides are able to deliver light with much greater
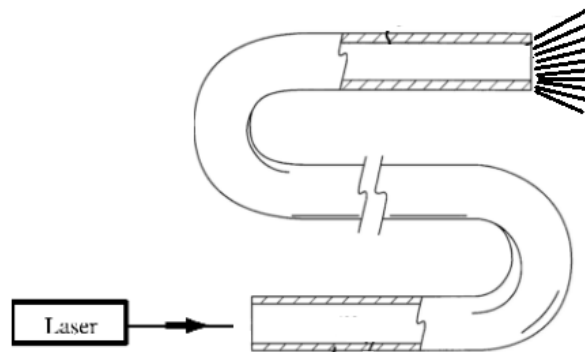
intensity to the target object.



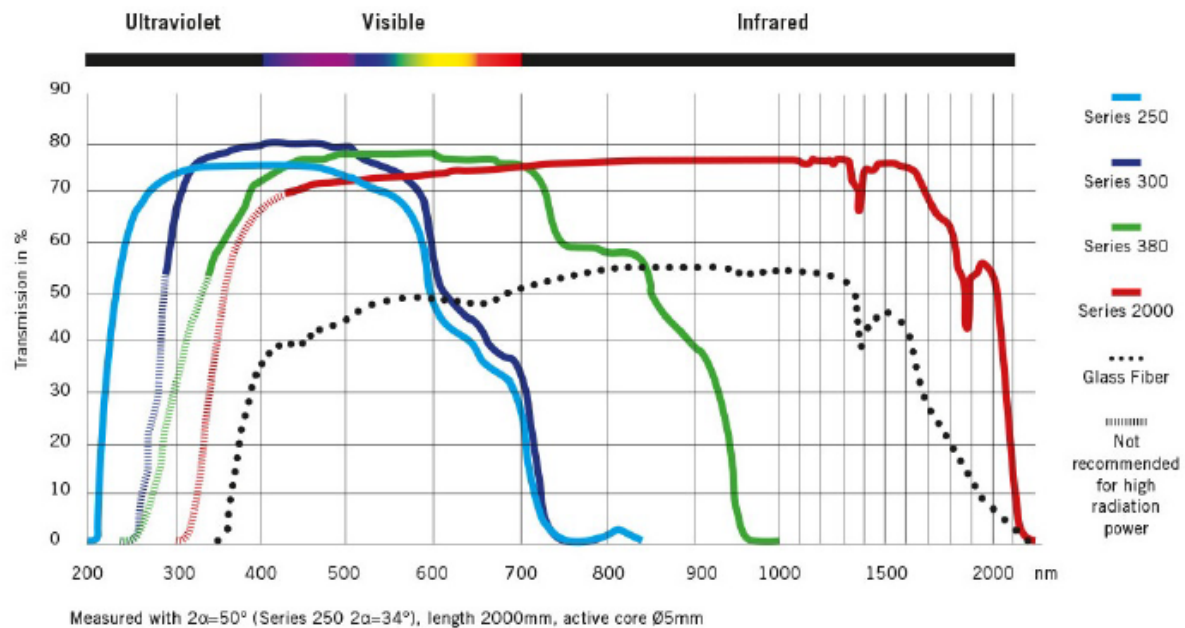**Figure 5.12:** *Liquid Light Guide Expander*



**Figure 5.13:** *Liquid Light Guide*

**Figure 5.14:** *Spectral Characteristics of Liquid Light Guides*

| Series | Core Diameters | NA 2α | Application Examples and Spectrum | Specific Properties |
|---|---|---|---|---|
| 250 | 3, 5, 8 mm | 50° | Wafer manufacturing, curing of UV adhesives with tack free surfaces. Lengths up to 5m (15ft). 220 nm–650 nm | Outstanding photo stability even in the UVC range, suitable for high power UV lasers. Recommended light sources: Deep UV Mercury, Xenon, Excimer. Temperature range (long term): +5 °C to +30 °C |
| 300 | 2, 3, 5, 6.5, 8, 10 mm | 72° | UV adhesive curing and UV fluorescence inspection at lengths of up to 20 m (60 ft). 280 nm–650 nm | Superior transmission of up to 5W of UV radiation. Suitable for very rugged environments. Recommended light sources: Mercury and Xenon, Tungsten Halogen, LED. Temperature range (long term): -5 °C to + 35 °C |
| 380 | 2, 3, 5, 6.5, 8, 10 mm | 72° | Outstanding white light illumination at lengths of up to 30 m (100ft). 340 nm–800 nm | Excellent transmission from the near UV to the far red even at a length of 30 m. Suitable for very rugged environments. Recommended lightsources: Tungsten Halogen, LED, Xenon, Metal Halide. Temperature range (long term): -5 °C to +35 °C |
| 2000 | 3, 5, 8 mm | 62° | Visible and near infrared illumination. Lengths up to 4 m (12ft). 420 nm–2000 nm | Transmission of high power near infrared radiation in the multi-watt range. Integrated long pass filter for radiation below 420 nm. Recommended light sources: Xenon or Tungsten Halogen lamps, Nd-YAG or Diode Lasers. Temperature range (long term): +5 °C to +35 °C |

**Figure 5.15:** *Specifications of Liquid Light Guides*

# Chapter 6

# Temporal Laser Speckle Imager

## 6.1    First measurments

In order to built a **Temporal Laser Speckle Imager** we used the setup that discribed in the previous chapter. The object we studied with Temporal Laser Speckle Imaging method was a piece of plywood (figure 6.1). We chose this object because it is very sensitive to mechanical vibrations, so the speckle pattern will change easily.



**Figure 6.1:** *Sensitive to Vibrations Wood Surface*

In order to vibrate our surface and reduce the speckle contrast we used a Vibration Motor (figure 6.2) and a voltage generator. Vibration frequency gets higher when we grow the vibration motors voltage from 0V (off) to 2V (maximum vibration frequency).
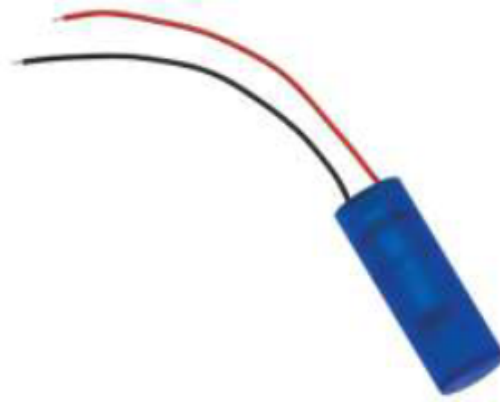


**Figure 6.2:** *Vibration Motor*

From our **Coherent Light Source** 5.2 we used only the 532nm(green) laser diode. A survey of the literature[18] indicates that the green laser light is the most suitable for Laser Speckle Imaging on rough surfaces. Our set up for our first experiment is shown in figure 6.3.



**Figure 6.3:** *Laser Speckle Imager first Setup*

Since we had our Setup we started to take some measurements with and without vibration. We started our measurements from 0V (without vibration) to 2V with a 400mV voltage step(figure 6.4).
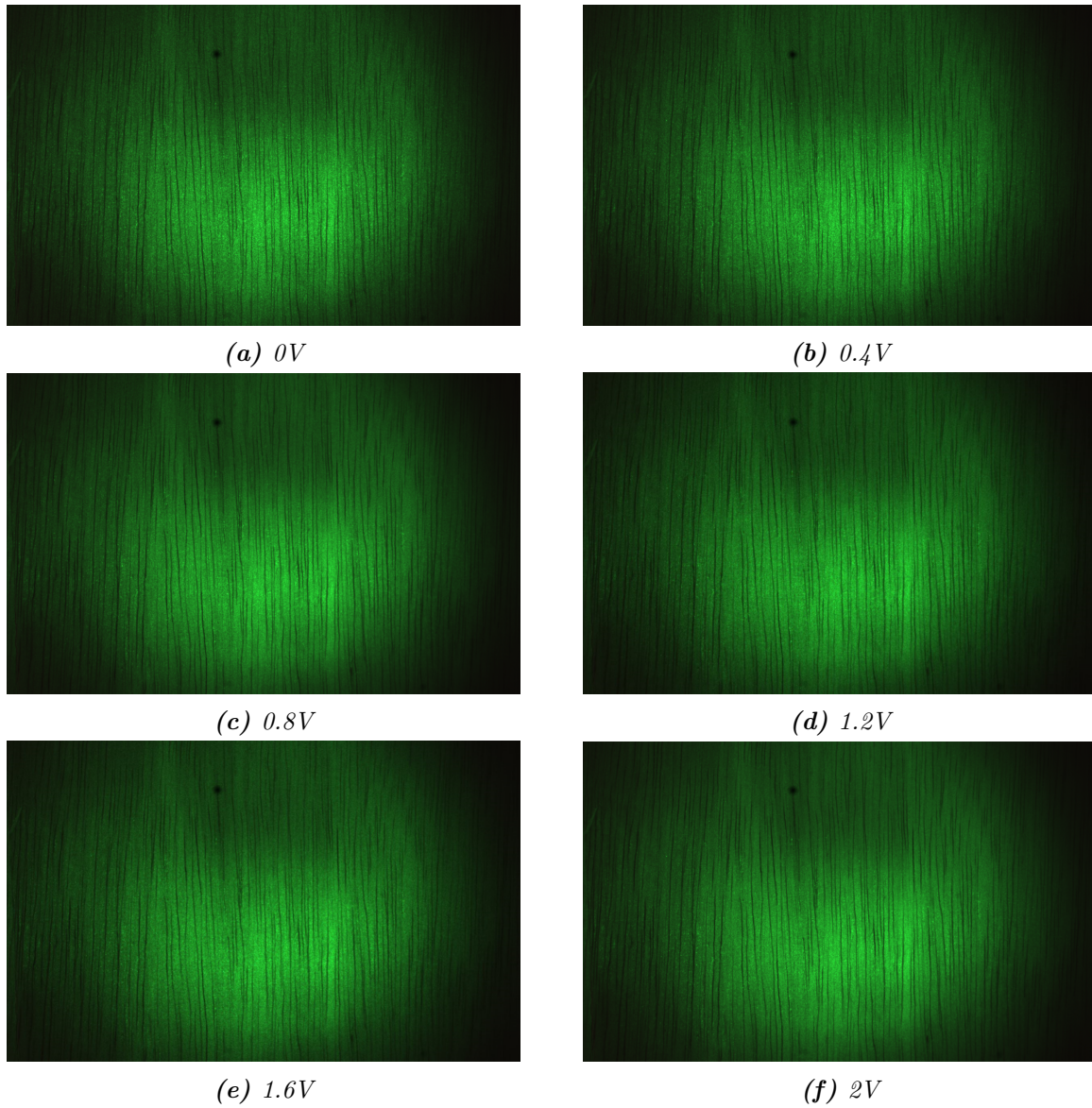

*(a) 0V*


*(b) 0.4V*


*(c) 0.8V*


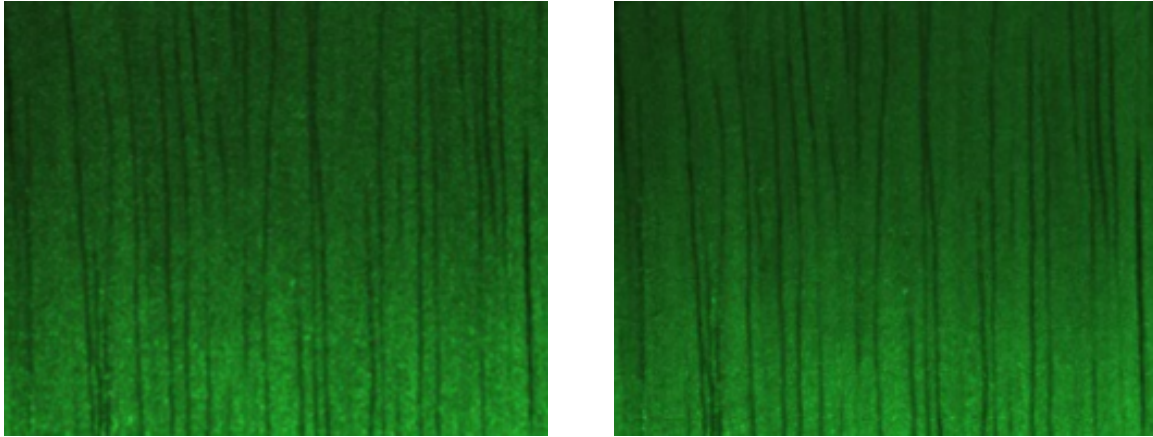*(d) 1.2V*


*(e) 1.6V*


*(f) 2V*

**Figure 6.4:** *Speckle Images With Vibration*

if we use zoom to the image that has no vibration and to the image that has 1.2V vibration we will easily notice that the speckle pattern is blurred (figure 6.5).

*(a) Speckle Image without Vibration*     *(b) Speckle Image with Vibration 1.2V*

***Figure 6.5:*** *Speckle Images with vs without Vibration*

So we can easily observe without the help of any additional algorithms that the Speckle Contrast is redused a lot with the little motor vibrator.

## 6.2   Green Channel and Pseudocolor Map

All the images that we have taken have 3 channels: The red, the blue and the green. In order to reduce the noise that is created from the blue and the red channel given that our laser is green we cat those channels and we reproduce the green channel as shown in figure 6.6. We did that with Matlab r2014a software.

Since we isolated the green channel we designed a pseudocolor map with colors : blue, green, red, yellow, white and we reproduced the pictures based in this colormap (figure 6.7).

From the pseudocolor map images we can now see clearly that the speckle contrast is redused while we use the vibrator. In addition we can note that the more we increase the vibrator's voltage it decreases the speckle contrast. So in the next section using temporal analysis we will quantify this reduction.
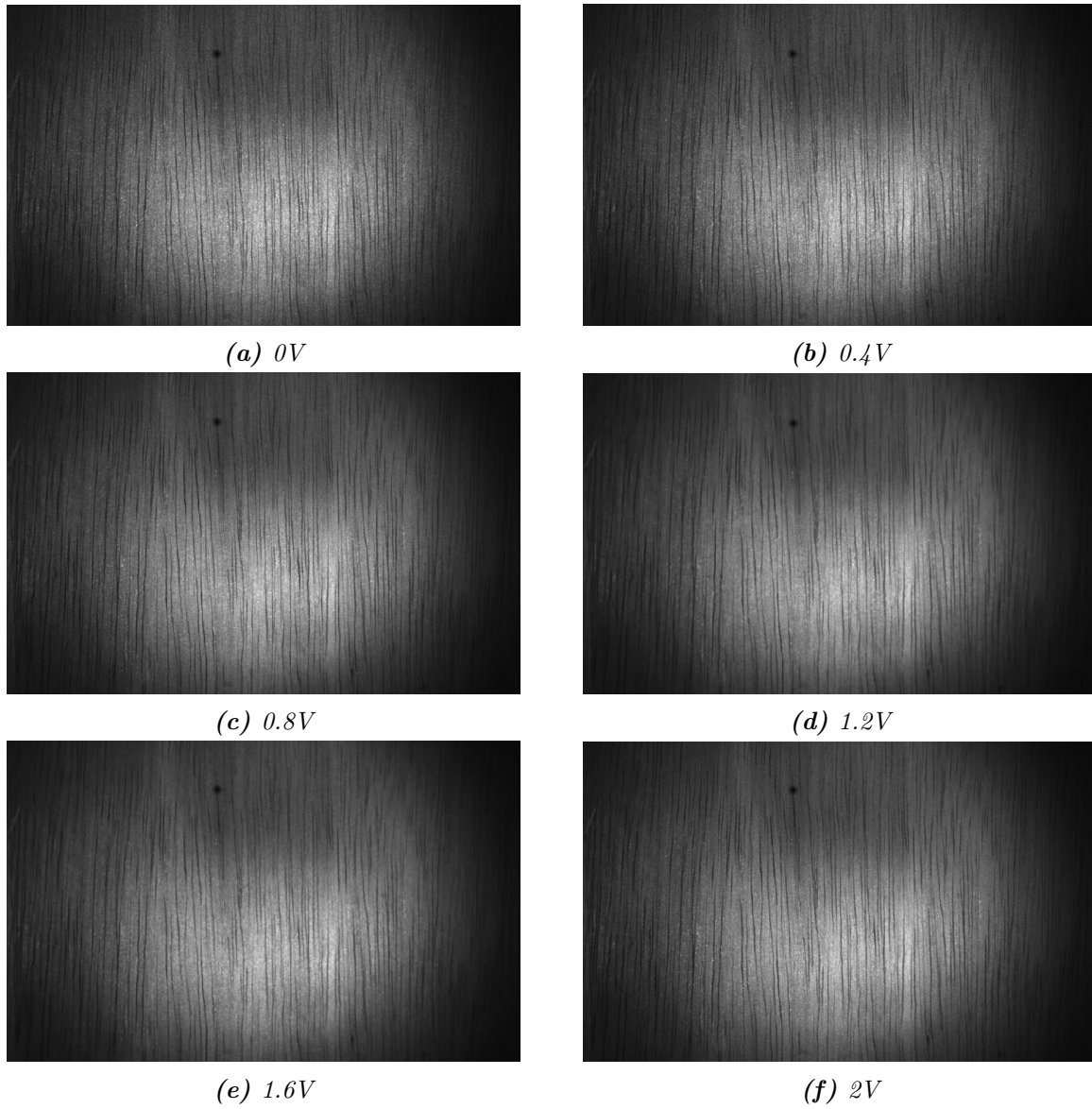
(a) *0V*

(b) *0.4V*

(c) *0.8V*

(d) *1.2V*

(e) *1.6V*

(f) *2V*

**Figure 6.6:** *Speckle Images With Vibration greyscale*

*(a)* 0V

*(b)* 0.4V

*(c)* 0.8V

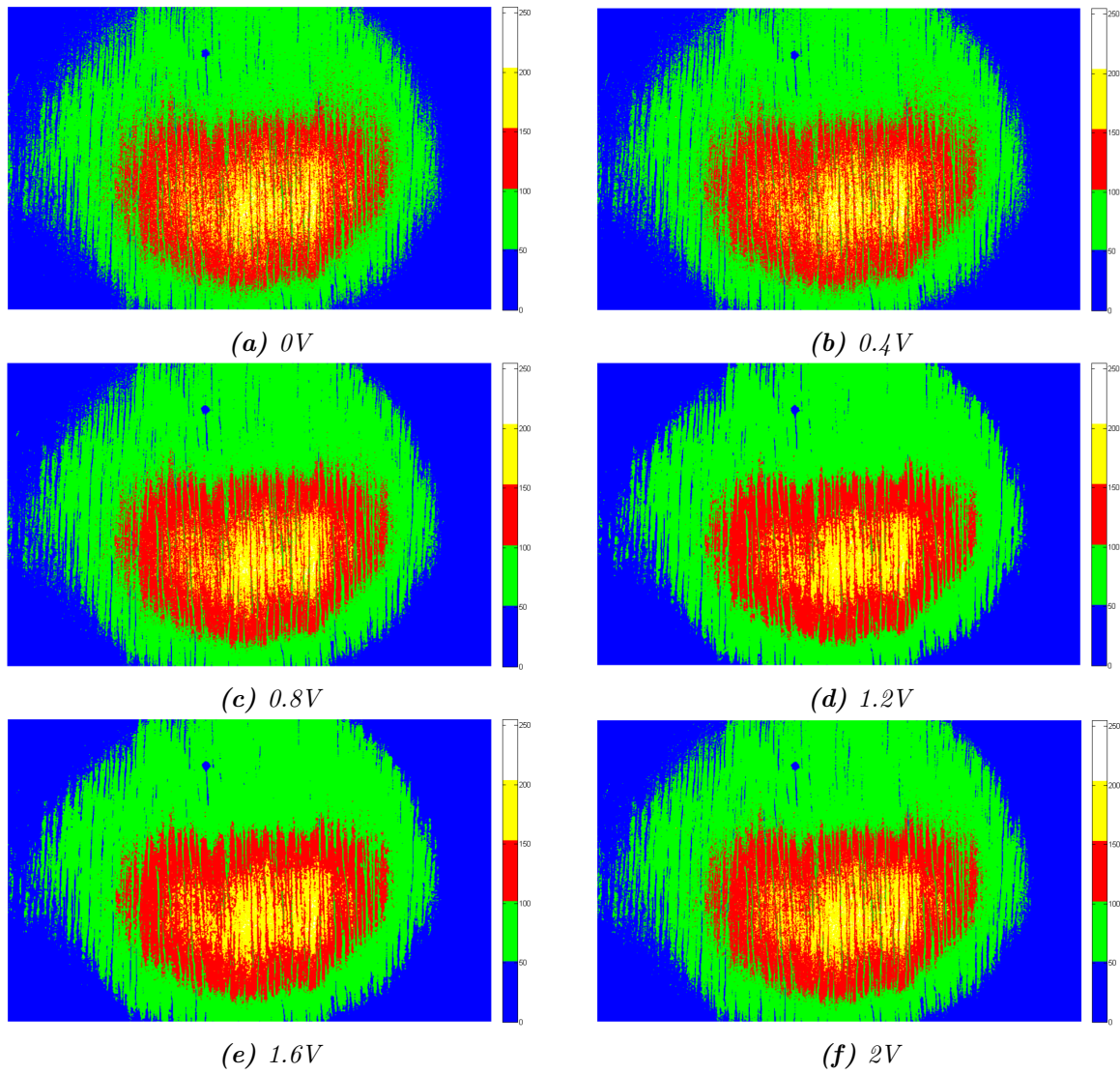*(d)* 1.2V

*(e)* 1.6V

*(f)* 2V

***Figure 6.7:*** *Speckle Images With Vibration pseudocolor map*

## 6.3  Temporal Contrast Algorithm

We designed an **Temporal Contrast Algorithm** based in the algorithm descripted in section 4.5.2 with Matlab r2014a. We took 4 statistically independent images for each vibration. For every quartet we calculate Speckle Contrast $K$ for each pixel across the images as shown in figure 4.5.Temporal Speckle Contrast is the ratio of standard deviation, $\sigma_I$ , to the mean intensity, $\langle I \rangle$ , of the quartet of pixels.

$$K_T = \frac{\sigma_I}{\langle I \rangle}$$

In order to image the temporal speckle contrast we designed a contrast table $K_{table}$ that in every coordinate (x,y) has the contrast value $K_T$ of the same (x,y) of quartet of pixels. In our implementation our images is $2080 \times 3096$ pixels but if we use the whole image the processing will be too slow and the r2014a matlab cannot image so huge tables. So we used the central $500 \times 500$ pixels. As a result our $K_{table}$ will be $500 \times 500$ as well.

In order to image the $K_{table}$ we used the pseudocolor map that we designed with the colors : blue, green, red, yellow, white. When we are close to blue the $K_T$ value is low so our surface is vibrating. When we image a temporal contrast table from four vibrating images we image next to it the temporal contrast table from four non-vibrating images in order to notice the differences. We can also compare to temporal contrast tables that comes from different vibration voltages in order to compare in which vibration the speckle contrast is redused more.

In figure 6.8 we can see the $K_{table}$ of the non vibrating surface (left half) versus the 0.4V vibrating surface (right half).
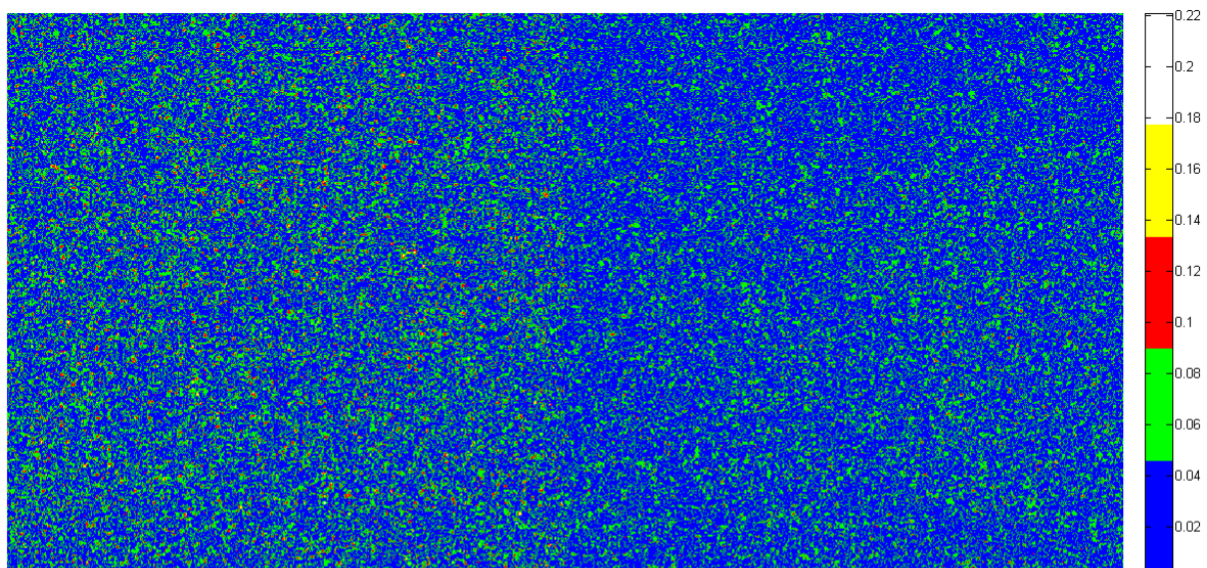


**Figure 6.8:** $K_{table}$ *for non-vibrating and for 0.4V vibrating surface*

In figure 6.9 we can see the $K_{table}$ of the non vibrating surface (left half) versus the 0.8V vibrating surface (right half).
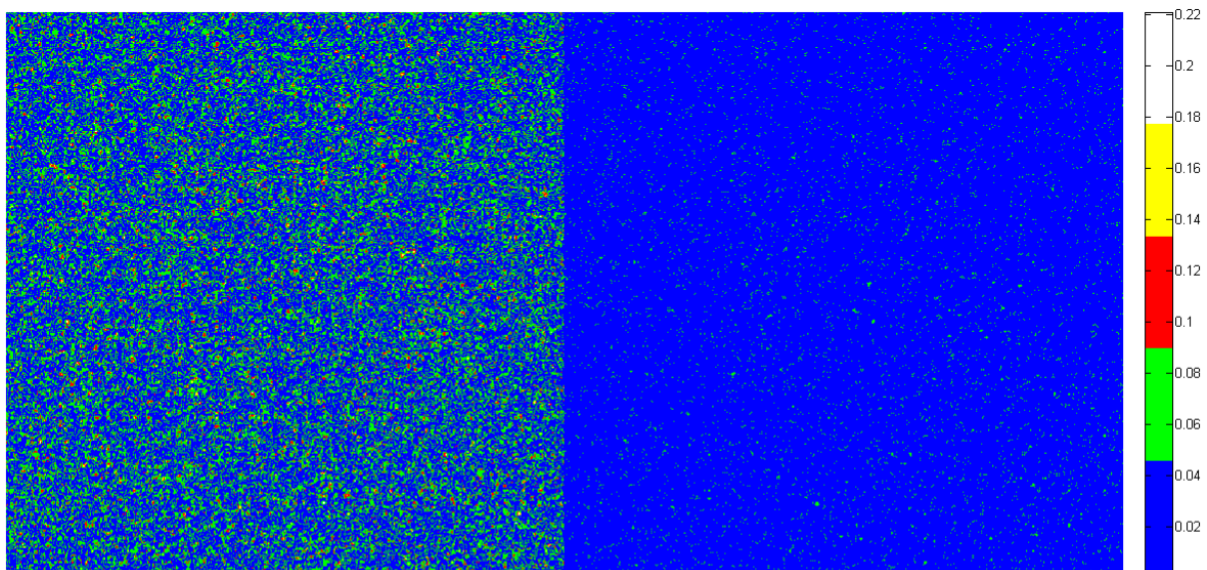


**Figure 6.9:** $K_{table}$ for non-vibrating and for 0.8V vibrating surface

In figure 6.10 we can see the $K_{table}$ of the non vibrating surface (left half) versus the 1.2V vibrating surface (right half).



**Figure 6.10:** $K_{table}$ for non-vibrating and for 1.2V vibrating surface

In figure 6.11 we can see the $K_{table}$ of the non vibrating surface (left half) versus the 1.6V vibrating surface (right half).



**Figure 6.11:** *$K_{table}$ for non-vibrating and for 1.6V vibrating surface*

In figure 6.12 we can see the $K_{table}$ of the non vibrating surface (left half) versus the 2V vibrating surface (right half).
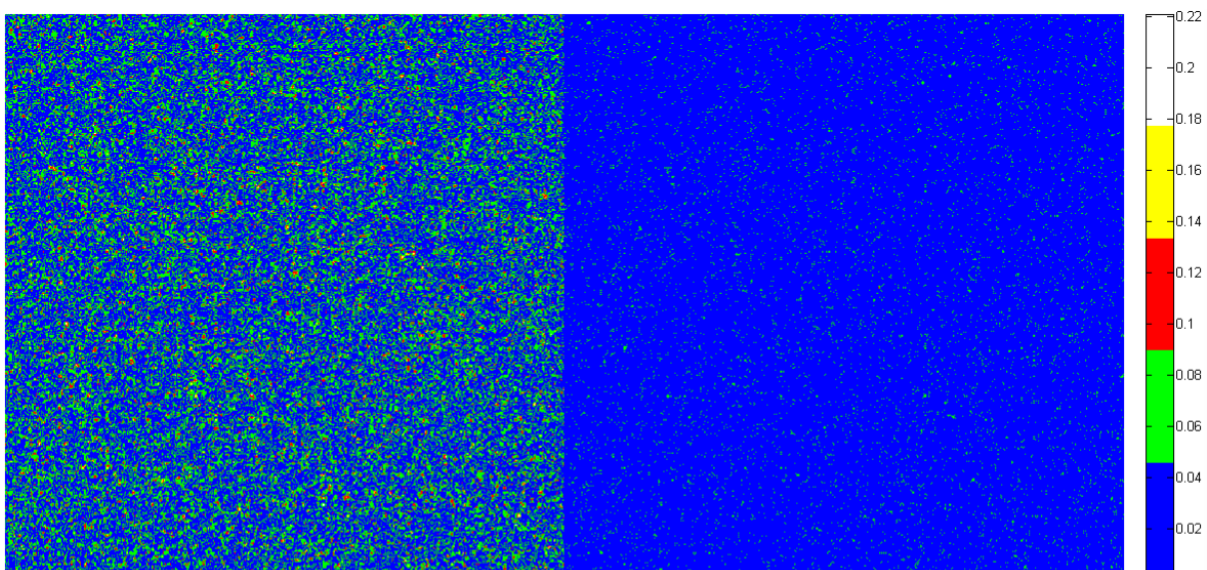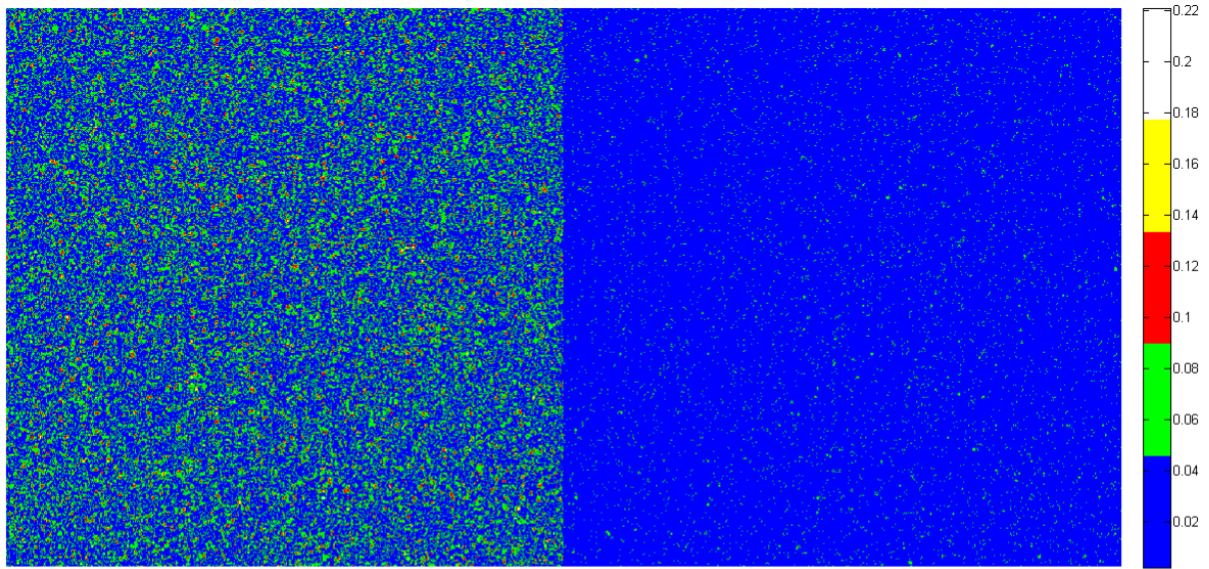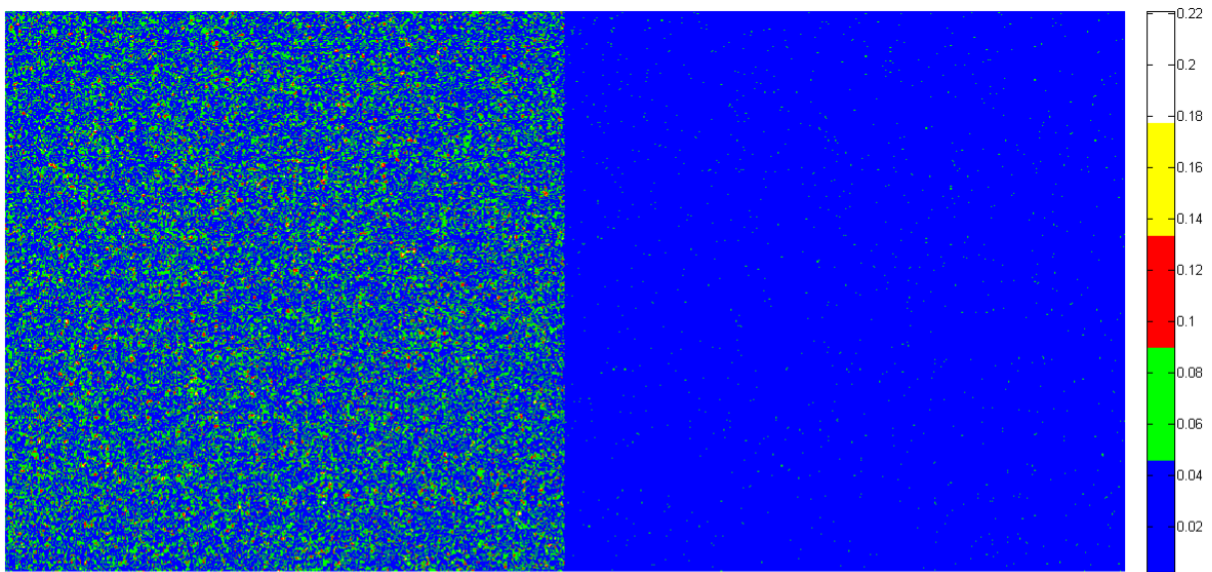


**Figure 6.12:** *$K_{table}$ for non-vibrating and for 2V vibrating surface*

The result of these measurements is that we prove that the more we increase the vibration the more the speckle contrast decreases. So we designed a **Laser Temporal Speckle Imager** that can quantify the vibration of a surface without knowing the vibration size.

## 6.4 Temporal Contrast Images with different zoom

In this section we took some speckle images with different zoom. We used the same algorithm to quantify the speckle contrast reduction and we compared the $K_{table}$ of each zoom. In order to do that we used the Navitar Zoom 7000 Macro Lens which is shown in figure 6.13.



**Figure 6.13:** *Navitar Zoom 7000 Macro Lens*

| | |
|---|---|
| **Back Focal Length** | 24.28 |
| **EFL (mm)** | 18-108 |
| **Exit Pupil Position** | 238.60 |
| **Field Angle 1/2 (HxV)** | Wide 19° 58' x 15° 06' / Tele 3° 23' x 2° 55' |
| **Field Angle 1/3 (HxV)** | Wide 14° 59' x 11° 20' / Tele 2° 32' x 1° 91' |
| **Field Angle 1/4 (HxV)** | Wide 9° 59' x 7° 33' / Tele 1° 41' x 1° 23' |
| **Field Angle 2/3 (HxV)** | Wide 27° 28' x 20° 46' / Tele 4° 39' x 3° 50' |
| **Filter Diameter** | Ø52 P=0.75 |
| **Focus Control** | Manual |
| **Focusing range from front of lens (m)** | 0.13 - inf. |
| **Format** | 2/3" |
| **F Stop** | 2.5-Close |
| **Iris Control** | Manual |
| **Mount** | C |
| **Object Area (mm) at M.O.D. (HxV) 1/2"** | Wide 183 x 142 / Tele 31 x 24 |
| **Object Area (mm) at M.O.D. (HxV) 1/3"** | Wide 138 x 106 / Tele 23 x 18 |
| **Object Area (mm) at M.O.D. (HxV) 1/4"** | Wide 91 x 71 / Tele 15 x 12 |
| **Object Area (mm) at M.O.D. (HxV) 2/3"** | Wide 252 x 195 / Tele 43 x 33 |
| **Weight (g)** | 595 |
| **Zoom Control** | Manual |

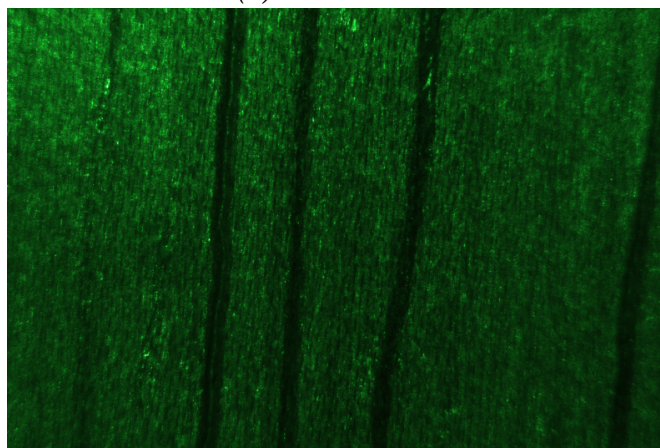**Figure 6.14:** *Navitar Zoom 7000 Macro Lens Specifications*

We took measurments in 3 different zooms as shown in figure 6.15
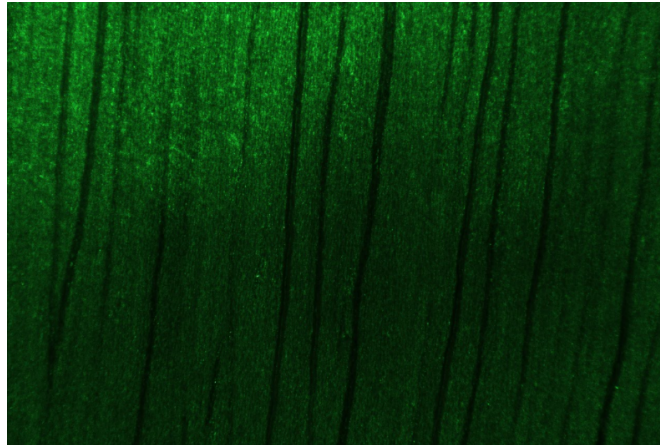


*(a) minimum zoom*
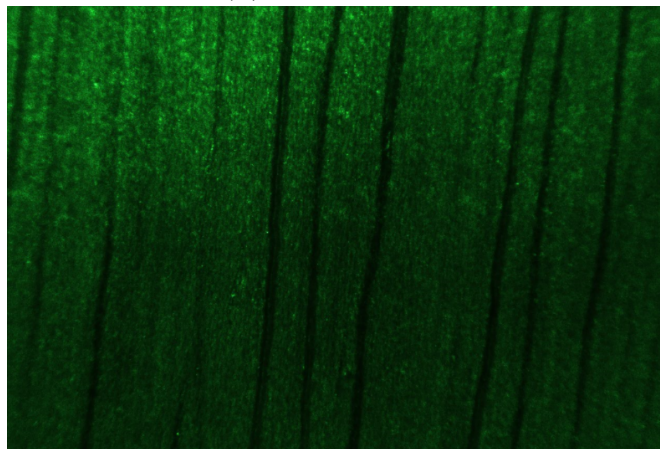


*(b) medium zoom*



*(c) maximum zoom*

***Figure 6.15:*** *Speckle Images With 3 different zooms*

We repeated the same measurements as in the previous section for each zoom separately.

### 6.4.1   Minimum zoom

In figure 6.16 we can see the $K_{table}$ of the non vibrating surface (left half) versus the 0.4V vibrating surface (right half) with the minimum zoom of Navitar zoom 7000 Macro Lens.



**Figure 6.16:** $K_{table}$ for non-vibrating and for 0.4V vibrating surface

In figure 6.17 we can see the $K_{table}$ of the non vibrating surface (left half) versus the 0.8V vibrating surface (right half) with the minimum zoom of Navitar zoom 7000 Macro Lens.



**Figure 6.17:** $K_{table}$ for non-vibrating and for 0.8V vibrating surface

In figure 6.18 we can see the $K_{table}$ of the non vibrating surface (left half) versus the 1.2V vibrating surface (right half) with the minimum zoom of Navitar zoom 7000 Macro Lens.
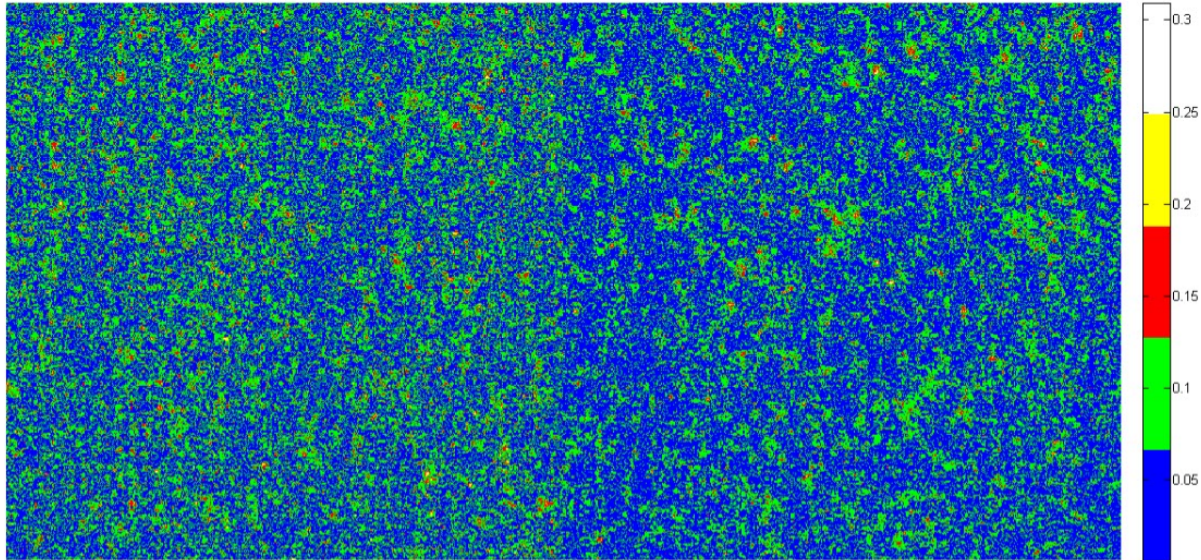


**Figure 6.18:** $K_{table}$ *for non-vibrating and for 1.2V vibrating surface*

In figure 6.19 we can see the $K_{table}$ of the non vibrating surface (left half) versus the 1.6V vibrating surface (right half) with the minimum zoom of Navitar zoom 7000 Macro Lens.
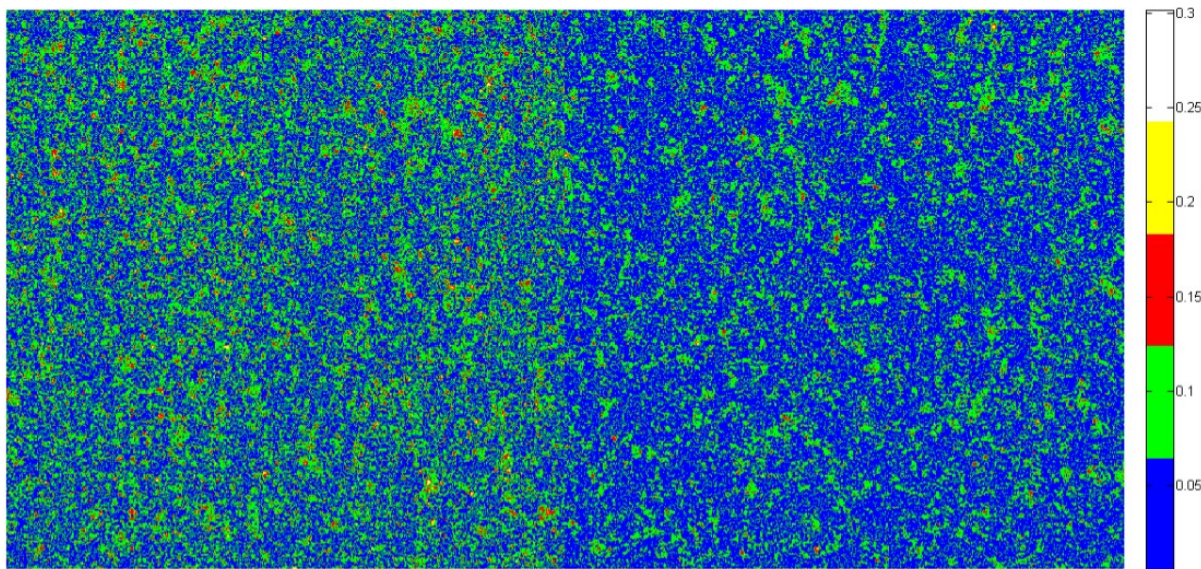


**Figure 6.19:** $K_{table}$ *for non-vibrating and for 1.6V vibrating surface*

In figure 6.20 we can see the $K_{table}$ of the non vibrating surface (left half) versus the 2V vibrating surface (right half) with the minimum zoom of Navitar zoom 7000 Macro Lens.
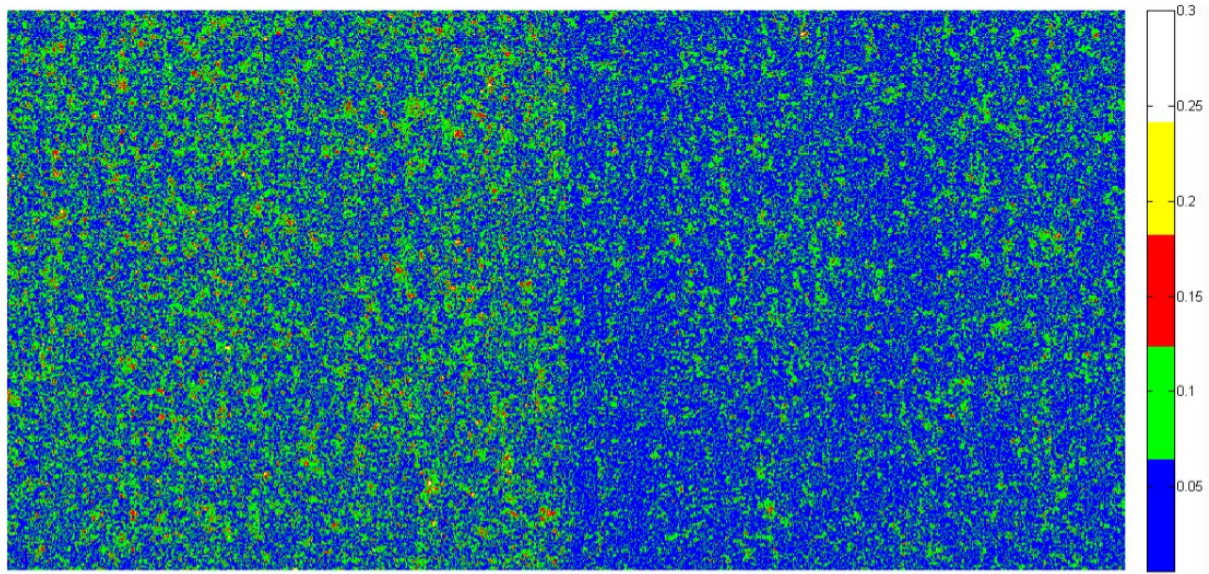


**Figure 6.20:** $K_{table}$ *for non-vibrating and for 2V vibrating surface*

### 6.4.2 Medium zoom

In figure 6.21 we can see the $K_{table}$ of the non vibrating surface (left half) versus the 0.4V vibrating surface (right half) with the medium zoom of Navitar zoom 7000 Macro Lens.



**Figure 6.21:** $K_{table}$ *for non-vibrating and for 0.4V vibrating surface*

In figure 6.22 we can see the $K_{table}$ of the non vibrating surface (left half) versus the 0.8V vibrating surface (right half) with the medium zoom of Navitar zoom 7000 Macro Lens.
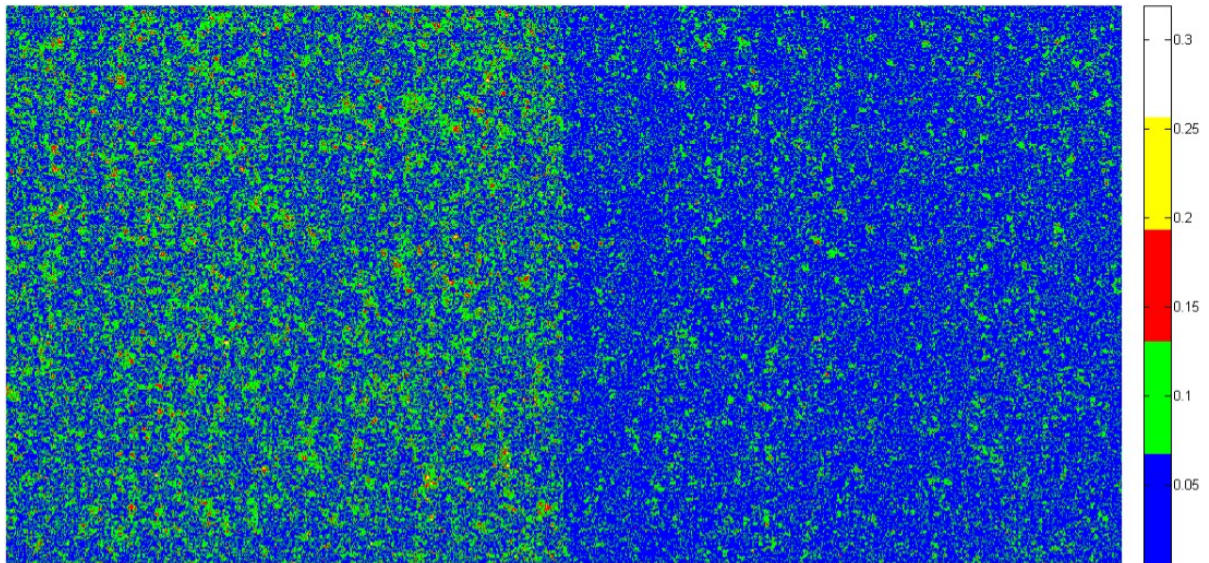


**Figure 6.22:** $K_{table}$ *for non-vibrating and for 0.8V vibrating surface*

In figure 6.23 we can see the $K_{table}$ of the non vibrating surface (left half) versus the 1.2V vibrating surface (right half) with the medium zoom of Navitar zoom 7000 Macro Lens.
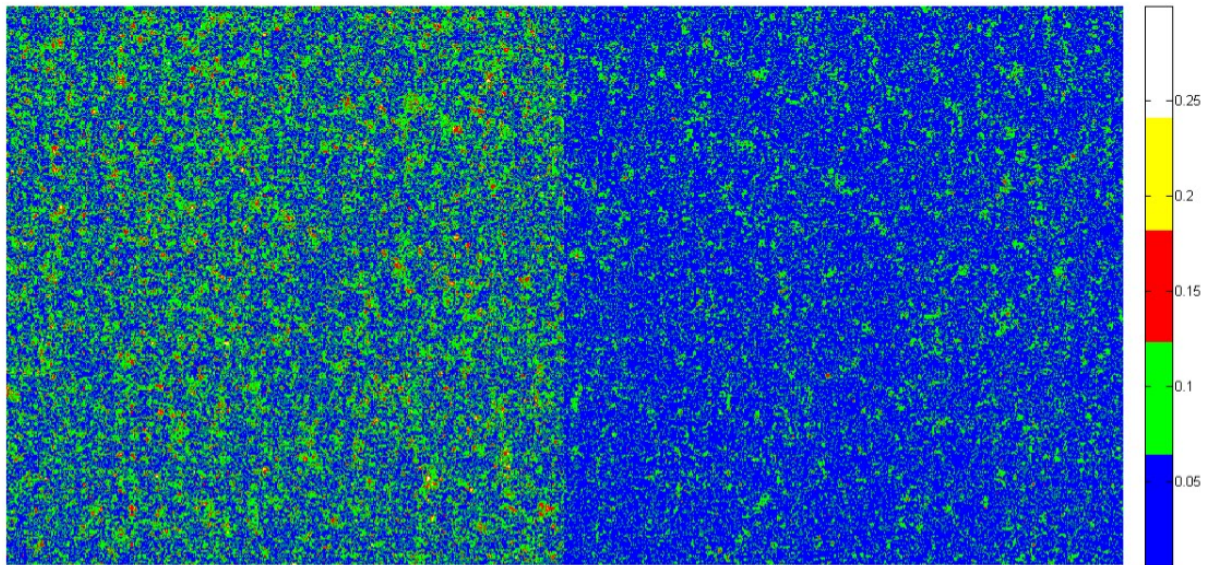


**Figure 6.23:** $K_{table}$ *for non-vibrating and for 1.2V vibrating surface*

In figure 6.24 we can see the $K_{table}$ of the non vibrating surface (left half) versus the 1.6V vibrating surface (right half) with the medium zoom of Navitar zoom 7000 Macro Lens.
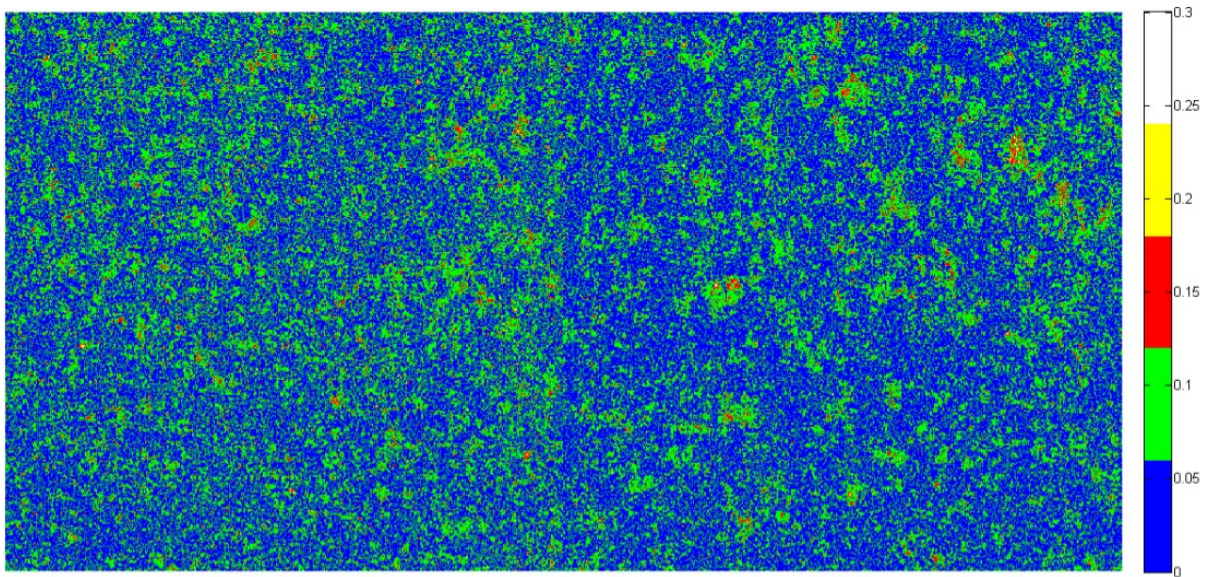


**Figure 6.24:** $K_{table}$ *for non-vibrating and for 1.6V vibrating surface*

In figure 6.25 we can see the $K_{table}$ of the non vibrating surface (left half) versus the 2V vibrating surface (right half) with the medium zoom of Navitar zoom 7000 Macro Lens.



**Figure 6.25:** $K_{table}$ *for non-vibrating and for 2V vibrating surface*

### 6.4.3 Maximum zoom

In figure 6.26 we can see the $K_{table}$ of the non vibrating surface (left half) versus the 0.4V vibrating surface (right half) with the maximum zoom of Navitar zoom 7000 Macro Lens.
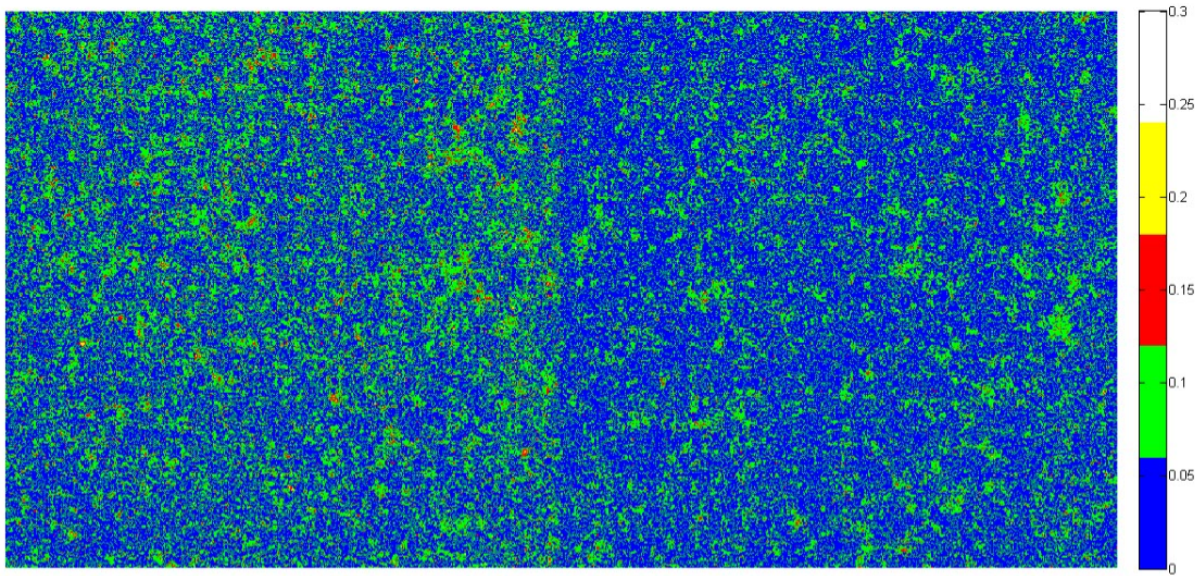


**Figure 6.26:** $K_{table}$ *for non-vibrating and for 0.4V vibrating surface*

In figure 6.27 we can see the $K_{table}$ of the non vibrating surface (left half) versus the 0.8V vibrating surface (right half) with the maximum zoom of Navitar zoom 7000 Macro Lens.
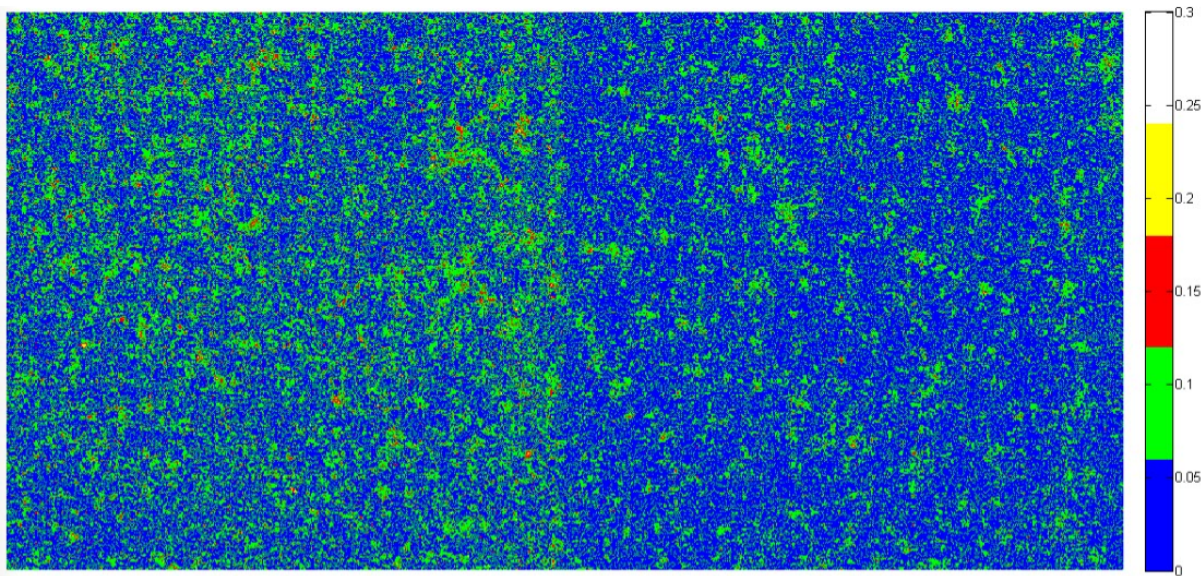


**Figure 6.27:** $K_{table}$ *for non-vibrating and for 0.8V vibrating surface*

In figure 6.28 we can see the $K_{table}$ of the non vibrating surface (left half) versus the 1.2V vibrating surface (right half) with the maximum zoom of Navitar zoom 7000 Macro Lens.
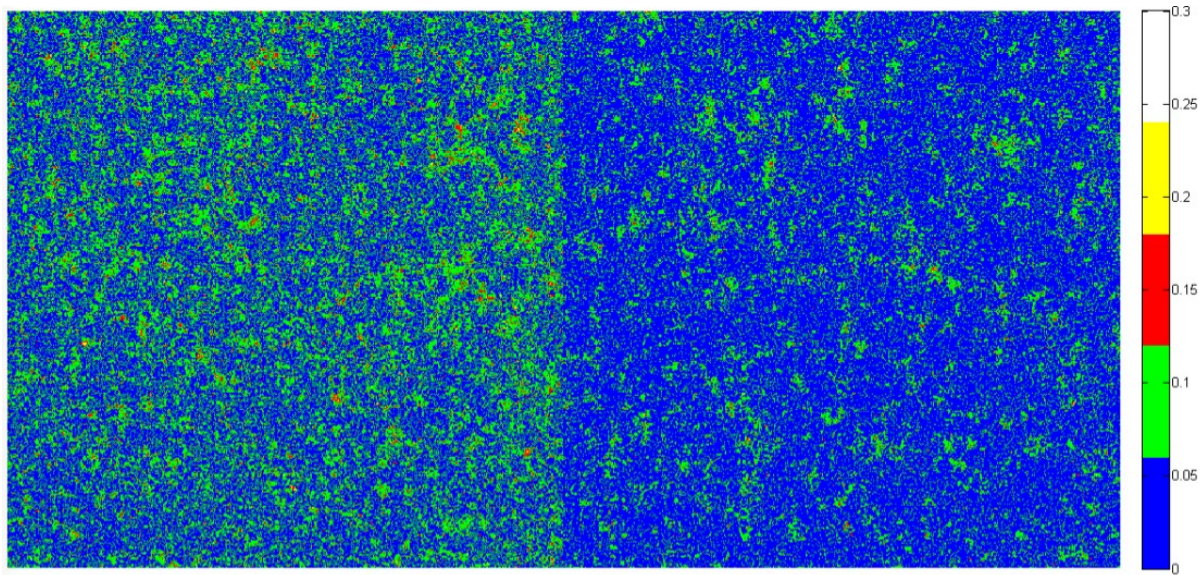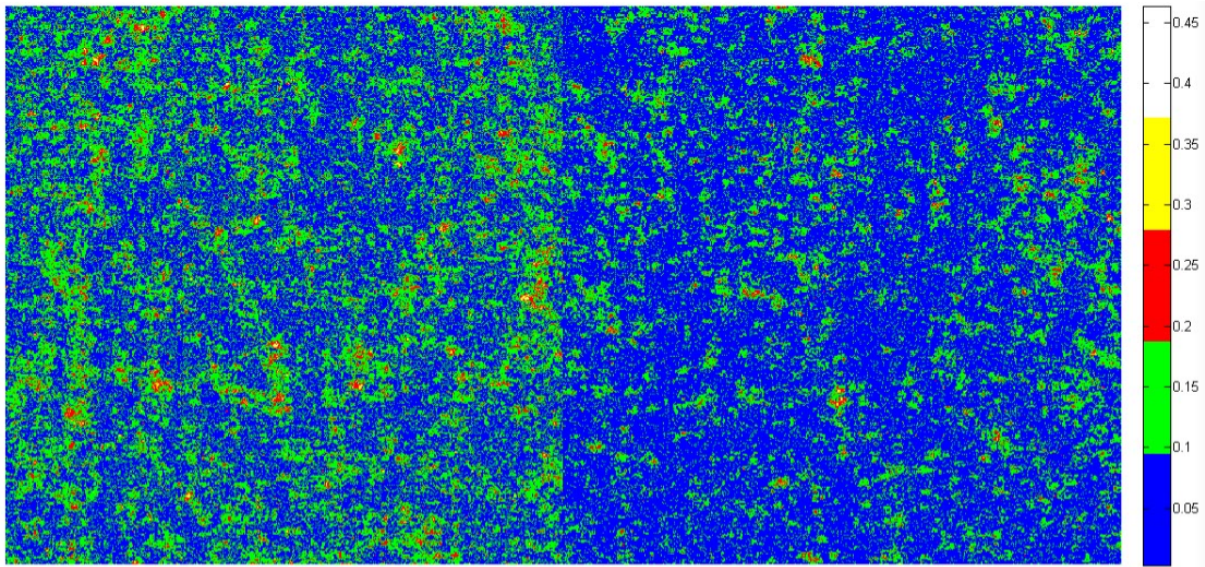


**Figure 6.28:** $K_{table}$ *for non-vibrating and for 1.2V vibrating surface*

In figure 6.29 we can see the $K_{table}$ of the non vibrating surface (left half) versus the 1.6V vibrating surface (right half) with the maximum zoom of Navitar zoom 7000 Macro Lens.
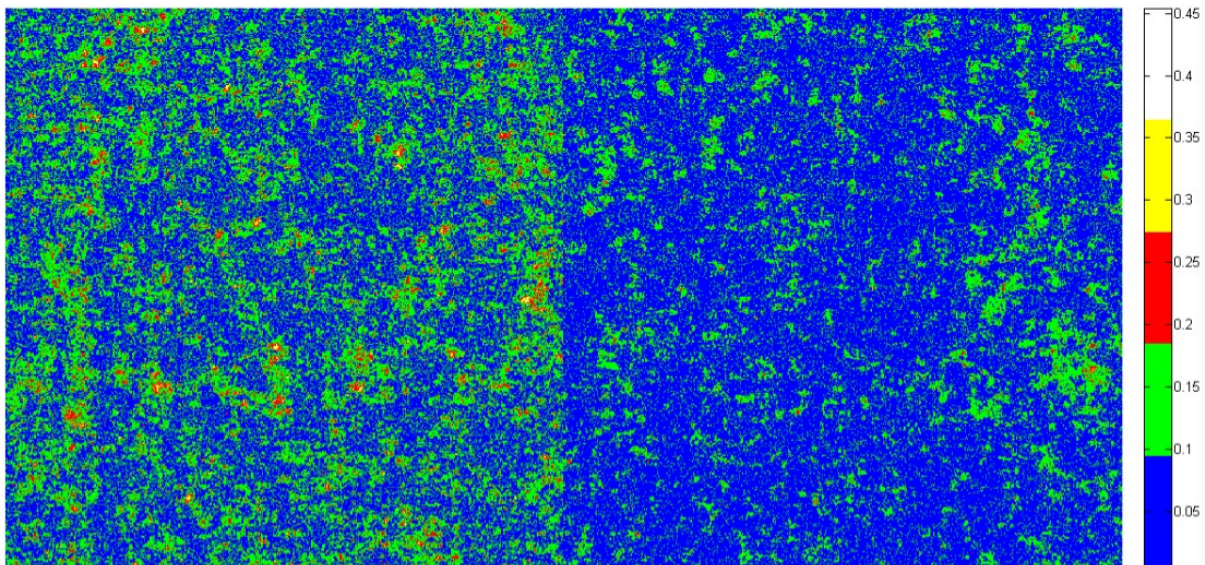


**Figure 6.29:** $K_{table}$ *for non-vibrating and for 1.6V vibrating surface*

In figure 6.30 we can see the $K_{table}$ of the non vibrating surface (left half) versus the 2V vibrating surface (right half) with the maximum zoom of Navitar zoom 7000 Macro Lens.
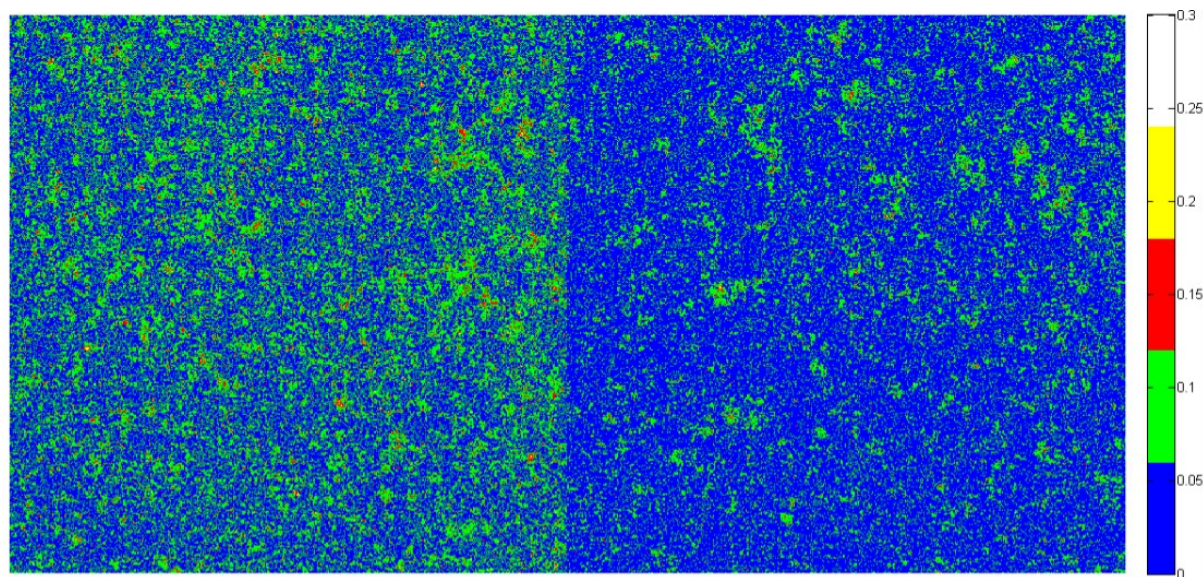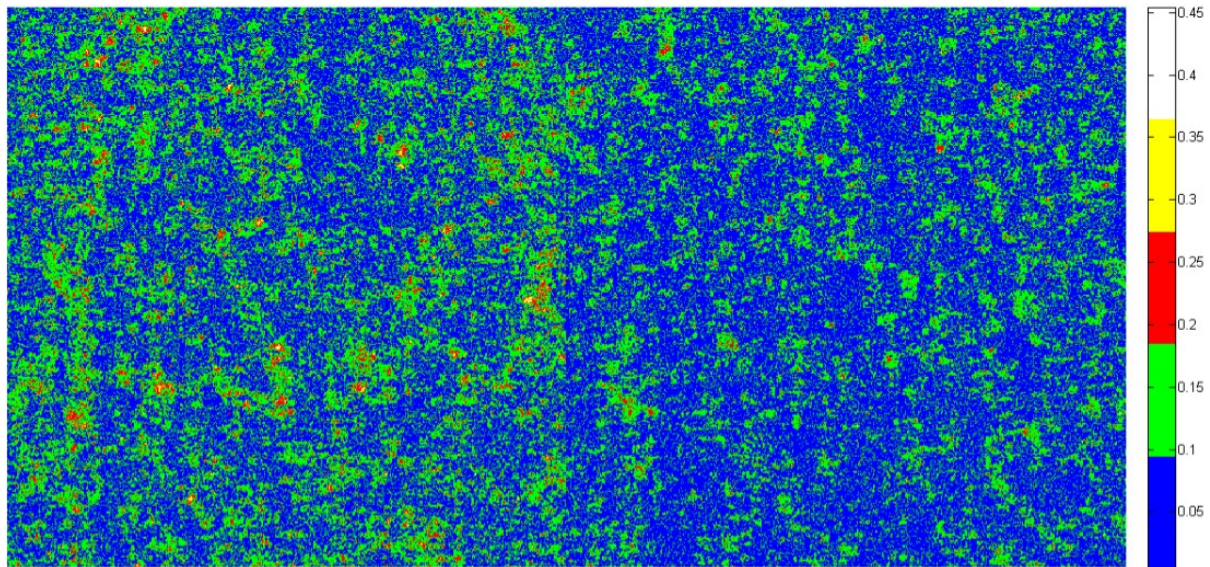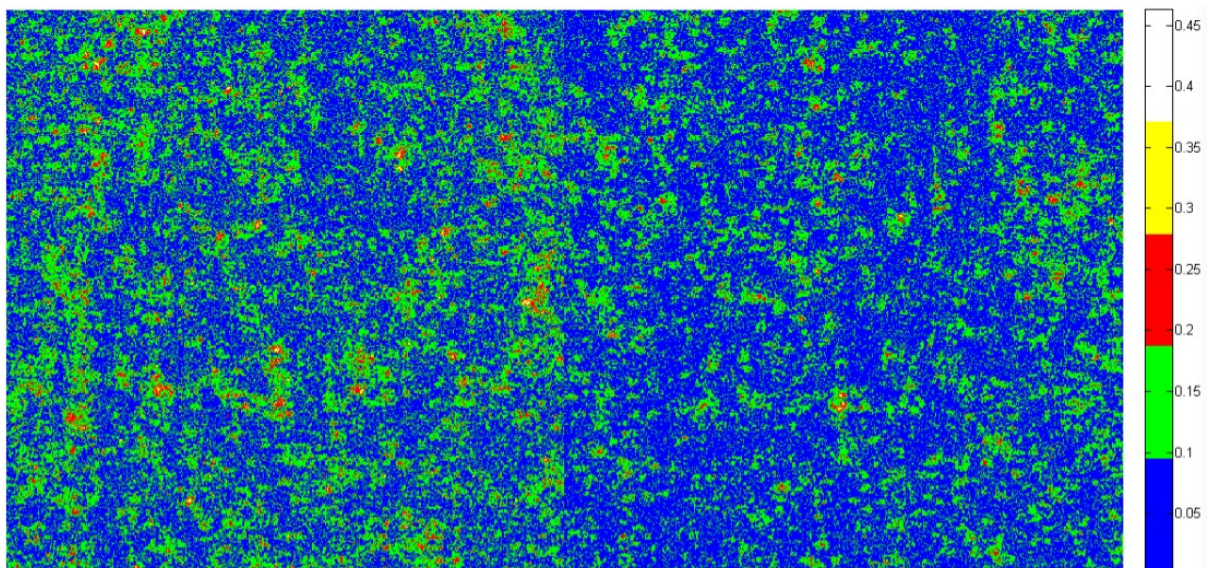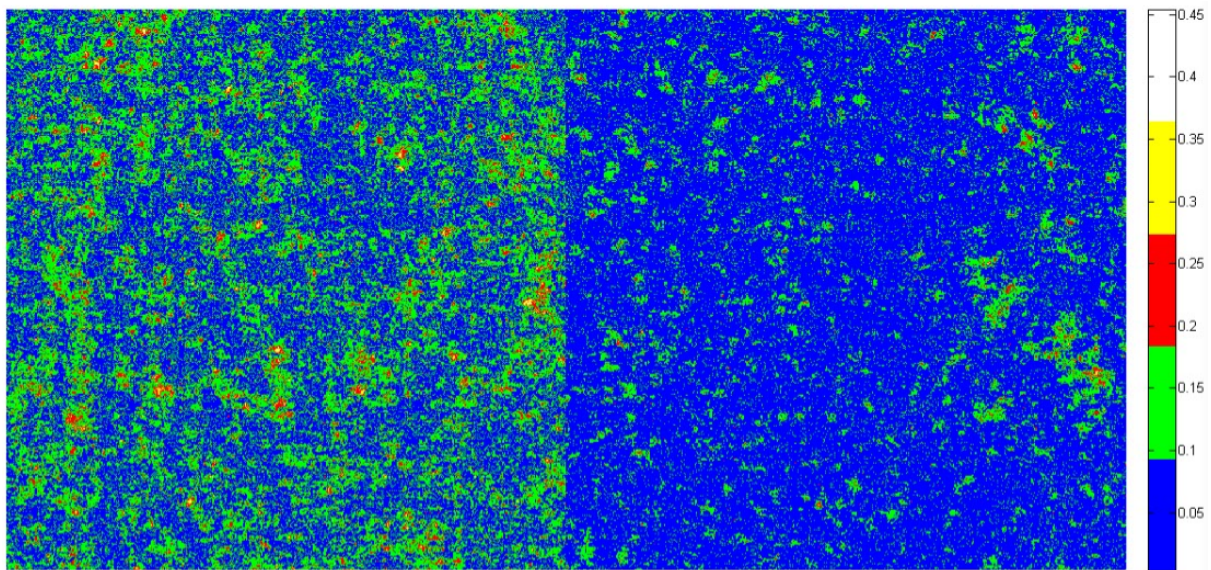


**Figure 6.30:** $K_{table}$ *for non-vibrating and for 2V vibrating surface*

# Chapter 7

# Spatial Laser Speckle Imager

## 7.1  Setup

In order to built a **Spatial Laser Speckle Imager** we used the setup that discribed in chapter 5. The object we studied with Spatial Laser Speckle Imaging method was a drum with white drum film as shown in figure 7.1. We used this object because it is very sensitive in impact and sound stimulations. In addition with this method we will study the Spatial Contrast so we will measure the speckle contrast in neighboring pixels. As a result we needed a surface that has no contrast on its own. That's why we used a white surface.



**_Figure 7.1:_** _White Film Drum_

In order to stimulate our surface in the first experiment we used a drumstick (figure 7.2)with which we just hit the film and in the second experiment a conventional speaker (figure 7.3) and a tone generator [31] software with which we produced acoustic tones in different frequencies.



**Figure 7.2:** *Drumstick*
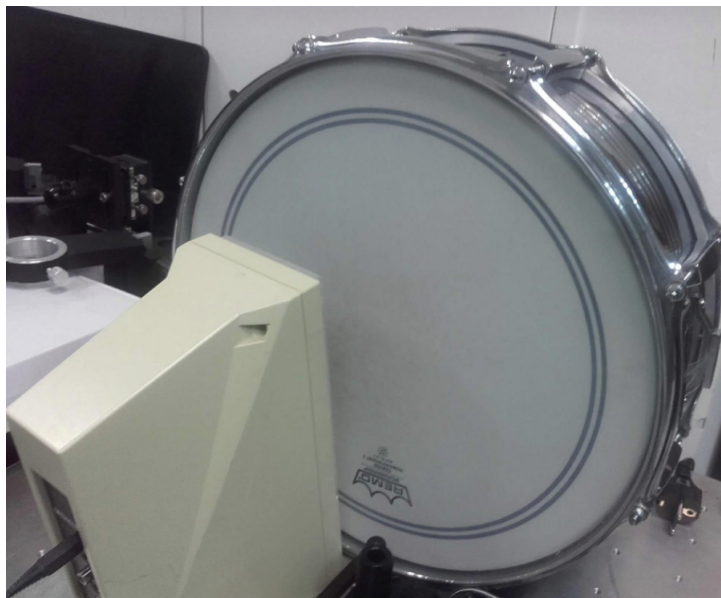


**Figure 7.3:** *Speaker*

We also used as a lens the Sofra L25F1.4 25mm F1.4 C-Mount Objective Lens (figure 7.4)



**Figure 7.4:** *Sofradir-EC*

| FEATURES | Universal C-Mount for cameras and viewers, manual focus, integral adjustable iris diaphragm, broadband lens coating for near-infrared imaging. |
|---|---|
| TECH SPECS | Objective Lens $\mapsto$ 25mm |

***Figure 7.5:*** *Sofradir-EC Specifications*

From our **Coherent Light Source** 5.2 we used only the 532nm(green) laser diode. A survey of the literature[18] indicates that the green laser light is the most suitable for Laser Speckle Imaging. Our set up for spatial laser speckle imaging experiment is shown in figure 7.6.
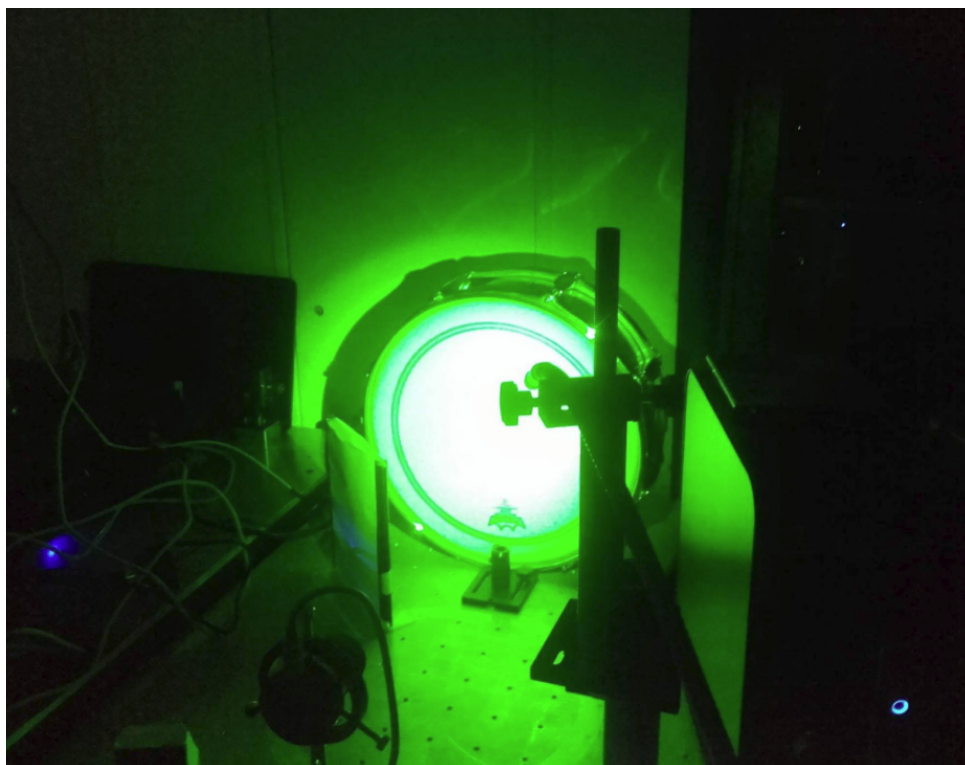


***Figure 7.6:*** *Laser Speckle Imager second Setup*

## 7.2    Spatial Contrast Algorithm

We designed an **Spatial Contrast Algorithm** based in the algorithm described in section 4.5.1 with Matlab r2014a. We intersected every image in subimages of variable size. According to the litaratute [27] typically we use $16 \times 16$ or $8 \times 8$ pixels for each subimage. For every subimage we calculate Speckle Contrast $K$ and we store it in a look-up table. Spatial Speckle Contrast is the ratio of standard deviation, $\sigma_I$ , to the mean intensity, $\langle I \rangle$ , of the pixels' values of the subimage.

$$K_s = \frac{\sigma_I}{\langle I \rangle}$$

So after the calculation of the contrast of every subimage the look up table is complete. In order to normalize the contrast reduction we use this simple equation:

$$I_{table} = \left[ 1 - \frac{(K_{reference} - K_{transient})}{K_{reference}} \right]$$

where $K_{reference}$ is the look-up table at the initial state for a given image, $K_{transient}$ is the look-up table at some point in time during forced/passive excitation. At this point, we are able to image the $I_{table}$ with a pseudocolor map in order to portray the contrast reduction.

In this algorithm as an input we used a video. From this video we built a Speckle Contrast look-up table from each frame. We use the first frame as the reference frame and all the others as the transient frames. Since we have $K_{reference}$ and $K_{transient}$ for each frame we extract and image the $I_{table}$ from every frame of the video. Then we reproduce the video but instead the original frames we use the $I_{table}$ frames.

In the end we find the average value of each $I_{table}$ and we match every frame with real time through the fps. So we produce a chart with axles: The average value of $I_{table}$ and the time. Through that chart we will known exactly how long did the oscillation last and how strong is this oscillation.

## 7.3    Spatial Laser Speckle Imaging with impact stimulation

In this experiment we used the set-up and the algorithm as we described them in the previous sections. In the first measurement we took a video and during the capture we hit the drum with the drumstick. We put our video in the algorithm and we produced a new video with the same number of frames as the original one but instead of images has the $I_{tables}$. We used the same pseudocolor map as in the temporal contrast algorithm in this algorithm as well. In figures 7.7 and 7.8 we can see all the frames of our video after the use of the algorithm.
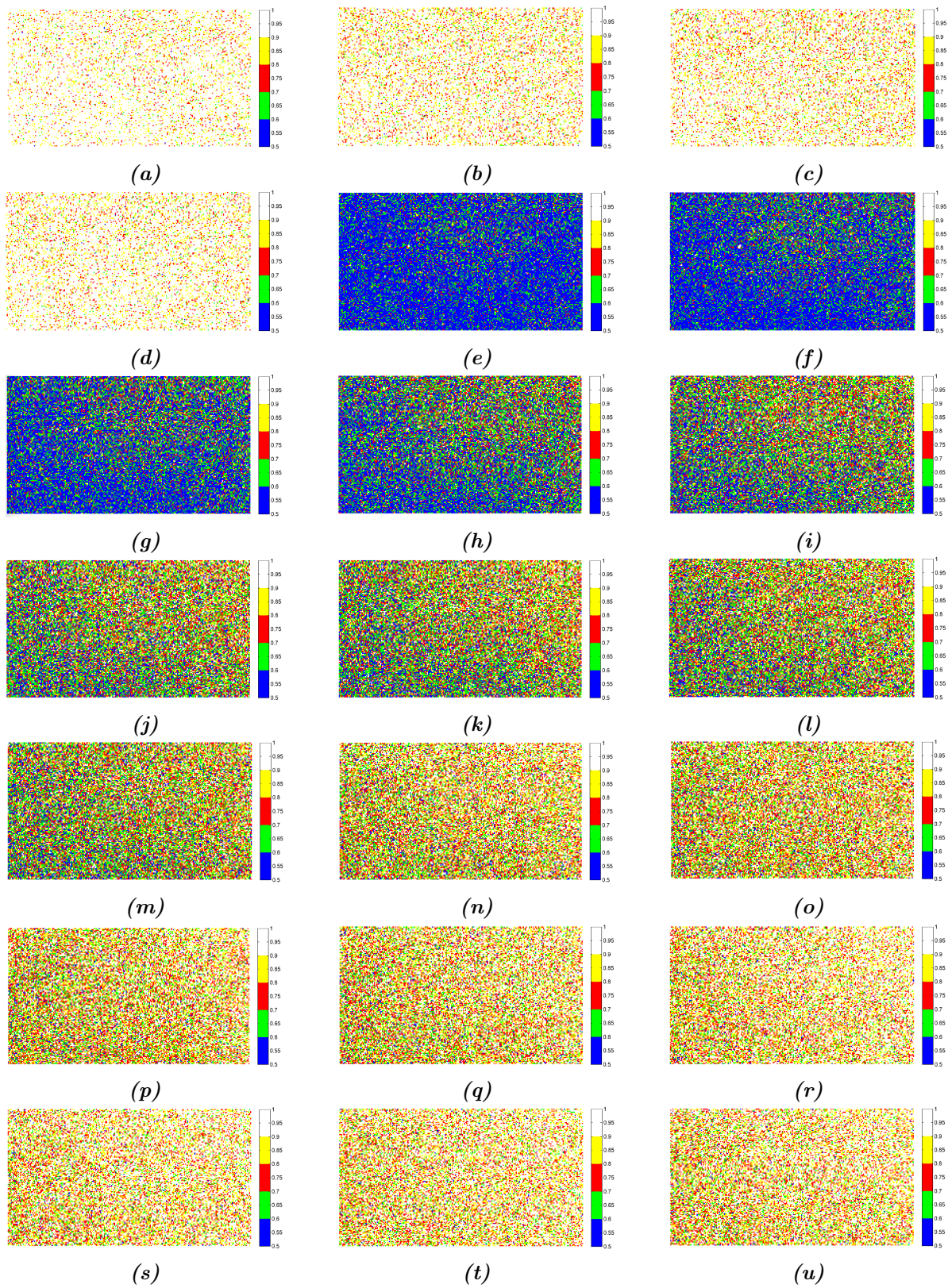
**Figure 7.7:** $I_{table}$ *frames(1)*

(a)

(b)

(c)

(d)

(e)

(f)

(g)

(h)

(i)

(j)

(k)

(l)

(m)

(n)

(o)

(p)

(q)

(r)

(s)

(t)

(u)
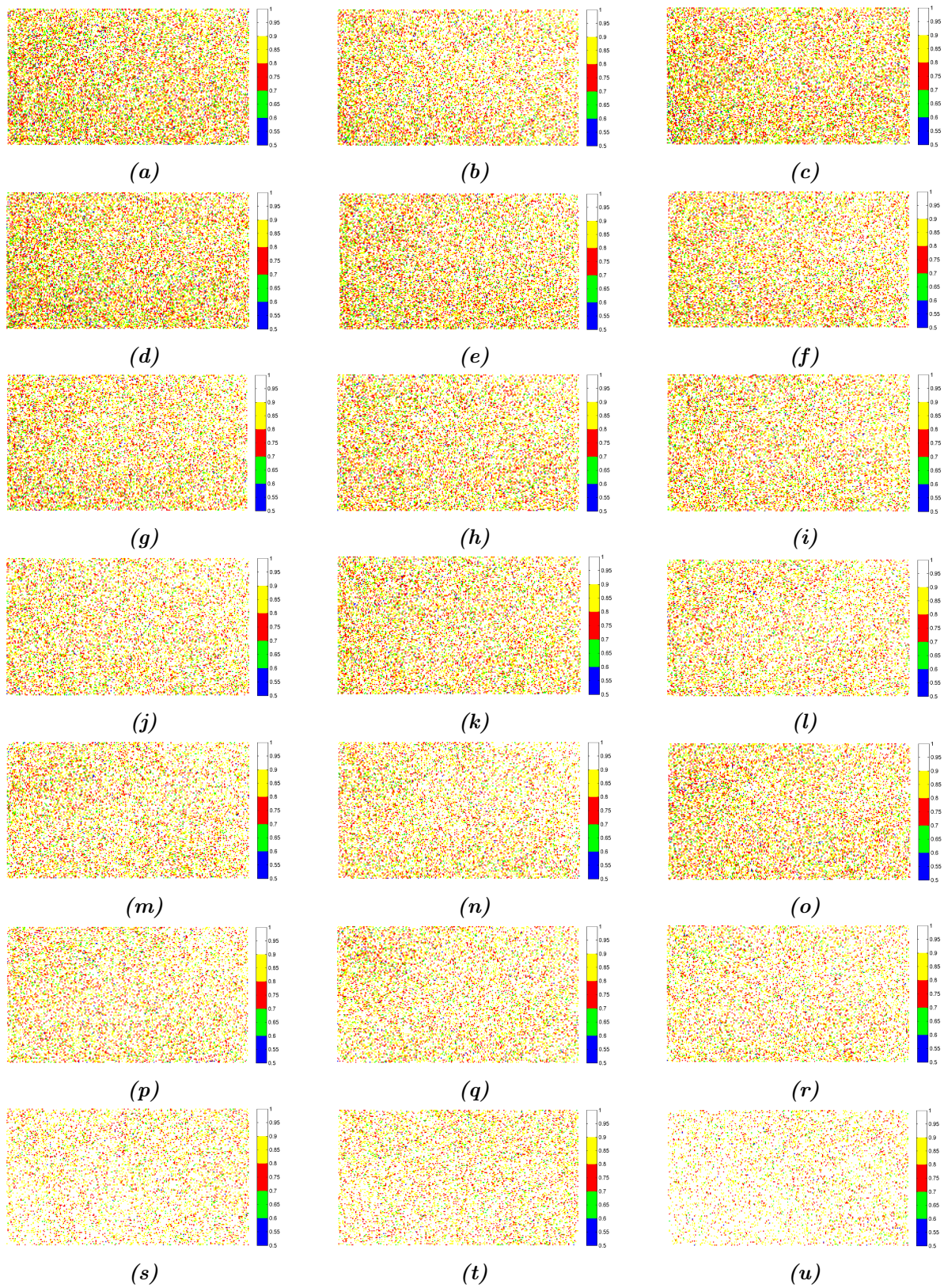
**Figure 7.8:** $I_{table}$ *frames(2)*

As we mentioned in previous section (7.2) from every video we produce a chart with axles: The average value of $I_{table}$ and the time. Figure 7.9 shows this chart for single hit measurement. The red line in the chart is the exact time that we hit the drum.
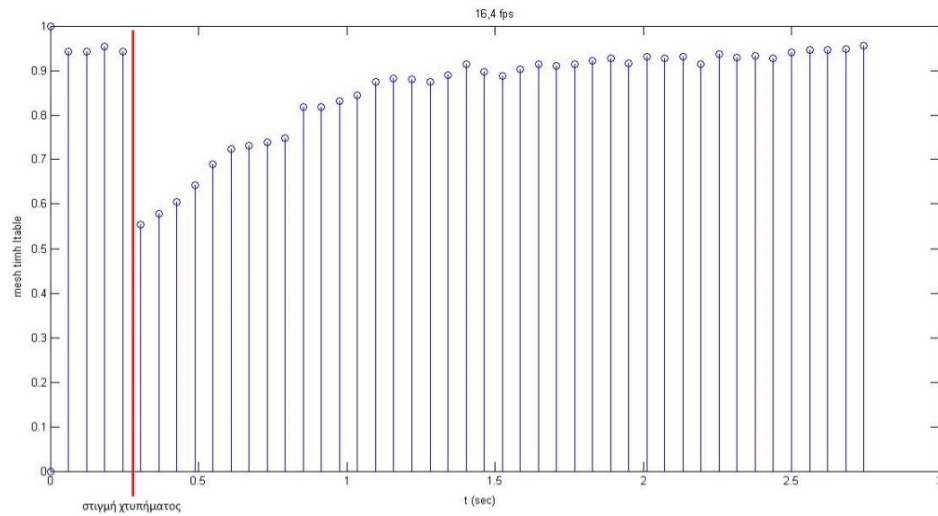


**Figure 7.9:** *Chart for single hit(16.4fps , 42 frames)*

In the next measurements we took longers videos and we hit the drum more than one time. As we can see in figure 7.10 through our implementation we can deduce the exact time that an oscillation lasts. The red line in the chart is the exact time that we hit the drum. The yellow one is the exact time that the oscillation stops. In the first hit we do not have a yellow line because we hit again the drum before the first oscillation stops.
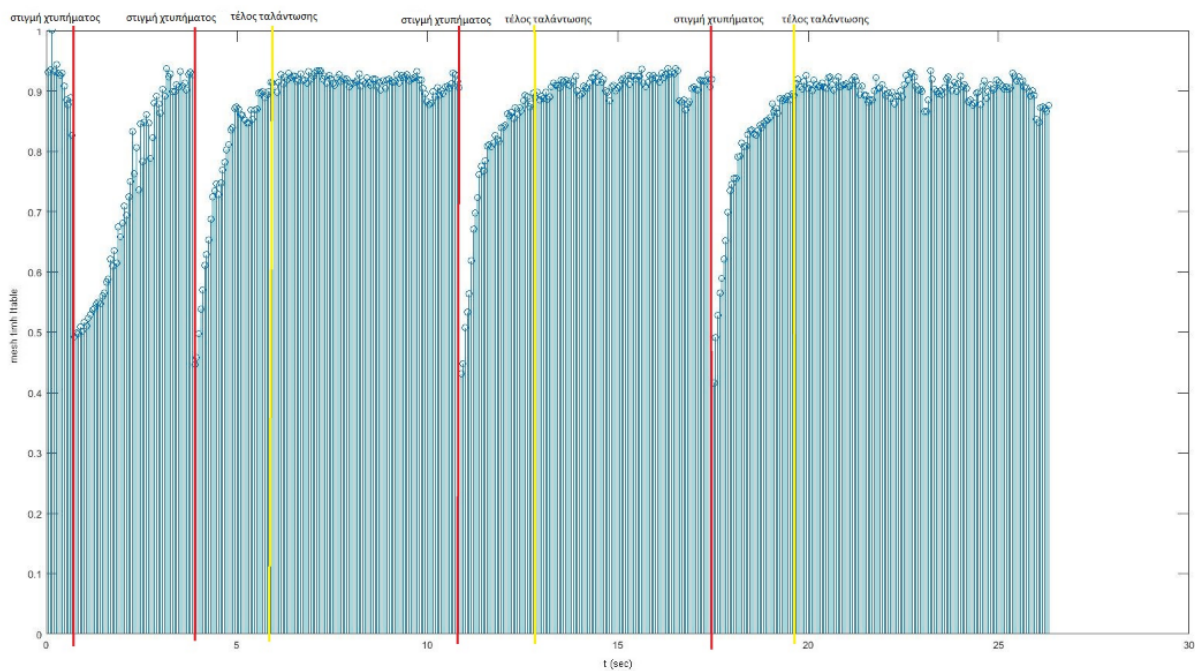


**Figure 7.10:** *Chart for multiple hits(19fps , 500 frames)*

## 7.4    Spatial Laser Speckle Imaging with sound stimulation

In this experiment we used the set-up with the speaker and the algorithm as we described them. With an online *tone generator*[31] we produced wav files with 1 second duration with frequencies from 100hz to 400hz with 50hz step. So we took seperate videos with each tone frequency in order to quantify the reduction of the speckle contrast. Using our algorithm we produced new videos with the same number of frames exactly as in the previous experiment. We also produced charts with axles: The average value of $I_{table}$ and the time, that show us exactly the reduction for each frequency. After we finished our measurements we repeated them but we place the speaker at a distance of one meter. In the end we produced a wav file with frequency escalation. Our escalation is from 50hz to 450hz at a steady pace for eight seconds. We took this measurment twice in order to ensure that the result is correct.

In figures 7.11 and 7.12 we can see the charts for 100Hz 1sec sound stimulation in 2 cases: the speaker near the drum and the speaker at a distance of one meter.



**Figure 7.11:** *Chart with sound stimulation 100hz*



**Figure 7.12:** *Chart with sound stimulation 100hz 1m*

In figures 7.13 and 7.14 we can see the charts for 150Hz 1sec sound stimulation in 2 cases: the speaker near the drum and the speaker at a distance of one meter.



**Figure 7.13:** *Chart with sound stimulation 150hz*



**Figure 7.14:** *Chart with sound stimulation 150hz 1m*

In figures 7.15 and 7.16 we can see the charts for 200Hz 1sec sound stimulation in 2 cases: the speaker near the drum and the speaker at a distance of one meter.



**Figure 7.15:** *Chart with sound stimulation 200hz*
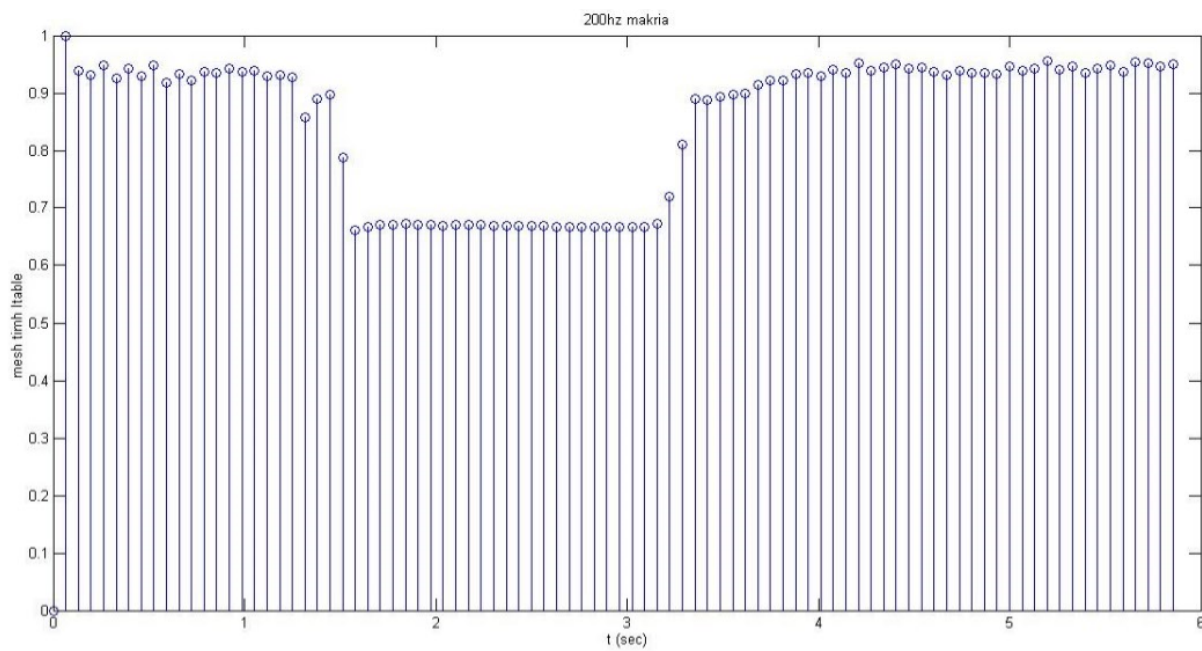


**Figure 7.16:** *Chart with sound stimulation 200hz 1m*

In figures 7.17 and 7.18 we can see the charts for 250Hz 1sec sound stimulation in 2 cases: the speaker near the drum and the speaker at a distance of one meter.
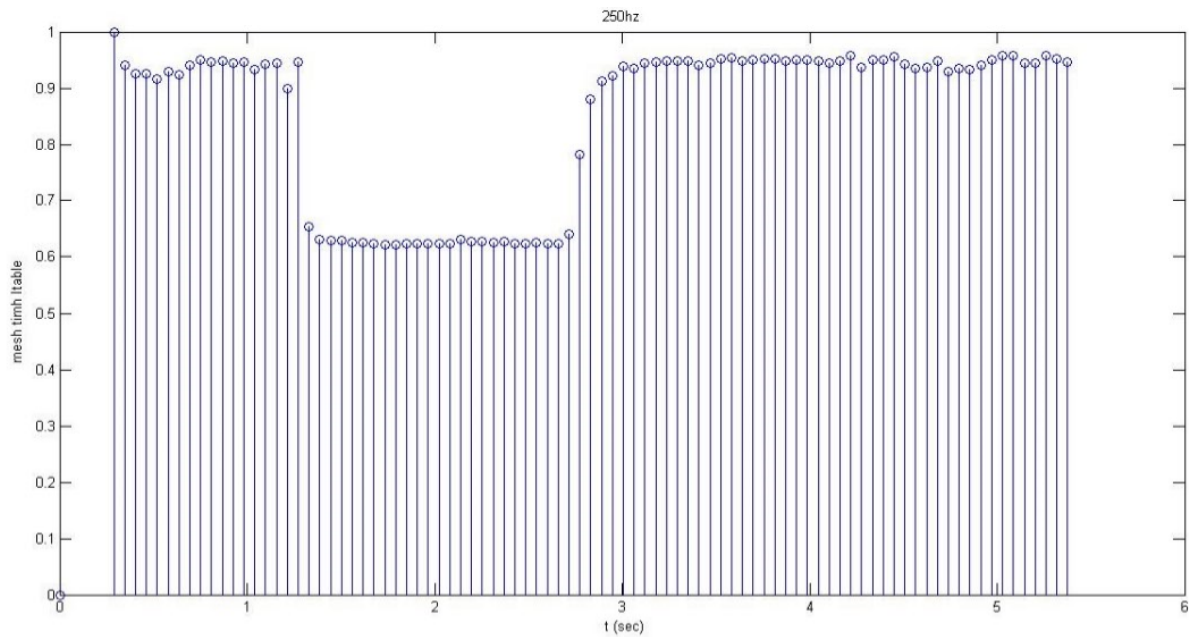


**Figure 7.17:** *Chart with sound stimulation 250hz*
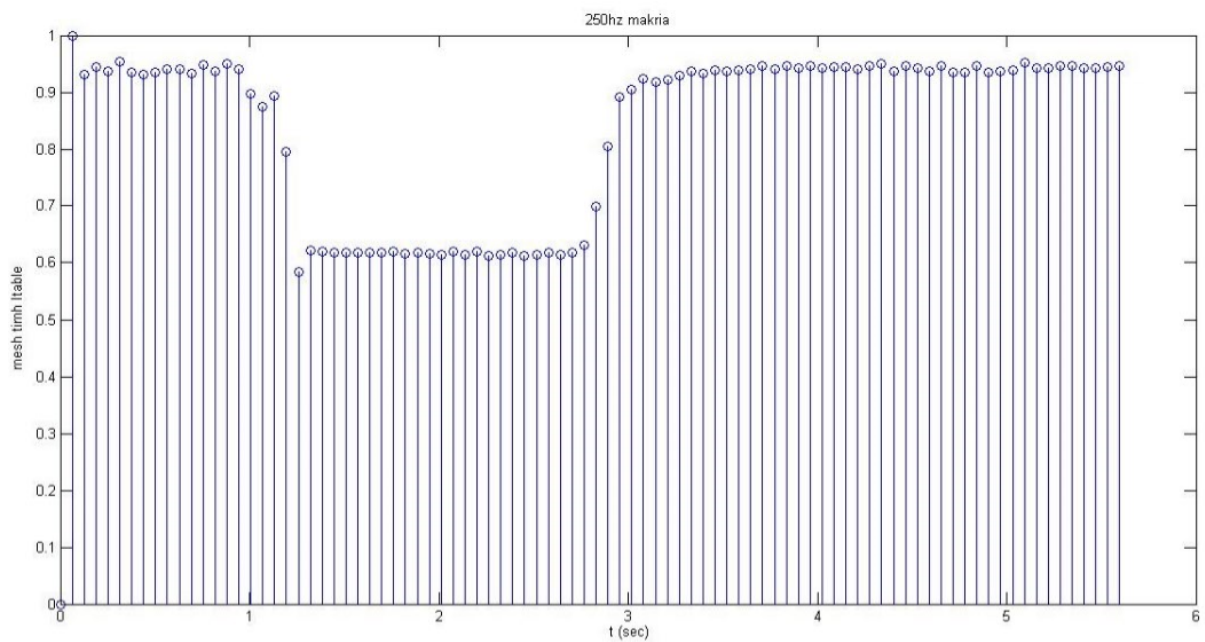


**Figure 7.18:** *Chart with sound stimulation 250hz 1m*

In figures 7.19 and 7.20 we can see the charts for 300Hz 1sec sound stimulation in 2 cases: the speaker near the drum and the speaker at a distance of one meter.
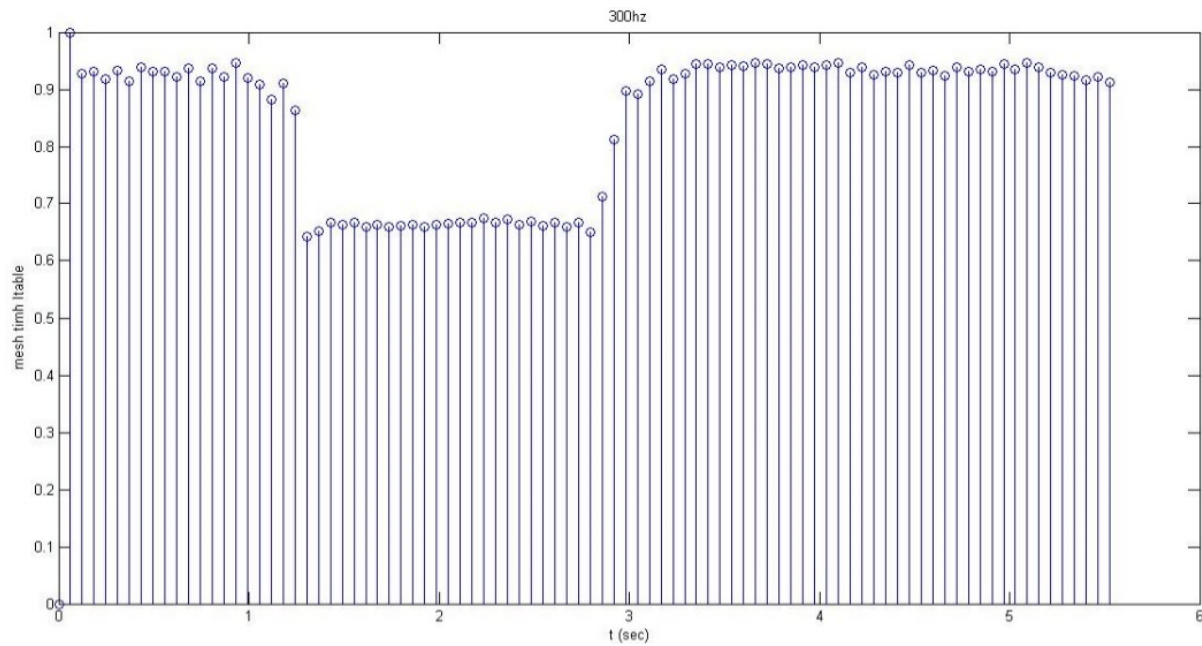


**Figure 7.19:** *Chart with sound stimulation 300hz*
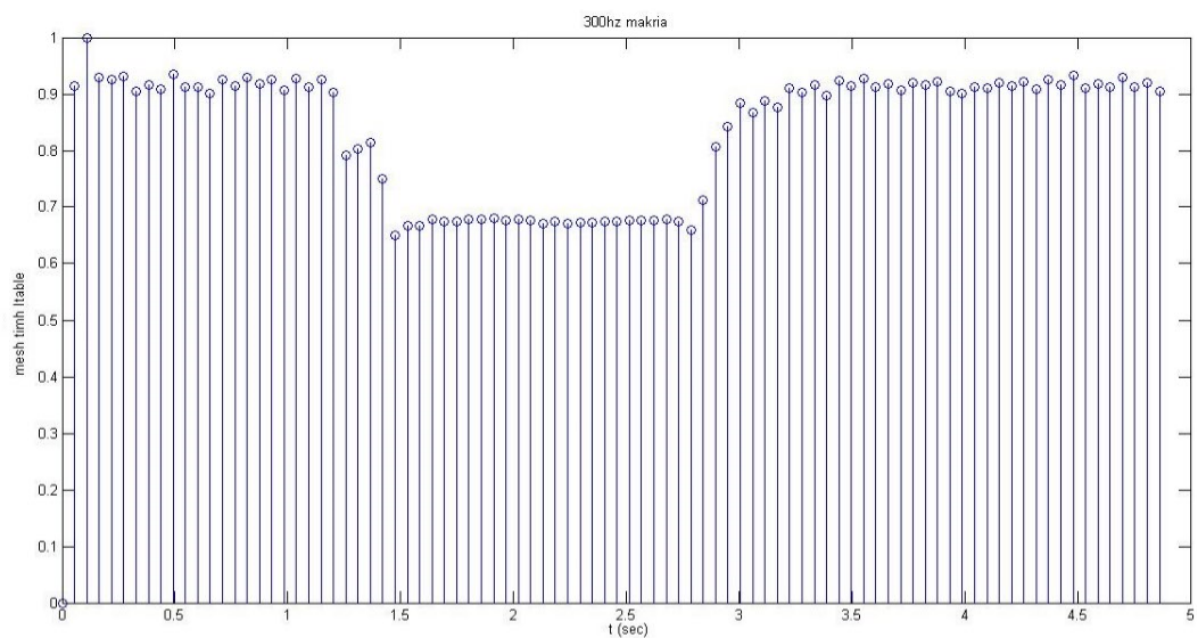


**Figure 7.20:** *Chart with sound stimulation 300hz 1m*

In figures 7.21 and 7.22 we can see the charts for 350Hz 1sec sound stimulation in 2 cases: the speaker near the drum and the speaker at a distance of one meter.
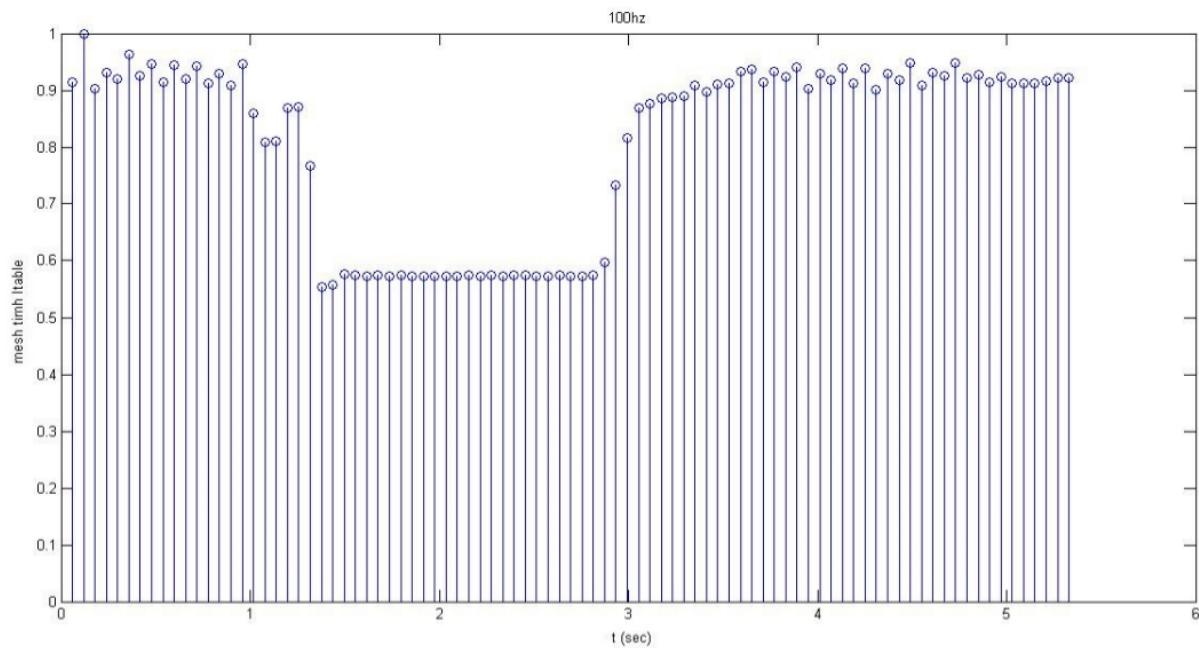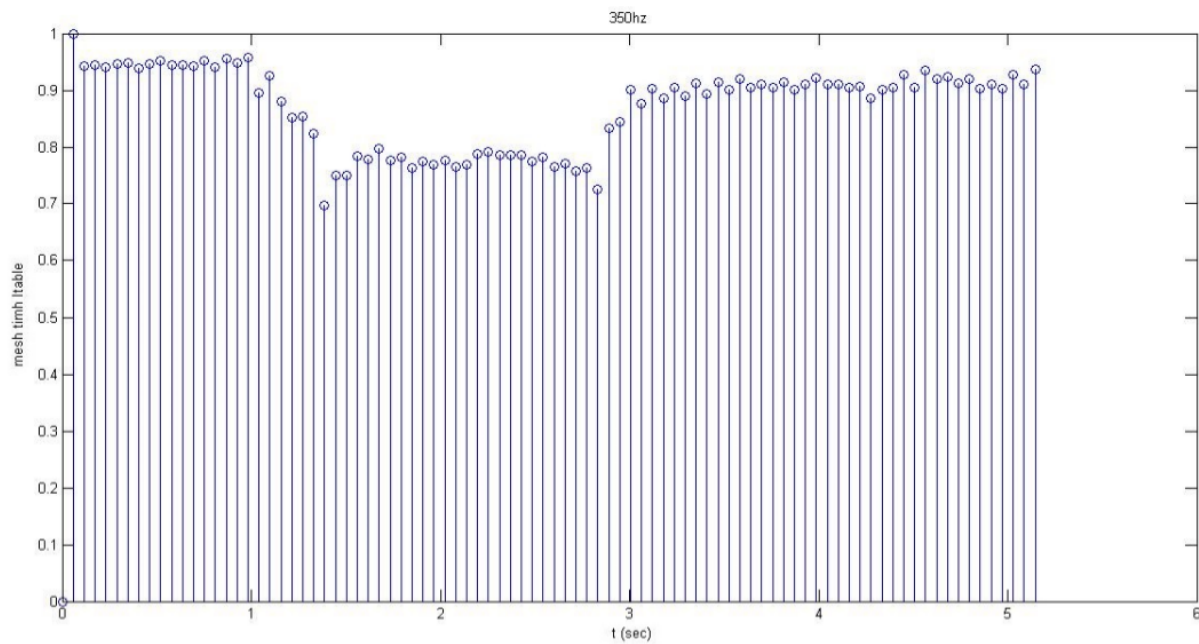


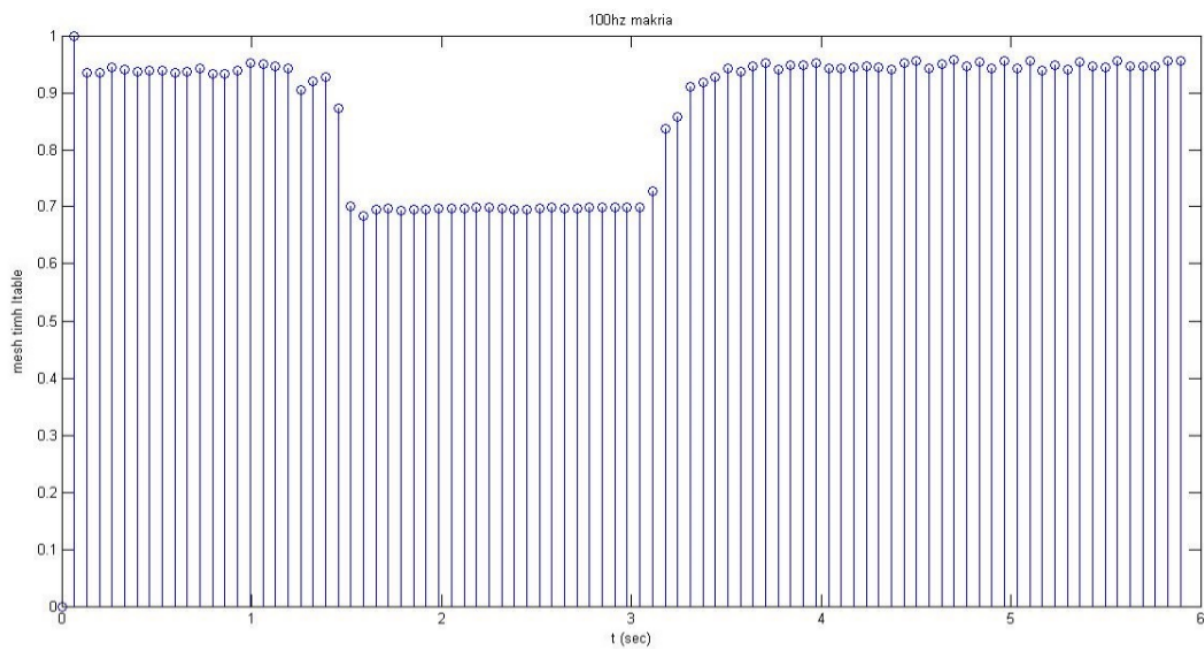**Figure 7.21:** *Chart with sound stimulation 350hz*
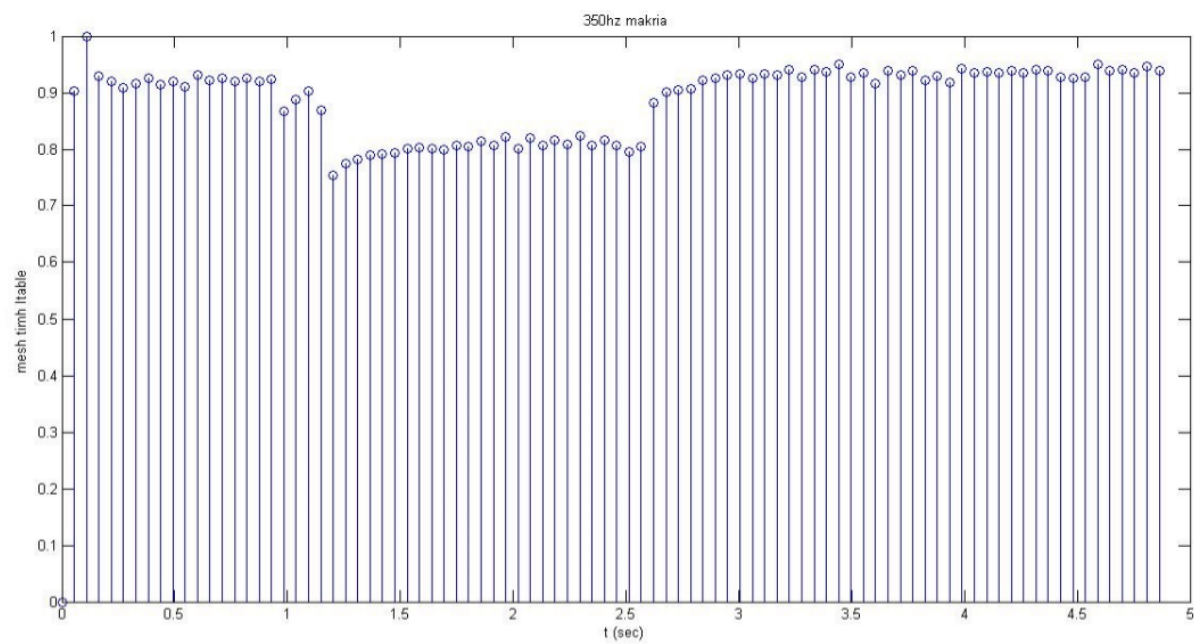


**Figure 7.22:** *Chart with sound stimulation 350hz 1m*

In figures 7.23 and 7.24 we can see the charts for 400Hz 1sec sound stimulation in 2 cases: the speaker near the drum and the speaker at a distance of one meter.
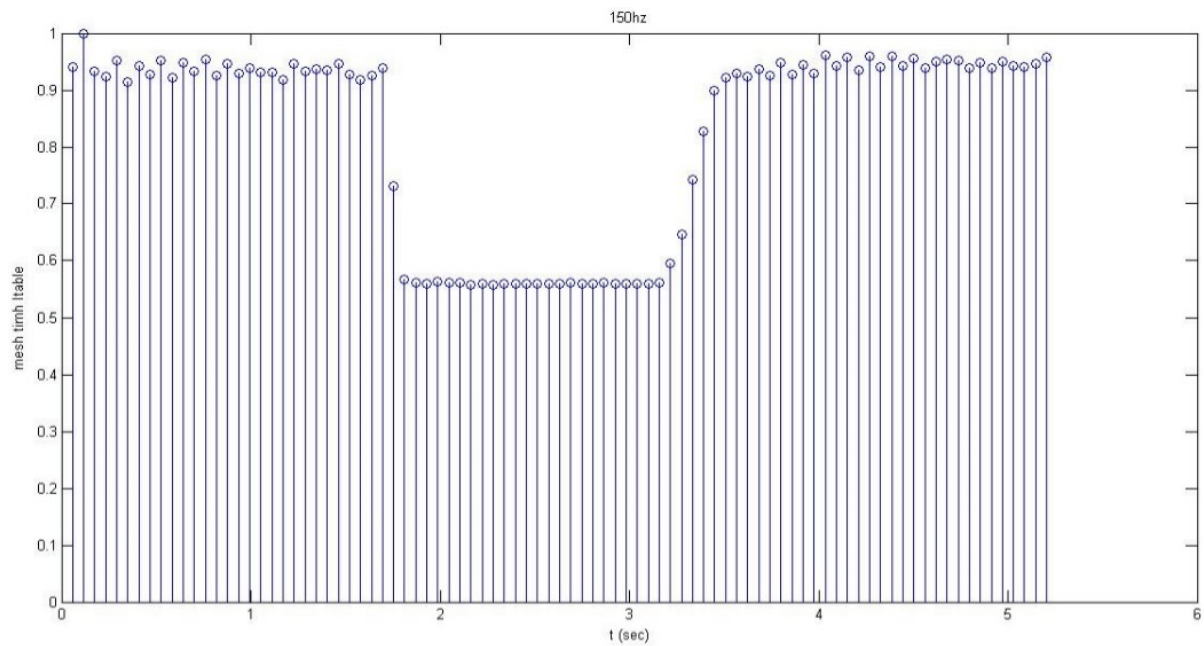


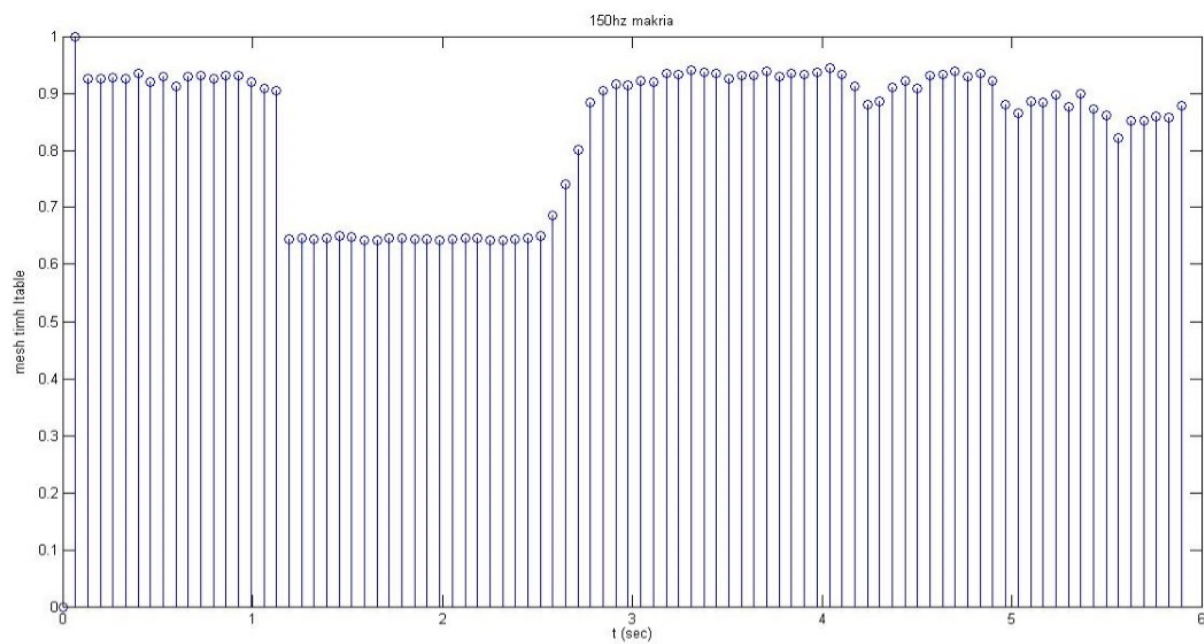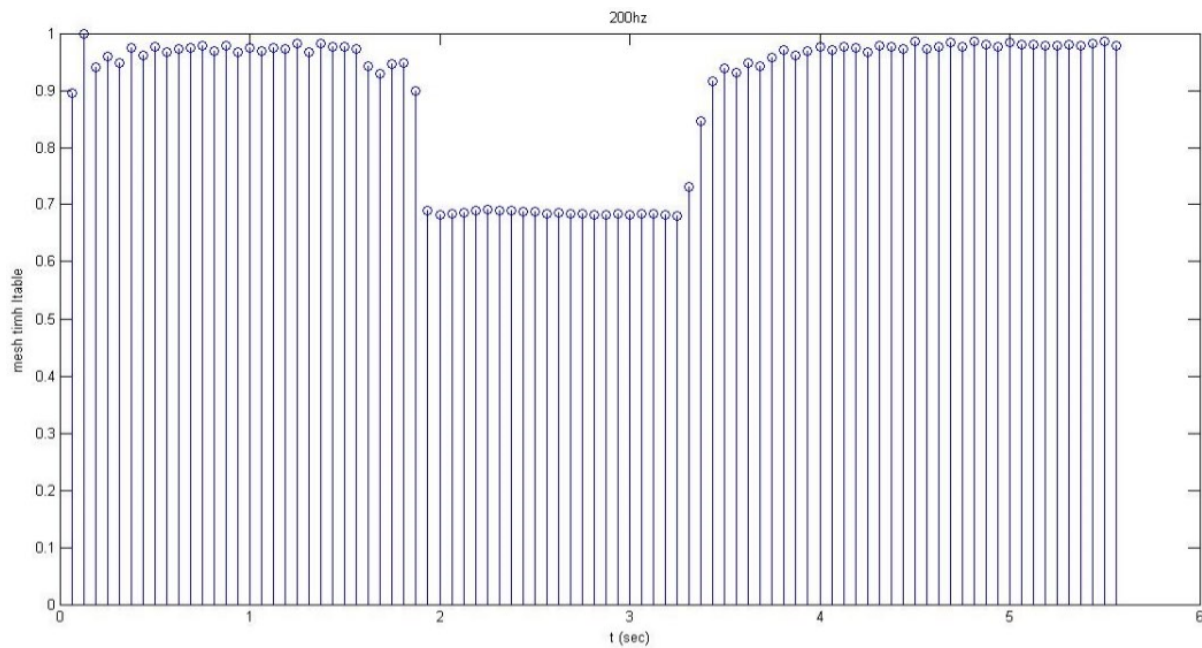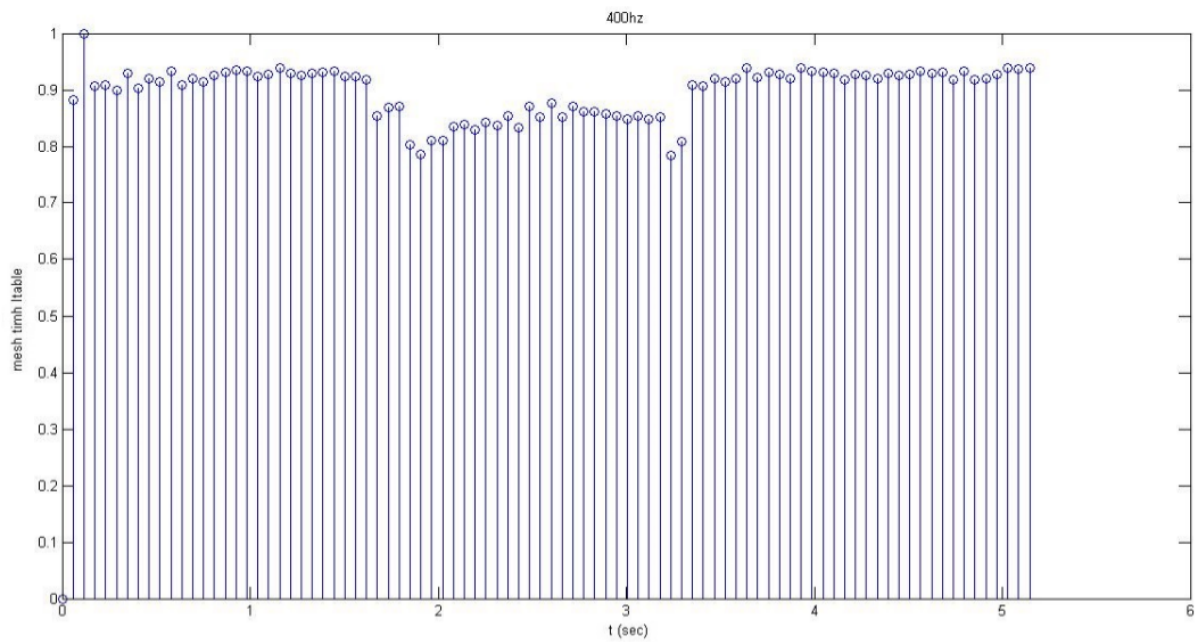**Figure 7.23:** *Chart with sound stimulation 400hz*
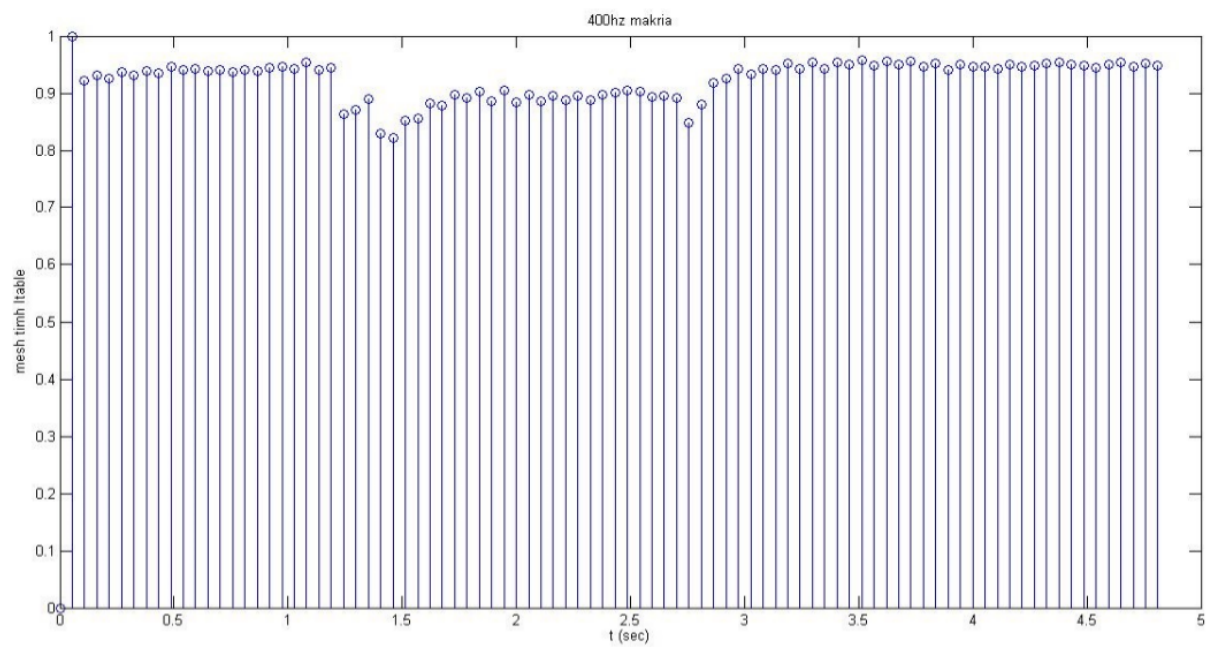


**Figure 7.24:** *Chart with sound stimulation 400hz 1m*

In figures 7.25 and 7.26 we can see the charts for escalated frequency from 50hz to 450hz in 8 seconds sound stimulation. We took this measurment twice in order to ensure that the result is correct.
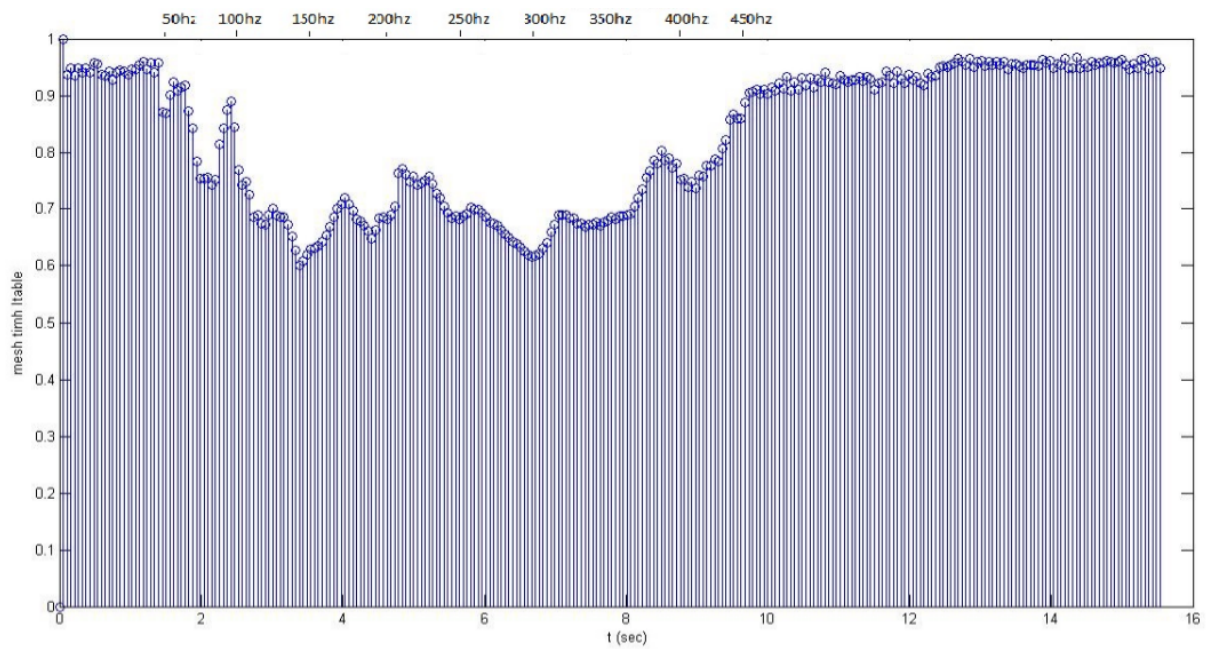


*Figure 7.25:* *Chart with frequency escalation 50-450hz 1st attempt*
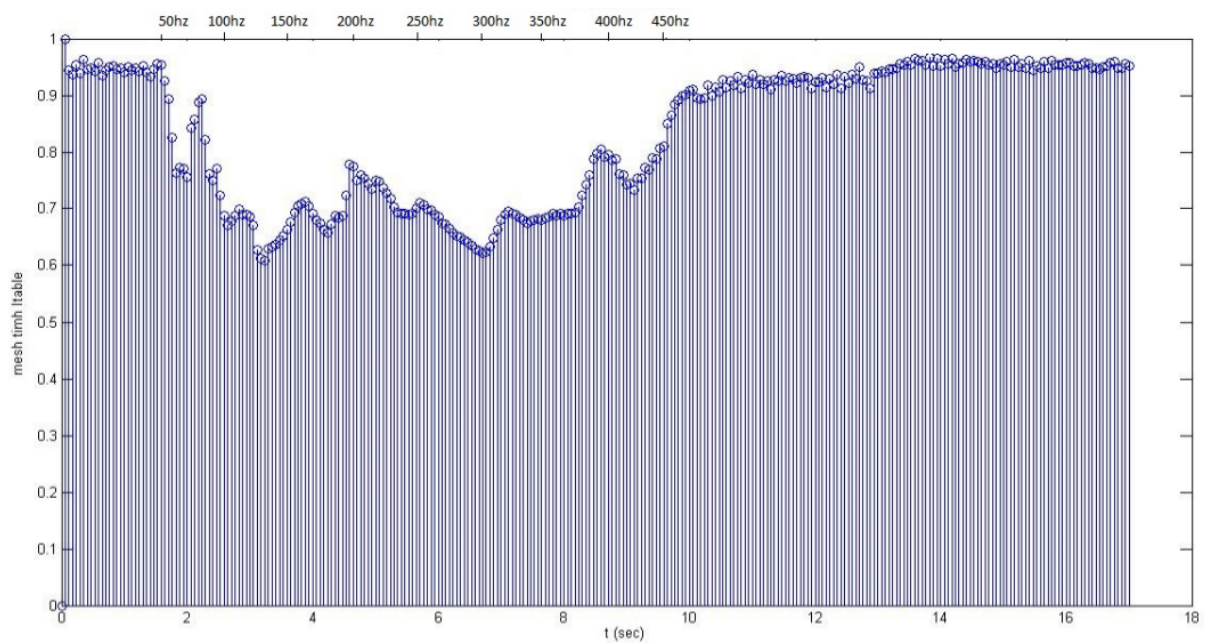


*Figure 7.26:* *Chart with frequency escalation 50-450hz 2nd attempt*

# Chapter 8

# Conclusion and Future work

## 8.1 Conclusion

In this diploma thesis we designed a Laser Speckle Imaging device in two ways. In the first way we measured and quantified the temporal speckle contrast reduction and in the second one we measured and quantified the spatial speckle contrast reduction. For both implementations we come to some interesting conclusions.

**Temporal Speckle Contrast Analysis**: After we completed all the measurements from the first implementation we concluded we cannot detect and quantify the vibration of a induced surface without the use of a temporal contrast analysis algorithm. We tried to take measurements with different zooms in this implementation and from all our measurements we came to the same conclusion: The more we increase the vibration of the surface the more the Speckle Contrast decreases.

So with our setup we can compare images from a surface with different vibrations and prove which vibration is more powerfull. In other words we can quantify the vibration's power without knowing anything about the vibrator or his source.

Because of the fact that we used a temporal algorithm and we have no lack of spatial resolution we can detect in a surface, which is not homogeneous, in which parts vibrates more. That fact can give as some usefull information about the surface.

**Spatial Speckle Contrast Analysis**: In this implementation we did four expirements that led us to different conclusions.

From the first experiment that was an instantaneous impact stimulation in a drum film we conclude that there is speckle contrast reduction in the surface just at the moment of the

impact. We also noticed that the speckle contrast reduced instantly but increased slowly as the drum's film oscillation stops.

From the second experiment that was the same as the previous one but with multiple impacts we conclude that it takes about 2 seconds for the film of the drum to stop the oscillation from the moment of the impact. Of course it depends on the impact's intensity. The stronger the impact, the longer the oscillation lasts.

From the third experiment which was with sound stimulation we conclude that the drum film has a different sensitivity in the different frequencies. Specifically, in the frequencies from 100 to 300hz the oscillation is very intense but after 300hz the oscillation is much less intense.

From the final experiment in which there is a frequency escalation we conclude that there isn't a linear ratio between the frequency and the speckle contrast reduction in a drum film. Instead, we noticed an irregular pattern. However we noticed that the frequencies that cause the most speckle contrast reduction are the 130hz and the 300hz.

## 8.2 Future work

**Spatiotemporal Algorithm**. We can design one new algorithm that combines those which we have already design. This algorithm will improve both spatial and temporal resolution and give as better results. Also we can design an algorithm that run in the same time our spatial and our temporal algorithm and give us both the results.

**Real-time**. The lack of computational power made our algorithm unable to work in real-time. So another possible future work can be the upgrade of our implementation into a real-time one. In order to do that we have to run our algorithm in a device that have much more computational power and we have to upgrade our source code into a C++ one.With this changes propably we can reach a real-time implementation goal.

**Imlpementation of a Graphical User Interface** In our implementation all the images or the videos are loaded directly through the source code. So we can design a GUI for all the functions of our device. A GUI could provide the user a more friendly environment to work.

# Appendix A

# Algorithms

## A.1   Temporal Contrast Imaging Algorithm

```matlab
1   clear all;
2   close all;
3
4
5   img = imread('Still003.bmp'); % First image without vibration
6   %red1 = img(:,:,1); % Red channel
7   green1 = img(:,:,2); % Green channel
8   %blue1 = img(:,:,3); % Blue channel
9   %[m,n]=size(red1);
10  [m,n]=size(green1);
11  %[m,n]=size(blue1);
12
13  img = imread('Still004.bmp'); % Second image without vibration
14  %red2 = img(:,:,1); % Red channel
15  green2 = img(:,:,2); % Green channel
16  %blue2 = img(:,:,3); % Blue channel
17  %[m,n]=size(red2);
18  %[m,n]=size(green2);
19  %[m,n]=size(blue2);
20
21  img = imread('Still005.bmp'); % Third image without vibration
22  %red3 = img(:,:,1); % Red channel
23  green3 = img(:,:,2); % Green channel
24  %blue3 = img(:,:,3); % Blue channel
25  %[m,n]=size(red3);
26  %[m,n]=size(green3);
27  %[m,n]=size(blue3);
28
29  img = imread('Still006.bmp'); % Fourth image without vibration
30  %red4 = img(:,:,1); % Red channel
31  green4 = img(:,:,2); % Green channel
32  %blue4 = img(:,:,3); % Blue channel
33  %[m,n]=size(red4);
34  %[m,n]=size(green4);
```

```matlab
35  %[m,n]=size(blue4);
36
37
38  img = imread('Still015.bmp'); % First image with vibration
39  %red5 = img(:,:,1); % Red channel
40  green5 = img(:,:,2); % Green channel
41  %blue5 = img(:,:,3); % Blue channel
42  %[m,n]=size(red5);
43  %[m,n]=size(green5);
44  %[m,n]=size(blue5);
45
46  img = imread('Still016.bmp'); % Second image with vibration
47  %red6 = img(:,:,1); % Red channel
48  green6 = img(:,:,2); % Green channel
49  %blue6 = img(:,:,3); % Blue channel
50  %[m,n]=size(red6);
51  %[m,n]=size(green6);
52  %[m,n]=size(blue6);
53
54  img = imread('Still017.bmp'); % Third image with vibration
55  %red7 = img(:,:,1); % Red channel
56  green7 = img(:,:,2); % Green channel
57  %blue7 = img(:,:,3); % Blue channel
58  %[m,n]=size(red7);
59  %[m,n]=size(green7);
60  %[m,n]=size(blue7);
61
62  img = imread('Still017.bmp'); % Fourth image with vibration
63  %red8 = img(:,:,1); % Red channel
64  green8 = img(:,:,2); % Green channel
65  %blue8 = img(:,:,3); % Blue channel
66  %[m,n]=size(red8);
67  %[m,n]=size(green8)
68  %[m,n]=size(blue8);
69
70
71
72  for x = 750:1250      %%Central area 500X500
73     for y = 1250:1750
74  %  for x = 1:m       %%For the whole image
75  %  for y = 1:n
76
77         B = [green1(x,y) , green2(x,y) , green3(x,y) , green4(x,y)];
78         C = [green5(x,y) , green6(x,y) , green7(x,y) , green8(x,y)];
79
80
81         B = double(B);
82         I=mean(B);
83         S=std(B);
84         Contrast(x,y) = S/I ;
85         C = double(C);
86         I=mean(C);
87         S=std(C);
88         Contrast(x,y+500) = S/I ; %Contrast(x,y+n) = S/I ; % for the whole image
89
```

```matlab
90
91
92
93        end
94    end
95
96     %If we use the whole image there is no need for this double for loop and
97     %no need of Contrast2. You have to replace it with Contrast
98
99        for x = 1:500
100       for y = 1:1000
101
102           Contrast2(x,y)= Contrast(x+750,y+1250);
103
104
105       end
106   end
107
108
109           sortedValues = unique(Contrast2(:));
110           maxValues = sortedValues(end-9:end) ;
111           minValues = sortedValues(1:10) ;
112           Max=mean(maxValues);
113           Min=mean(minValues);
114
115           for x = 1:500
116       for y = 1:1000
117           if Contrast2(x,y) <= minValues(10)
118             Contrast2(x,y) = Min;
119           elseif Contrast2(x,y) >= maxValues(1)
120               Contrast2(x,y) = Max;
121           end
122
123       end
124   end
125
126 mymap = [0 0 1
127      0 1 0
128      1 0 0
129      1 1 0
130      1 1 1];
131
132
133 figure();
134 imshow(Contrast2,[Min Max])
135
136 colormap(mymap)
137 colorbar
138
139
140
141 figure();
142 imhist(Contrast2);
```

## A.2   Spatial Contrast Imaging Algorithm

```matlab
1   clear all;
2   close all;
3
4
5   v = VideoReader('13_26_20 16fps.avi'); %Video for reading
6   fps=16 ; %frames per second of the original video capture
7   video1 = read(v);
8
9   [y,x,k,l]=size(video1);
10
11  A = video1(:,:,2,2); %reference frame
12
13
14  par=8; % window size
15  par1=par-1;
16
17  [y,x]=size(A);
18
19      x=fix(x/par)*par
20       y=fix(y/par)*par
21    % B=zeros(1,3);
22    e=1;
23
24     for n=1:par:y
25          r=1;
26  for m = 1:par:x
27      k=1;
28      for a = m:m+(par-1)
29       for d = n:n+(par-1)
30
31      B(k) = A(d,a)  ;
32      if k<(par*par)
33         k=k+1 ;
34         end
35
36      end
37      end
38      B = double(B);
39          I=mean(B);
40          S=std(B);
41          Contrast(e,r) = S/I ;
42
43          if r<(x/par)
44          r=r+1 ;
45          end
46
47  end
48  if e<(y/par)
49          e=e+1 ;
50  end
51      end
52
53
```

```matlab
54  %%
55  for i=1:10 % the frames that we want to study
56  A = video1(:,:,2,i);
57  [y,x]=size(A);
58
59   x=fix(x/par)*par;
60        y=fix(y/par)*par ;
61
62     % B=zeros(1,3);
63     e=1;
64
65      for n=1:par:y
66          r=1;
67  for m = 1:par:x
68      k=1;
69      for a = m:m+(par-1)
70       for d = n:n+(par-1)
71
72       B(k) = A(d,a)  ;
73      if k<(par*par)
74         k=k+1  ;
75         end
76
77       end
78      end
79      B = double(B);
80         I=mean(B);
81         S=std(B);
82         Contrast2(e,r) = S/I ;
83
84         if r<(x/par)
85         r=r+1  ;
86         end
87
88  end
89  if e<(y/par)
90         e=e+1  ;
91  end
92      end
93
94
95         [y1,x1]=size(Contrast);
96         [y2,x2]=size(Contrast2);
97
98   %%
99   O=ones(y1,x1);
100     Itable= O-((Contrast-Contrast2)./Contrast) ;
101     [y,x]=size(A);
102      x=fix(x/par)*par
103        y=fix(y/par)*par
104
105
106     %Itablebig=zeros(y,x);
107     for t=1:y
108         for z=1:x
```

```matlab
109             z1=fix((z+par1)/par);
110             t1=fix((t+par1)/par);
111
112
113             if Itable(t1,z1)<1
114             Itablebig(t,z)=Itable(t1,z1);
115             else
116                 Itablebig(t,z)=1;
117             end
118         end
119     end
120  N=Itablebig;
121     N = double(N);
122         K=mean(N,2);
123         L(i)=mean(K);
124
125
126         mymap = [0 0 1
127     0 1 0
128     1 0 0
129     1 1 0
130     1 1 1];
131
132   fig=figure();
133 imshow(Itablebig,[0.6 1])  ;
134 colormap(mymap);
135  colorbar   ;
136
137  print(fig,['images',num2str(i+100)],'-dpng');
138
139         N=Itablebig;
140     N = double(N);
141         K=mean(N,2);
142         L(i)=mean(K);
143
144       F(i)=(i)/fps;
145 end
146
147 myFolder = 'C:\Users\pakos\Desktop\kefalaio 5\mat5'; %path for the reproduction of video
148 if ~isdir(myFolder)
149     errorMessage = sprintf('Error: The following folder does not exist:\n%s', myFolder);
150     uiwait(warndlg(errorMessage));
151     return;
152 end
153 % Get a directory listing.
154 filePattern = fullfile(myFolder, '*.PNG');
155 pngFiles = dir(filePattern);
156 % Open the video writer object.
157
158 writerObj = VideoWriter('klimakwsh_50-450hz.avi');
159 %writerObj.FrameRate=1;
160 open(writerObj);
161 % Go through image by image writing it out to the AVI file.
162 for frameNumber = 1 : length(pngFiles)
163     % Construct the full filename.
```

```matlab
164        baseFileName = pngFiles(frameNumber).name;
165        fullFileName = fullfile(myFolder, baseFileName);
166        % Display image name in the command window.
167        fprintf(1, 'Now reading %s\n', fullFileName);
168        % Display image in an axes control.
169        thisimage = imread(fullFileName);
170        %imshow(imageArray);  % Display image.
171        drawnow; % Force display to update immediately.
172        % Write this frame out to the AVI file.
173        writeVideo(writerObj, thisimage);
174    end
175    % Close down the video writer object to finish the file.
176    close(writerObj);
177
178
179    figure();
180    title('100hz')
181    plot(F,L)
182
183    figure();
184
185    stem(F,L)
186    title('100hz')
```

# Bibliography

[1] D.A. Boas, C. Pitris, and N. Ramanujam. *Handbook of Biomedical Optics*, chapter 7, pages 131–164. Taylor & Francis, 2011.

[2] Le Thinh M., Paul J. S., Al-Nashash H., Tan A., Luft A. R., Sheu F. S. and Ong S. H.(2007) *New insights into image processing of cortical blood flow monitors using laser speckle imaging* IEEE Trans. Med. Imaging 26, 833842 .

[3] Cheng H.(2003) *Modified laser speckle imaging method with improved spatial resolution* J. Biomed. Opt. 8(3), 559564

[4] D. A. Boas and A. K. Dunn (January 2010) *Laser speckle contrast imaging in biomedical optics* Journal of Biomedical Optics , Spie Digital Library

[5] A. F. Fercher and J. D. Briers (1981) *Flow visualization by means of single-exposure speckle photography* Optics Communications, vol. 37, no. 5, pp. 326-330

[6] J. D. Rigden and E. I. Gordon (1962) *"The granularity of scattered optical laser light"* Proceedings of the Institute of Radio Engineers, vol. 50, pp. 2367-2368

[7] J. C. Ramirez-San-Juan, C. Regar, B. Coyotl-Oceloty and B. Choi(October 2014) *Spatial versus temporal laser speckle contrast analyses in the presence of static optical scatterers* Journal of Biomedical Optics , Spie Digital Library

[8] Bryan H. Bunch, Hellemans Alexander (April 2004). *The History of Science and Technology*.

[9] P. Hariharan (2007). *Basics of Interferometry*.

[10] Albert Michelson, Edward Morley (1887). *On the Relative Motion of the Earth and the Luminiferous Ether*, American Journal of Science.

[11] B. P. Abbot (15 June 2016). *Observation of Gravitational Waves from a 22-Solar-Mass Binary Black Hole Coalescence*, Physical Review Letters .

[12] C. Dainty (1984) *Laser Speckle and Related Phenomena* Sprinter Verlag.

[13] Tao Hua, Simon Wang, Zhenxing Hu, Pengwan Chen, Qingming Zhang. *Evaluation of the quality of a speckle pattern in the digital image correlation method by mean subset fluctuation.* Optics and Laser Technology.

[14] D. Lecompte, A. Smits, Sven Bossuyt, H. Sol, J. Vantomme, D. Hemelrijck, A.M. Habraken. *Quality assessment of speckle patterns for digital image correlation.* Optics and Lasers in Engineering.

[15] Lukasz Lasyk, Michal Lukomski (January 2011). *Simple digital speckle pattern interferometer for investigation of art objects* Optica Applicata.

[16] K. Hinsch (2007). *Laser speckle metrology a tool serving the conservation of cultural heritage, [In] Oscillation, Waves and Interaction* Universitatsverlag Gottingen, Germany.

[17] E. Bernikola, A. Nevin, V. Tornari (2009). *Rapid initial dimensional changes in wooden panel paintings due to simulated climate-induced alterations monitored by digital coherent out-of-plane interferometry* Applied Physics.

[18] T.R. Moore(2004). *A simple design for an electronic speckle pattern interferometer* American Journal of Physics.

[19] M. Sjodahl (2001). *Digital speckle photography in digital speckle pattern interferometry and related techniques, [In] Digital Speckle Pattern Interferometry and Related Techniques* [Ed.]Rastogi P.K., John Wiley.

[20] K. Creath, G.A. Slettemoen (1985). *Vibration-observation techniques for digital speckle-pattern interferometry* Journal of optical society of America.

[21] Tom W. J., Ponticorvo A. and Dunn A. K. (2008),*Efficient processing of laser speckle contrast images* IEEE Trans. Med. Imaging 27, 17281738 .

[22] Briers J. D. and Fercher A. F.(1982) *Retinal blood-flow visualization by means of laser speckle photography* Invest. Ophthalmol. Visual Sci. 22, 255259 .

[23] Yi Chang Shih, Abe Davis, Samuel W. Hasinoff , Fredo Durand, William T. Freeman *Laser Speckle Photography for Surface Tampering Detection* MIT CSAIL

[24] Briers J. D. and Webster S.(1996) *Laser speckle contrast analysis (LASCA): a nonscanning, full-field technique for monitoring capillary blood flow* J. Biomed. Opt. 1, 174179

[25] Nelson H. Koshoji, Sandra K. Bussadori, Carolina C. Bortoletto, Renato A. Prates, Marcelo T. Oliveira, and Alessandro M. Deana (February 2015)*Laser Speckle Imaging: A Novel Method for Detecting Dental Erosion*

[26] D. D. Duncan, S. J. Kirkpatrick and R. K. Wang (2008) *Statistics of local speckle contrast* Journal of optical society of America.

[27] Lionel Keene, Fu-Pen Chiang(January 2008) *Real-time anti-node visualization of vibrating distributed systems in noisy environments using defocused laser speckle contrast analysis* Journal of Sound and Vibration 320 472-481

[28] Albert Einstein (2001).*Relativity: The Special and the General Theory* (Reprint of 1920 translation by Robert W. Lawson ed.). Routledge. p. 48.

[29] Barish, Barry C.; Weiss, Rainer (October 1999). *LIGO and the Detection of Gravitational Waves.* Physics Today.

**Online sources**

[30] https://www.rp-photonics.com/optical_power.html

[31] http://www.wavtones.com/functiongenerator.php